

Zur Erlangung des akademischen Grades
doctor rerum naturalium (Dr. rer. nat.)
des FB08 Biologie und Chemie
der Justus-Liebig-Universität Gießen

A twostep affinity purification of nuclear mRNPs

Vorgelegt von

Christoph Wierschem

(Master of Science in Biochemistry)

Lasserg Dezember 2020

Die vorliegende Arbeit wurde am Institut für Biochemie des Fachbereiches 08 der Justus-Liebig-Universität Gießen in der Zeit von März 2015 bis März 20120 unter der Leitung von Prof. Dr. Katja Strässer angefertigt.

“Honor iis antecesserunt et me fecerunt eum, qui sum.

Utinam spiritus eorum prosit ut ego in viis Domini ambulare possim.”

Dissertation eingereicht im Januar 2021

Erstgutachterin: Prof. Dr. Katja Sträßer
Institut für Biochemie
Fachbereich für Biologie und Chemie
Justus-Liebig-Universität Gießen

Zweitgutachter: Apl. Prof. Dr. Elena Evguenieva-Hackenberg
Institut für Mikrobiologie und Molekularbiologie
Fachbereich für Biologie und Chemie
Justus-Liebig-Universität Gießen

Summary

Gene expression is an extraordinarily complex and highly regulated process during which mRNA is exported from the nucleus to the cytoplasm. A particularly important step in gene expression is the formation of a particle consisting of proteins and mRNA called mRNP. In *S. cerevisiae*, the conserved TREX complex supports synthesis and export of mRNA and mediates mRNP formation. Although many RNA binding proteins (RBPs) have been studied in yeast, the composition and structure of a nuclear mRNP remains elusive. Various diseases such as cancer or amyotrophic lateral sclerosis (ALS) are linked to nuclear proteins involved in mRNP formation. Therefore, understanding mRNP formation in yeast will expand our knowledge of gene expression in higher eukaryotes and enhance the understanding of this complex process in humans.

To investigate mRNP formation, this study explored the purification protocol for nuclear mRNPs in *S. cerevisiae*. The goal was to purify the total pool of a single nuclear mRNP from a yeast whole cell extract (WCE). This unity of identical mRNPs was called a specific mRNP.

First, the total pool of nuclear mRNPs from WCE was enriched via an affinity purification step. The target was the 5' cap of the mRNA. To further purify the specific nuclear mRNP of *CCW12* or *ILV5* of the selected mRNAs of the study, a specific 2'-O-methylated antisense oligonucleotide was used. To improve the purification outcome, different incubation times, temperatures, and buffers were tested. To evaluate the impact on the purified sample, the mRNA levels were monitored with qPCR and the protein levels detected on western blots. As additional sample quality control, all purified complexes were examined under the electron microscope (EM). Particles were found in the expected size of the *CCW12* mRNPs reported in literature.

The protocol described in this study can be used to purify any specific nuclear mRNP of interest. This specific nuclear mRNP can be used in downstream applications like quantitative mass spectrometry or cryogenic electron microscopy (cryo-EM).

Understanding mRNP formation and the structural composition of each stage in the life cycle of a yeast nuclear mRNP might explain why the absence or presence (at elevated levels) of their human homologues are connected to cancer or neuronal diseases.

Zusammenfassung

Die Genexpression ist ein hochkomplexer und streng regulierter Prozess, bei dem die Boten-RNA (mRNA) vom Zellkern ins Zytoplasma transportiert und dort übersetzt wird. Ein wichtiger Schritt der Genexpression ist die Bildung eines Komplexes aus einer mRNA und vielen Proteinen, welcher mRNP genannt wird. Ein in *S. cerevisiae* konservierter Proteinkomplex TREX ist neben der Synthese und dem Export von mRNA auch an der Bildung dieser mRNPs beteiligt. Obwohl in Hefe viele RNA-bindende Proteine (RBPs) untersucht sind, ist die Zusammensetzung und die Struktur der nuklearen mRNPs bis heute unbekannt. Da beim Menschen einige Arten von Krebs und neurologische Erkrankungen wie amyotrophe Lateralsklerose (ALS) ihren Ursprung in der Fehlregulation von Proteinen haben, welche an der mRNP Formation beteiligt sind, ist es essenziell, den Prozess der mRNP Formation in Hefe zu studieren und dieses Wissen auf die menschliche Genexpression zu übertragen.

Zur Untersuchung der mRNP Formation in Hefe stellt diese Studie ein Reinigungsprotokoll für nukleare mRNPs vor. Das Ziel ist die Reinigung eines spezifischen nuklearen mRNP. Das Wort spezifisch beschreibt, dass nur Kopien eines mRNPs von einer zuvor ausgewählten mRNA aus dem Zellextrakt gereinigt werden.

Im ersten Schritt werden alle nuklearen mRNPs über eine Affinitätsreinigung angereichert. Dies geschieht über die Selektion nach der 5' Kappe der mRNAs. Im nächsten Schritt wird die mRNA von *CCW12* oder *ILV5*, deren mRNPs gereinigt werden sollen, durch einen biotinylierten 2'-O-methylierten Antisense-Oligonukleotid erkannt und gebunden. Zur Verbesserung der Reinigung wurden unterschiedliche Inkubationszeiten und Temperaturen, sowie verschiedene Puffer getestet. Um die Auswirkung der Änderung auf die Reinigung zu untersuchen, wurden die mRNA Level mit qPCR bestimmt und die aufgereinigten Proteine auf Western Blot analysiert. Des Weiteren wurden die gereinigten mRNP Komplexe unter dem Elektronen Mikroskop (EM) untersucht. Es wurden Partikel gefunden, die in Form und Größe den Voraussagen für *CCW12* mRNPs in der Literatur entsprechen.

Das hier veröffentlichte Protokoll kann zur Reinigung jedes spezifischen nuklearen mRNP verwendet werden. Die gereinigten Proben dienen der weiteren Charakterisierung des mRNP. Dazu zählen unter anderem die Bestimmung der Masse, der Struktur und die Ladung des Komplexes.

Das Verständnis der mRNP Formation und das Wissen über jeden Zustand des Komplexes während seines Lebens-Zyklus liefert möglicherweise Antworten auf die Frage, warum Proteine, die für die mRNP Formation beim Menschen verantwortlich sind, zur Ausprägung diverser Krebsarten und neurologischer Krankheiten beitragen.

Table of Content

Table of Content.....	IV
1 Introduction.....	1
1.1 Gene expression.....	1
1.1.1 Transcription.....	1
1.1.2 mRNA processing.....	2
1.1.3 mRNP formation and nuclear export.....	4
1.1.4 Coupling of transcription, mRNP formation and mRNA export.....	6
1.2 THO/ TREX complex.....	8
1.3 PAF complex.....	10
1.4 Nab2, Npl3 and SR-Proteins in mammalian cells.....	10
1.5 Mex67-Mtr2 the main mRNA exporter in <i>S. cerevisiae</i>	11
1.6 Sub2 and human UAP56 (DDX39B).....	11
1.7 Tho1 and human CIP29.....	12
1.8 linking miss regulated mRNP assembly to disease.....	12
1.9 Aim of this study.....	14
2 Materials and Methods.....	16
2.1 Materials.....	16
2.1.1 Consumables and Chemicals.....	16
2.1.2 Equipment.....	16
2.1.3 Yeast and e.Coli strains.....	17
2.1.4 Plasmids.....	18
2.1.5 Oligonucleotide sequences.....	19
2.1.6 Growth media, Buffers and solutions.....	20
2.1.7 Kits and Antibodies.....	22
2.2 Methods.....	23
2.2.1 Standard technics.....	23
2.2.2 Yeast technics.....	27
3 Results.....	34
3.1 Role of Tho1 in Transcription.....	34
3.1.1 Tho1 overexpression does not influence the occupancy of Paf1 on transcribed genes.....	34
3.1.2 Tho1 deletion of does not influence the occupancy of Spt5 on transcribed genes.....	38
3.1.3 A Δ tho1 deletion increases the Paf1-TAP occupancy on transcribed genes.....	41
3.1.4 Additional ChIP experiments to study Tho1 function in yeast.....	42
3.2 Purification of a specific nuclear mRNP in <i>saccharomyces cerevisiae</i>	43
3.2.1 Selecting CCW12 and ILV5 as targets for specific nuclear mRNP in yeast.....	43
3.2.2 mRNP purification from RS 453 WCE.....	44
3.2.3 Optimization the pull-down for nuclear mRNP purification.....	46
3.2.4 Optimization of the input culture in terms of strain and optical density.....	47
3.2.5 Comparing a mixture of good CCW12 ASOs with ASO 2 from CCW12 and modifying the ultracentrifugation step (UZ).....	50

3.2.6	Cross-linking of Hpr1-TAP with formaldehyde and glutaraldehyde	54
3.2.7	ATP- γ -S a trap for Sub2 in TAP purification with or without MgCl ₂	55
3.2.8	Anti-sense oligo optimization: biotin vs desthiobiotin	56
3.2.9	Purification of nuclear mRNPs using a temperature sensitive yeast mutant	60
3.2.10	Testing the good buffers HEPES and TRIS in CCW12 mRNP purification and dilution of TEV eluate.....	62
3.2.11	Testing three annealing temperatures of CCW12 ASO 3 in mRNP purification	63
3.2.12	Introducing the “Gerber wash buffer” in mRNP purification.....	65
3.2.13	Testing biotin and desthiobiotin CCW12 ASO 3 at 4 °C vs RT annealing temperature and performing the whole mRNP purification at 4 °C vs RT.....	66
3.2.14	Analysing the binding efficiency of CCW12 ASO 1-3 to their mRNA via dilution and via RNase H assay	68
3.2.15	Purifying nuclear CCW12 mRNPs at the different pH values	69
3.2.16	Specific nuclear mRNP in Δ ccw12 and Δ ilv5 as control strains.....	73
4	<i>Discussion</i>	75
4.1	A role for Tho1 in transcription.....	75
4.2	A purification for specific nuclear mRNPs.....	76
4.3	Comparing the combined mRNP purification with other methods from the literature.	78
5	Abbreviations	81
6	Acknowledgements	83
7	Figures	86
8	Tables	87
9	Equations	88
10	References	89

1 Introduction

1.1 Gene expression

The most fundamental process of each living cell is the so-called gene expression. It describes the translation of information stored in the nuclear-localised DNA into proteins in the cytoplasm. During this process, an intermediate storage of information, the messenger RNA (mRNA), is synthesised by RNA polymerase II (RNAPII). Various proteins interact with the mRNA to form a messenger ribonucleoparticle (mRNP) to travel from the nucleus to the cytoplasm. This process is tightly regulated to ensure cell viability.

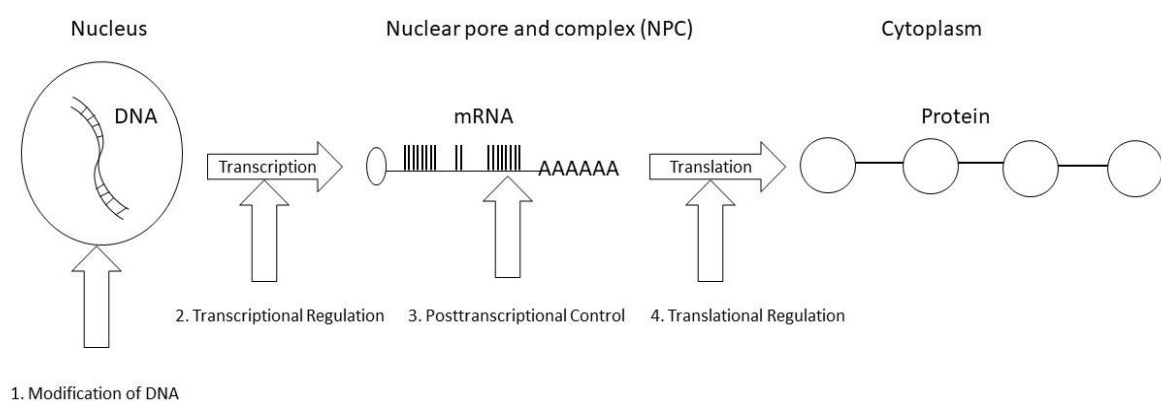


Figure 1. Regulation of gene expression

The scheme illustrates how the information stored in DNA is translated to a protein. The four arrows indicate specific mechanism of regulation for gene expression.

1.1.1 Transcription

As seen in Figure 1, transcription is the first step in gene expression to transform the code of life from DNA into RNA. The synthesis of mRNA takes place in the nucleus of the cell. The process itself consists of three stages thus, initiation, elongation and termination, and ends with the matured mRNA transcript which is modified and bound by RNA binding proteins (RBPs) to form the mRNP.

The first step of this cycle is the formation of the RNAPII, the preinitiation complex (PIC) (Hahn *et al.* 2004), to the promoter of the gene. The complex consists of the initiation factors TFIIA, TFIIB, TFIID, TFIIIE, TFIIF and TFIIF. The last binding TFIIF is a complex with helicase and kinase activity. The helicase activity is required to unwind the DNA while the kinase activity is important to phosphorylate the heptapeptide residues in the C-terminal domain (CTD) of Rpb1, the largest subunit of RNAPII. The CTD plays an important role in the regulation of the whole transcription cycle via the phosphorylation of its heptapeptide repetition YSPTSPS (see Figure 3).

After the DNA duplex is opened, transcription by RNAPII is initiated and the RNAPII starts to synthesize the RNA (Hahn *et al.* 2004). At this stage of transcription, the RNA synthesis works error prone and up to the first 8 nucleotides, several abortive rounds of initiation might take place until the early elongation phase is reached (Margaritis *et al.* 2008).

In the elongation phase, various transcription elongation factors join the RNAPII to synthesis nascent mRNA. To unwind the DNA from its packed form, the chromatin remodelling factors such as Paf1 complex and Elf1 are recruited (Sims *et al.* 2004). Additional, factors like Spt4/5 and TFIIIS, empower the RNAPII to overcome blockages in elongation (Cramer *et al.* 2004). During the elongation phase, the pre-mRNA is co-transcriptionally 5' capped and spliced.

Transcription is terminated by the release of the pre mRNA from RNAPII which dissociates from the RNA of the transcribed gene. Two models have been published on how this event occurs (Loya *et al.* 2016). The first model is the 'allosteric model' according to which, the presence of a poly(A) signal together with the recruitment of factors like cleavage and polyadenylation factor (CPF) leads to conformational changes of the active elongation complex causing RNAPII stalling and termination. The second process is the "torpedo model". In this model, the protein, Rat1, enters at the poly A site and the 5'-3' exonuclease is degraded, leaving the 3' end of the RNA. When Rat1 reaches the RNAPII, it disassociates from the chromatin. (Richard and Manley 2009 and Proudfoot *et al.* 2011).

1.1.2 mRNA processing

The first maturation step in the mRNP formation takes place co-transcriptionally and is called capping. The mRNA capping enzyme adds a m⁷Gppp "cap" in several steps to the 5' end of the mRNA (Topisirovic *et al.* 2011).

The final cap structure interacts with the cap binding complex (CBC). This complex is composed of the subunits Cbp20 and Cbp80. The small subunit directly binds to the 5' m⁷-G-cap while the large subunit interacts with other proteins. Between the CBC and the cap structure is a direct interaction. CBC protects the mRNA from degradation and is also involved in transcription elongation, splicing, nuclear mRNP export, and translation (Gonatopoulos-Pournatzis and Cowling 2014 and Meinel and Sträßer 2015).

The next step in the formation of nuclear mRNPs is the splicing process. In this complex reaction, several splice factors and RNA work together to remove the non-coding regions (introns) of the mRNA to fuse the exons together. This two-step chemical reaction is catalysed by spliceosomes (Figure 2). In yeast, roughly 4 % of all genes contain introns but the amounts of expressed mRNAs make up for 27 % of the total mRNA in each cell (Ares *et al.* 1999).

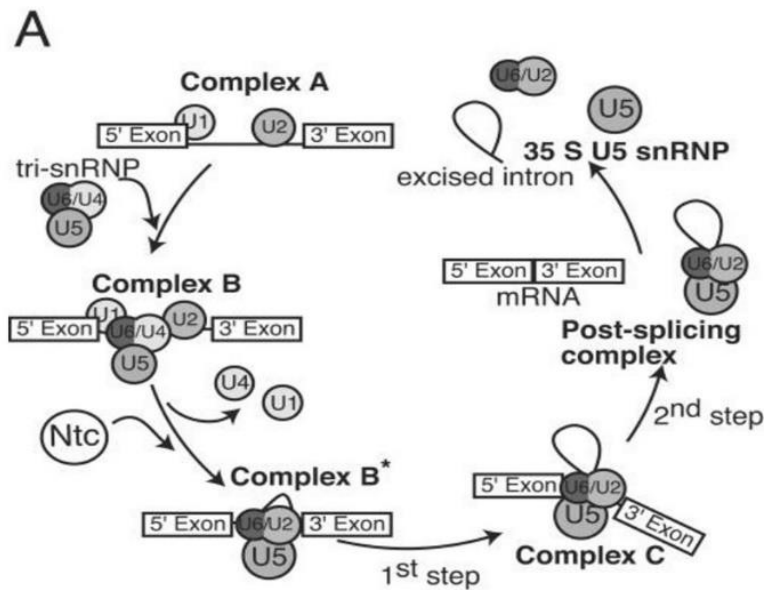


Figure 2. A schematic showing pre-mRNA splicing in yeast

The beginning of splicing is marked by the recognition of 5' and 3' of the splice site by U1 and U2 snRNAs, forming the Complex A. It is then followed by the association of U5/U4/U6 tri-snRNP forming the Complex B, which after a series of rearrangements leads to the formation of an active spliceosome intermediate (Complex C). After the splicing reaction, the post-splicing complex and the spliced mRNA are released and factors involved in the process are recycled (Ohi *et al.* 2005)

The last maturation step involves the processing of the 3' end of the mRNA. It consists of two coupled steps: the cleavage of the pre-mRNA and the synthesis of a poly (A) tail. The mRNA is cleaved by the cleavage 3' end processing complex, which in yeast consists of the Cleavage and Polyadenylation Factor (CPF) and the Cleavage Factors I A and B (CFIA and CFIB). In this complex, routine binding to the efficiency element (EE) and positioning element (PE) upstream of the cleavage site in the mRNA by all these processing factors must be ensured (Mandel *et al.* 2008). The cleavage site itself is marked by a sequence element containing a pyrimidine followed by an adenosine stretch (Zhao *et al.* 1999). Cleavage and poly-adenylation are coupled *in vivo* by being functions of the 3' end processing complex. The major enzyme for 3' poly adenylation is the polyA-polymerase (Pap1). It defines the proper length of the poly (A) tail by interacting with the 3' end processing complex (Mandel *et al.* 2008). In yeasts, a poly(A) consists of around 70-90 adenosines and in humans, 200-300 adenosines. The length is important for the mRNA stability and therefore, the half-life of the mRNA. PAPI controls the poly A tail length of the polyadenylation reaction. The poly A binding protein Nab2 is also involved in poly A length control (Hector *et al.* 2002) (see Section 1.3)

Interestingly most genes have several cleavage and pol(A) sites (Wilkening *et al.* 2013 and Ozsolak *et al.* 2010). The number of this sites is important for +/- miRNA supported expression leading to precise regulation of mRNA levels (Sandberg *et al.* 2008). Alternative cleavage and polyadenylation might lead to truncated protein or omitted binding sites for RNA binding proteins, altering the transcript stability or leading to miss localisation (Tian and Manley 2013). The loss of cleavage and pol(A) sites might even activate oncogenes (Mayr and Bartel 2009).

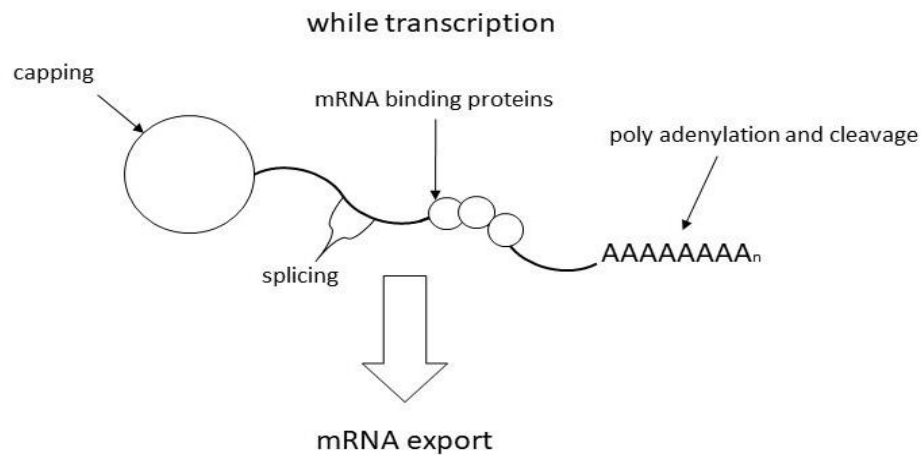


Figure 3. Schema of early mRNP formation during mRNA processing

mRNP formation has its starting point during transcription with the nascent RNA (black line). The capping, splicing, packaging by mRNA binding proteins and the cleavage and polyadenylation process contribute to the formation of a mature mRNP in the nucleus. All processes are highly coupled, and are mostly cotranscriptionally to ensure a highly efficient gene expression.

1.1.3 mRNP formation and nuclear export

Many proteins are bound co-transcriptionally and post-transcriptionally during the transcription and processing of a mature mRNA (Figure 3). After leaving the transcription site, a new set of RBP interacts with the mRNA to build a transport competent mRNP. These travel through the interchromatin region most likely undergoing further maturation steps to be able to interact with the nuclear pore. After leaving the pore, the matured mRNPs can be translated in the cytoplasm (Bjork and Wieslander *et al.* 2017).

In yeast the nuclear pore complex (NPC) is around 66 MDa (Rout *et al.* 1993) while in human cells it can even be 124 MDa (Reichelt *et al.* 1990). NPC is a huge multimeric protein complex of approximately 30 proteins called nucleoporins (Nups). Half of all Nups contain solenoid protein domains while the other half is mostly intrinsically disordered (Denning *et al.* 2003). These intrinsically disordered proteins (IDP) are important and forming the with their FG repeats (Phe-Gly) (Peters *et al.* 2006) the channel of the nuclear pore. They serve as mRNA export and other transport proteins. (Oeffinger *et al.* 2012)

The structure of the NPC is comprised of eight spokes, which form a central channel. The NPC can be divided into three segments: the nuclear face with the basket, the central channel, and the cytoplasmic face with the fibrils. The whole diameter of a nuclear pore from vertebrates is about 120 nm, and diameter of the channel is 5.2 nm in humans (Mohr *et al.* 2009) and 10.7 nm in *xenopus laevis* respectively (Keminer *et al.* 1999).

Mature mRNPs are too big to diffuse through the pore (limit for small particle is 60 kDa). For this export, the heterodimer Mex67-Mtr2 is essential (Santos-Rosa *et al.* 1998). Its function is highly

conserved from yeast (Mex67-Mtr2) to humans (NXF1-NXT1) (Strasser *et al.* 2002) that a lethal knockout of Mex67-Mtr2 in yeast can be rescued with the human homologue (Katahira *et al.* 1999). The binding of the export dimer to RNA is exceptionally low (Katahira *et al.* 1999, Strasser and Hurt *et al.* 2000). With the help of so-called export adapters (see 1.5), the affinity to mRNA is increased and Mex67-Mtr2 shuttles its substrates through the nuclear pore driven by the interaction of Mex67 with the FG repeats of the pore channel. (Katahira *et al.* 1999, Strasser *et al.* 2000, Hobeika *et al.* 2009).

To keep the mRNA on the cytoplasmic side, an ATP-dependent DEAD box helicase Dbp5 removes the RBPs from the mRNA. Dbp5 travels with the mature mRNP but can only be activated by Nup Gle1 (outside of nucleus via hCG1 binding to NPC, Strahm *et al.* 1999) and Inositol hexakisphosphate (IP6). The remodeling of the mRNP by Dbp5 (Tran *et al.* 2007, Noble *et al.* 2011, Alcázar-Román *et al.* 2006) leads to the release of several proteins from RNA exports like Nab2 and Mex67 (Lund and Guthrie 2005 and Tran *et al.* 2007), and the mRNA is further released into the cytoplasm for further translation into proteins.

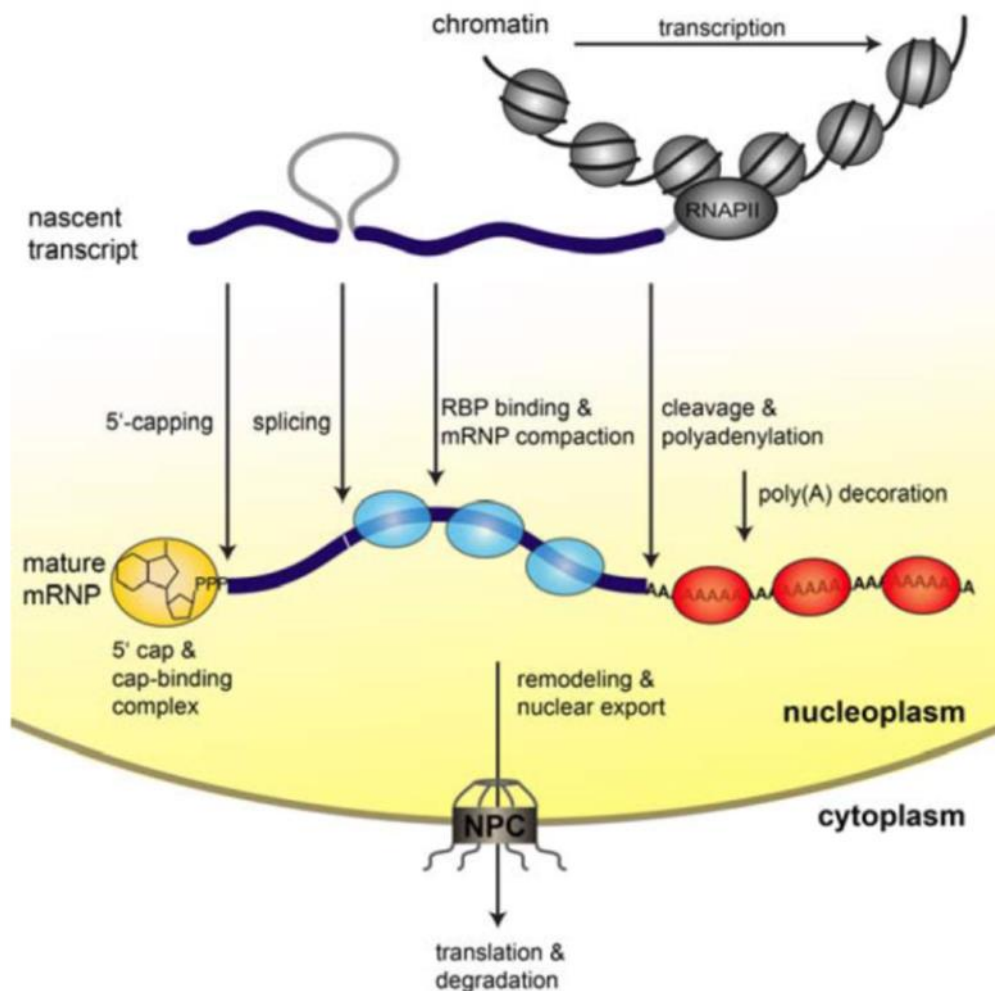


Figure 4. Steps of mRNP biogenesis

The nascent mRNA transcribed by RNA Polymerase II (RNAPII) undergoes various processing events such as capping at the 5' end, removal of introns (splicing), cleavage and polyadenylation at the 3' end. It is also bound by many RNA binding proteins, which followed by various remodeling events, leads to the formation of a matured messenger ribonucleoprotein particle (mRNP). This mRNP is finally exported from the nucleus to the cytoplasm for translation (Meinel and Strasser 2015).

1.1.4 Coupling of transcription, mRNP formation and mRNA export

All steps involved in gene expression (Figure 1) are tightly coupled and controlled by a huge number of proteins. Many processes like capping and slicing happen co-transcriptionally. The TREX complex play an important role in coupling transcription and export. By providing three different recruitment platforms at the level of transcription the cell can put all the key players in such proximity and allow the process to function. These platforms are the CTD of RNAPII, the RNA and the Spt5-CTR.

1.1.4.1 CTD of RNA polymerase II

RNAPII is the most important multi enzyme complex in transcription. Rbp1 and its largest subunit, has a very long extended C-terminal domain (CTD) which consists of unstructured heptad-repeats, with a consensus sequence of YSPTSPS. In yeast there are 26 of these repeats and in human 52 (Zhang *et al.* 2012). Not all the repeats are equally important for the viability of the cell, but yeast needs a minimum of eight repeats to survive (West and Corden 1995).

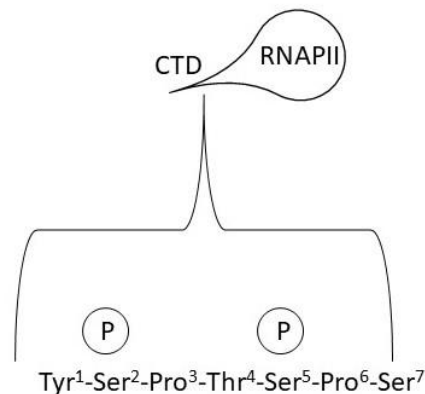


Figure 5. Schema of the Rbp1 CTD repeats

The CTD of Rbp1, largest subunit of RNAPII consists of heptapeptide repeats of the consensus sequence YSPTSPS. The phosphorylated, and these phosphorylation-dephosphorylation patterns among these residues except for proline, provide a fine platform for the recruitment of various mRNA binding proteins and mRNP biogenesis factors at the site of transcription.

The most prominent modification of the CTD is phosphorylation, which serves as a recruitment platform for proteins involved in the transcription cycle. Transcription initiation is marked by phosphorylation of Ser5. In yeast, this is achieved by Kin28 or Srb10, and in higher eukaryotes, the cyclin-dependent kinases 7 and 8 (Zhang *et al.* 2012). Two other proteins like Set, which trimethylates H3K4 histone, is involved in early chromatin remodelling, and the capping enzyme complex subunit Ceg1 (in yeast), a guanylyltransferase, can directly interact with Ser5 phosphorylation. (Cho *et al.* 1997). Even in higher eukaryotes, the capping enzyme interacts with ser5 phosphorylation of CTD for its recruitment (Fabrega 2003 *et al.* and Ghosh *et al.* 2011).

Pull down experiments in yeast reveal the interaction of Ser5 phosphorylated CTD with the spliceosome complex and in higher eukaryotes, several splicing intermediates were found claiming a significant role CTD in co-transcriptional splicing (Harlen *et al.* 2016, Harlen and Churchman 2017). So far, the main role of Ser7 phosphorylation is unknown but it is known to be phosphorylated by Kin28 in yeast and higher humans during transcription initiation, and in humans, processing of snRNA genes (Egloff *et al.* 2012).

During the elongation phase the phosphorylation pattern at the Rbp1-CTD is changed. While levels of Ser5 phosphorylation continuously decrease, an increase in Ser2 phosphorylation is observed. The Bur1 Kinase (human Cdc9) is recruited by phosphorylated Ser5 carry out initial Ser2 phosphorylation (Qiu *et al.* 2009). Bur1 kinase is also able to phosphorylate Ser7 (Tietjen *et al.* 2010, Bataille *et al.* 2012). The phosphorylated Ser2 (Ser2P) is now able to recruit the Ctk1 kinase complex (human Cdk12), which is the major Ser2 kinase, to propagate its own Ser2 phosphorylation state (Cho *et al.* 2001).

Simultaneously, the removal of the phosphate at Ser 5 in yeast is achieved by the phosphatase Rtr1 and Ssu72 to a basal level (Krishnamurthy *et al.* 2004, Mosley *et al.* 2009, Kim *et al.* 2009, Bataille *et al.* 2012). The Ser2 phosphorylation of the RNAPII CTD plays a pivotal role in various processes like chromatin remodelling and termination, and mRNA processing. In yeast, the protein Prp40, a protein involved in splicing, is recruited to CTD hyper phosphorylated repeats (Morris *et al.* 2000). To mammalian phosphorylated CTP binds the splicing protein U2AF65 which increases the recruitment of Prp19C and itself to activate the splicing process (David *et al.* 2011). Another prominent binder of Ser2P is Npl3 (see 1.4), an RNA binding protein involved in elongation, termination, 3' prime end processing and export (Zhang *et al.* 2012). The cleavage and poly adenylation complex which marks the termination of the transcription cycle is recruited to Ser2P. Yeast Pcf1, a component of the cleavage factor IA binds to Ser2P. The Ser2P also bind to Rtt103, another protein involved in the termination of transcription (Harlen and Churchmann. 2017). Tyr1 phosphorylation is detected during elongation and its role is to block termination factors Pcf1 and Rtt103 from interacting with the mRNA at the poly (A) site. This explains why close to the termination site, Tyr 1 is dephosphorylated (Mayer *et al.* 2012). In the early phase of termination when RNAPII reaches the poly (A) side of the gene body, the level of phosphorylated Thr4 of the CTD increases. The phosphorylated Thr4 interacts with termination factor Rtt103. It is suggested that phosphorylation of Ser2 and Thr4 by interacting with Rtt103 controls the transition from elongation to termination. (Harlen *et al.* 2016). The CTD phosphorylation pattern during the transcription cycle is shown in Table 1.

Table 1. The level of CTD modifications through the transcription cycle

modification	Initiation level	Elongation level	Termination level
phosphorylated Ser2	0	+	--
phosphorylated Ser5	+	--	0
phosphorylated Ser7	+	-	0
phosphorylated Tyr1	0	+	-
phosphorylated Thr4	0	0	+

0 = no change (+) + = (strong) increase (-) - = (strong) decrease. Table 1 point out that the dephosphorylation of Ser5 is stronger as for Ser7 and therefore the basal level of Ser5 is lower compared to Ser7.

1.1.4.2 RNA as recruitment platform

Nascent RNA provides by its sequence, the platform for various RBPs involved in mRNP biogenesis like Nab2 which binds only to A-rich motifs. Other proteins that bind directly to RNA are involved in the 3' end processing and recognise certain motifs like the positioning element or the efficiency element (Mandel *et al.* 2008). The SR-like proteins Gbp2 and Hrb1 which are part of the TREX complex binding highly specific to degenerated RNA sequence motifs.

Apart from protein/RNA interaction RNA/RNA interactions are also observed. During splicing snRNPS promote the interaction of the spliceosome with nascent RNA (with their own RNA component) (Will and Luhrmann 2011 and Meinel and Strasser *et al.* 2015).

1.1.4.3 Spt5 an adapter and important elongation factor

The general elongation factor Spt5 was shown to bind to RNAPII (Klein *et al.* 2011, Martinez-Rucobo *et al.* 2011). It is a part of the highly conserved Spt4-Spt5 complex and can be found in all three kingdoms (Werner *et al.* 2011). In humans this complex affects transcription elongation (Hartzog *et al.* 2013). Spt5 has been identified as a recruitment platform for various processing and transcription factors. Co-purification of Spt5 in yeast analysed by mass spectrometry revealed possible interaction with many proteins involved in mRNP biogenesis. (Lindstrom *et al.* 2003). Similar to the RNAPII CTD, Spt5 has a C-terminal region (CTR) with sequence repetitive motifs that can be phosphorylated by Bur1 kinase in yeast and the P-TEFb in human (Liu *et al.* 2009, Yamada *et al.* 2006 and Zhou *et al.* 2009). During transcription elongation, Bur1 kinase phosphorylates the Ser1 of the Spt5 CTR, which in yeast consists of 16 hexa-repeats. Among famous Spt5 CTR binders are Cleavage Factor I (CFI) (Mayer, Schreieck *et al.* 2012b) and the Paf1 complex (Jaehning 2010). This multi enzyme complex is linked to several processes like chromatin remodelling and 3' end processing. It can only bind to a specific pattern at the Spt5-CTR (Qiu *et al.* 2012a). Another modification pattern is the interaction with the capping enzyme (Lidschreiber *et al.* 2013). Yeast cells without Spt5-CTR are sensitive to 6-azauracil (6AU) (Mayer, Schreieck *et al.* 2012b). Therefore Spt5-CTR can be called an important recruitment platform.

1.2 THO/ TREX complex

For the co-transcriptional formation of nuclear mRNPs another multi enzyme complex called *TREX* was found, coupling transcription to export and promote transcription elongation (Strasser *et al.* 2002).

The hetero pentameric THO complex (consist of Tho2, Mft1, Hpr1, Thp2 and Tex1), the nuclear mRNA export factors Sub2 and Yra1, and the SR-like proteins Gbp2 and Nab2 are all part of TREX (Hurt *et al.* 2004, Strasser *et al.* 2002).

THO interacts with the phosphorylated CTD (S2 and S2-S5) (Meinel, *et al.* 2013) and the nascent RNA via several subunits to recruit TREX to the transcription site (Abruzzi *et al.* 2004). The pentameric complex was found initially in transcription elongation studies and null mutants of the components have been linked to R-loop formation in yeast (Chávez *et al.* 2000, Chavez *et al.* 2001) and higher eukaryotes (Dominguez-Sanchez *et al.* 2011a). This hybrid formed from backfolding nascent mRNA interacting with the DNA leads to severe damage like replication impairment or single strand breaks in the unbound DNA strand. In the absence of TREX, an increased number of backfolding events have been observed (Huertas and Aguilera 2003, Dominguez-Sanchez *et al.* 2011a) and indicate that the complex helps to pack mRNA into mRNPs.

The TREX components Sub2 (a DEAD-box helicase member) and Yra1, interreact physically and genetically with THO. They form a stable dimer to interact with the mRNP. Yra1 interacts with Mex67 (Strasser and Hurt 2000, Strasser and Hurt 2001 and Strasser *et al.* 2002) therefore bringing the main export dimer in yeast Mex67-Mtr2 to the mRNP. Mutation studies with Sub2 and Yra1 revealed temperature sensitive mutants which show phenotypes like some mutants of THO leading to hyper recombination in cells. An overexpression of Sub2 can rescue the Δ hpr1 phenotype (Jimeno *et al.* 2002).

TREX recruitment is extraordinarily complex as seen with Yra1 which can facilitate interaction depending on its partner with RNA (Yra1 itself) (Meinel *et al.* 2013), mRNP (Sub2, PCf1) (Strasser and Hurt 2001 and Johnson *et al.* 2009), mRNA (Dbp1, H2B and Swd2 (which are ubiquitylated) (Ma *et al.* 2013 and Vitaliano-Prunier *et al.* 2012).

Gbp2 and Hrb1, which belong to the serine-arginine-rich (SR) family of proteins, interact with Ctk1 kinase and are also important for efficient transcription elongation (Hurt *et al.* 2004).

The co-transcriptional recruitment of TREX to the genes in a transcription-dependent manner in *S. cerevisiae* has already been described (Strasser *et al.* 2002, Zenklusen *et al.* 2002).

The function of TREX seems to be conserved in many organisms, indicating physiological importance (Heath *et al.* 2016). In humans, the recruitment of TREX is rather during splicing. ALYREF (ALY), the human homologue of Yra1 interacts with the exon junction complex (EJC) component of eIF4AIII (Gromadzka *et al.* 2016 and Masuda *et al.* 2005).

TREX also interacts with the human PRP19C, which is a splicing complex in *S. cerevisiae*, and therefore PRP19C might recruit TREX to the mRNP in higher eukaryotes (Chanarat *et al.* 2012). In yeast it was demonstrated that the Prp19C is able to ensure full occupancy by binding to TREX in the 3' end of the genes (Chanarat *et al.* 2011). ALY interacts with the human cap binding complex (CBC) to recruit TREX to the 5' end of the mRNA (Cheng *et al.* 2006 and Nojima *et al.* 2007). A new transcriptome wide study revealed that ALY is not only present at the 5' mRNA in a CBC80-dependant manner but also at the 3' of the mRNA in a polyadenylate-binding nuclear protein 1(PABPN1)-dependant manner (Shi *et al.* 2017). Similar to its yeast homolog, Yra1 ALY is a good example for the complex recruitment of TREX in human cells. Interaction with the human homologue of Sub 2 UAP56 brings ALY to the mRNA where it can recruit the export receptor, NXF1-NXT1, the human homologue of Mex67-Mtr2 to the mRNP. There are more adapters known to bring the exporter NXF1-NXT1 to the mRNA (Luo *et al.* 2001; Taniguchi and Ohno 2008) and this includes UIF (Hautbergue *et al.* 2009) or CHTOP which requires ALY UAP56 to load into the mRNA (Chang *et al.* 2013). In yeasts, TREX associated with proteins in an ATP-dependent manner, and in mammalian cells, there are two proteins thus, POLDIP3 and ZC3H11A, which interact with TREX in similar fashion during mRNA export (Folco *et al.* 2012).

Also, in mammalian cells, the connection between chromatin and mRNA export is mediated via the TREX complex. IWS1, a chromatin remodeler, is known to interact with the transcription elongation factor Spt6 (recruited via S2 phosphorylated CTD to transcription machinery) (Yoh *et al.* 2007) and ALY. Decreased levels of ALY at genes and a nuclear export defect can be found in ISW1 depleted cells.

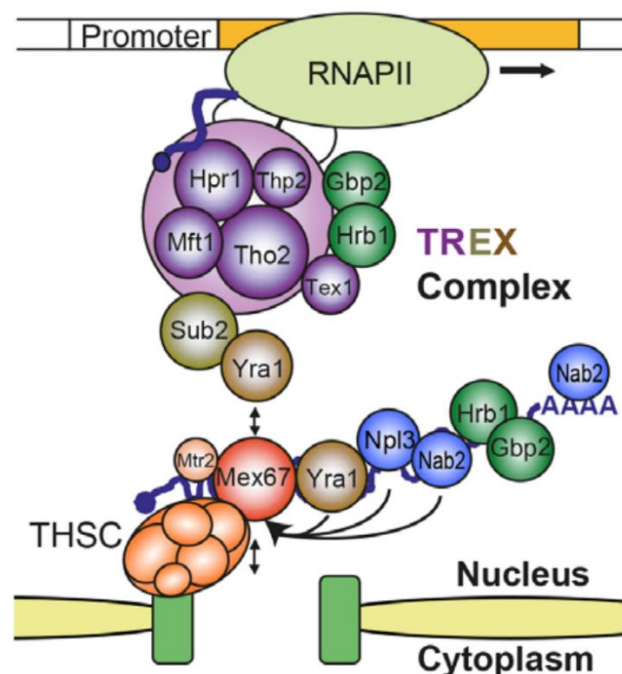


Figure 6. Scheme of TREX function in transcription and mRNA export

TREX binding to RNAPII via interaction of Hpr1 (part of THO in purple) with CTD of Rpb1. Before mRNA can be exported Yra1 interacted with export heterodimer Mex67-Mtr2 and TREX component Hrb1 and Gbp2 are present on mRNA. After interaction with THSC (TREX2) and the NPC the mRNP is released into the cytoplasm (Strasser 2013)

1.3 PAF complex

The PAF complex yeast consist of five proteins namely, Paf1, Cdc73, Ctr9, RTf1 and Leo1 (Krogan *et al.* 2002a, Mueller and Jaehning 2002 and Squazzo *et al.* 2002). By chromatin immunoprecipitation (ChIP) it was shown that PAF complex is located at active open reading frames (ORFs) (Krogan *et al.*, 2002a and Pokholok *et al.* 2002) and physically and genetically interacts with transcription elongation factors like Spt4-Spt5. Apart from phosphorylation of elongation factors, PAF complex was linked with H3 methylation carried out by Set1 or Set2 methyltransferase (Krogan *et al.* 2003a, Krogan *et al.* 2003b and Ng *et al.* 2003). In a pull-down experiment of RNAP II associated proteins, Cdc73, Paf1 and Hpr1 were found (Chang *et al.* 1999). The deletion of Paf1 and Ctr9 have the most severe phenotypes and being like deletions of THO but, in contrast, were not linked to hyper-recombination. A double mutant of Hpr1 and Paf1 is lethal (Chang *et al.* 1999) suggesting a functional relationship between PAF complex and TREX.

1.4 Nab2, Npl3 and SR-Proteins in mammalian cells

Npl3 and Nab2 are RBPs of the SR (serine, arginine)- and SR-like family, respectively. Npl3 as SR-like protein functions in splicing, transcription elongation, 3' end processing and nuclear mRNA export (Bucheli and Buratowski 2005, Dermody *et al.* 2008, Kress *et al.* 2008 and Lee *et al.* 1996). Via direct interaction with the S2 phosphorylated CTD and the mRNA, Npl3 is recruited co-transcriptionally to the mRNA early (Dermody *et al.* 2008 and Meinel *et al.* 2013). The binding and dissociation of Npl3 to mRNA is regulated by phosphorylation. In this cycle, Glc7, a nuclear phosphatase, dephosphorylates Npl3 and binds to RNA to recruit the export complex Mex67-Mtr2 (Gilbert and Guthrie 2004). In the cytoplasm, phosphorylation at one of the eight SR motifs by Sky1 leads to release from the mRNA (Gilbert *et al.* 2001). Npl3 is seen as a component of the mRNP that recruit Mex67-Mtr2 and travels along with the mRNA from the nucleus to the cytoplasm.

Nuclear polyadenylated RNA-binding protein (Nab2) is a serine-rich RNA binding protein that functions in nuclear export, poly (A) tail length control and mRNP assembly (Batisse *et al.* 2009; Green *et al.* 2002; Hector *et al.* 2002). RNA is needed to recruit Nab2 to the transcription site therefore Nab2 interact directly with RNA (Anderson *et al.* 1993 and Meinel *et al.* 2013). Nab2 dimerizes upon binding to RNA (Aibara *et al.* 2017). Yra1 recruitment ubiquitylation of H2B and Swd2 plus the presence of the RNA helicase Dbp2 are necessary for Nab2 recruitment (Ma *et al.* 2013 and Vitaliano-Prunier *et al.* 2012).

Several SR- proteins serve in human cells as adapter for the main export receptor NXF1-NXT1 (Huang *et al.* 2003, Lai and Tarn 2004 and Muller-McNicoll *et al.* 2016).

ALY compete for its NXF1 binding with the two SR-proteins 9G8 and SRSF3 (Huang *et al.* 2003). SRSF3 as the strongest binder of seven SRSF proteins regulates the 3' UTR length opposite to as the function of SRSF7 (Muller-McNicoll *et al.* 2016). Like yeast Npl3, unphosphorylated SR-proteins like ASF/SF2 interact with the NXF1 (Lai and Tarn 2004).

ZC3H14, the human homolog of Nab2 has its function in poly (a) length control conserved from mammals to *drosophila melanogaster* (Kelly *et al.* 2014). It is unknown if ZC3H14 functions in mRNP assembly and nuclear export or not. Nonetheless, various SR-like and SR-proteins play critical roles in mRNP maturation, composition, and mRNA export.

1.5 Mex67-Mtr2 the main mRNA exporter in *S. cerevisiae*

The exporter, Mex67-Mtr2, shuttles the mRNP from the nucleus to the cytoplasm via direct interaction with nuclear pore proteins harbouring TREX2 (THSC) and the mRNA (Segref *et al.* 1997 and Strasser *et al.* 2000). The complex is recruited to mRNA during transcription by various proteins described before. The human homologue is named NXF1-NXT1. Proteins of TREX like Hpr1 and Yra1 or others like Nab2 and Npl3 which recruit the complex to the mRNA are named export adapters (Gilbert and Guthrie 2004, Gwizdek *et al.* 2006, Iglesias *et al.* 2010 and Strasser and Hurt 2000). In mammalian cells, there are many proteins to recruit NXF1-NXT1 to the mRNA for example, THOC5, ALY (both TREX), several SR-proteins, ZC3H3 and CHTOP (Chang *et al.* 2013; Huang *et al.* 2003; Hurt *et al.* 2009; Viphakone *et al.* 2012). The function of the adapters seems to increase the weak binding of Mex67-MTr2/NXF1-NXT1 to RNA. The interaction is regulated via ubiquitylation (Nino *et al.* 2013) and phosphorylation (mentioned 1.2). Yet, it remains unknown if some export adapter is specific for certain mRNPs.

1.6 Sub2 and human UAP56 (DDX39B)

Human UAP56 (has a paralog DDX39) and yeast suppressor of *brr1-1* (Sub2) have been vividly identified in splicing (Fleckner *et al.* 1997 and Noble and Guthrie 1996). Later, it was found that Sub2 is a component of the TREX complex and is therefore involved in mRNP assembly by direct interaction with Yra1/ALY (Strasser and Hurt 2001; Strasser *et al.* 2002). In an ATP-dependent manner, THO interacts with UAP56, ALY and CIP29 (yeast Tho1) (Chi *et al.* 2013 and Kota *et al.* 2008) to form the human TREX complex coupling mRNA processing to export (Zhou *et al.* 2000). The nuclear export function of Sub2 and its orthologue is well conserved and documented for several species like humans (Luo *et al.* 2001), *Drosophila melanogaster* (Gatfield *et al.* 2001 and Ma *et al.* 2013), *S. cerevisiae* (Jensen *et al.* 2001, Strasser *et al.* 2002) and *C. elegans* (MacMorris *et al.* 2003). Additional functions of Sub2 like R-loop prevention (Gaillard *et al.* 2007; Gomez-Gonzalez *et al.* 2011) and RNA transport and storage (Meignin and Davis 2008) have been demonstrated. *In vitro*, yeast and human Sub2 are ATPases and bind ssRNA (Shen *et al.* 2007, Ma *et al.* 2013 and Saguez *et al.* 2013). Their substrate for unwinding is a partial duplex strand of RNA/DNA with a 3' overhang. When ATP is bound, UAP56 forms a complex with ssRNA and ALY or CHTOP or CIP29. The ATPase activity is stimulated by ALY and the helicase activity by CIP29 leading to the abandoning of the complex by UAP56 (Chang *et al.* 2013, Dufu *et al.* 2010 and Taniguchi and Ohno 2008). As a result, ALY binds to NXF1 (Hautbergue *et al.* 2008 and Taniguchi and Ohno 2008). This is similar in yeast where Sub2 dissociates after the ATPase was activated by C-terminal fragment of Yra1 (Ren *et al.* 2017), Apart from unwinding, Sub2 can also displace Mud2 from the mRNA during splicing (Kistler and Guthrie 2001 and Linder and Jankowsky 2011).

1.7 Tho1 and human CIP29

Tho1 is a conserved nuclear RBP when overexpressed in cells, it rescues the phenotype of a Hpr1 deletion (Jimeno *et al.* 2006), comparable to an overexpression of Sub2 which might indicate that both proteins have similar functions. The recruitment of Tho1 to transcribed genes happens in a THO- and RNA- dependent manner (Jimeno *et al.* 2006). The C-terminal part of Tho1 binds strongly to RNA in vitro, and a single SAP (scaffold associated protein) domain in the protein was identified via NMR to be important for the suppression of Hpr1 deletion and binds to double strand DNA in vitro (Jimeno *et al.* 2006). Deletion of Tho1 rescues a temperature sensitive phenotype of the nab2-1 mutant (Jimeno *et al.* 2006). Interestingly, the human CIP29, the orthologue of Tho1, co-purifies with human TREX (Dufu *et al.* 2010). However, in yeasts, no co-purification of Tho1 with TREX is observed. CIP29 is recruited to mRNA in a splicing- and cap-dependent manner (Chi *et al.* 2013). In a yeast two-hybrid system (Y2H) CIP29 binds to the DEAD-box helicases UAP56 (Sub2) and DDX39 in an ATP-dependant manner (Dufu *et al.* 2010 and Leaw *et al.* 2004). Deletion of Tho1 (MOS11) in *arabidopsis thaliana* exhibit nuclear poly (A) accumulation (Germain *et al.* 2010). Therefore, the protein might be necessary for nuclear export, but its function and recruitment must be elucidated.

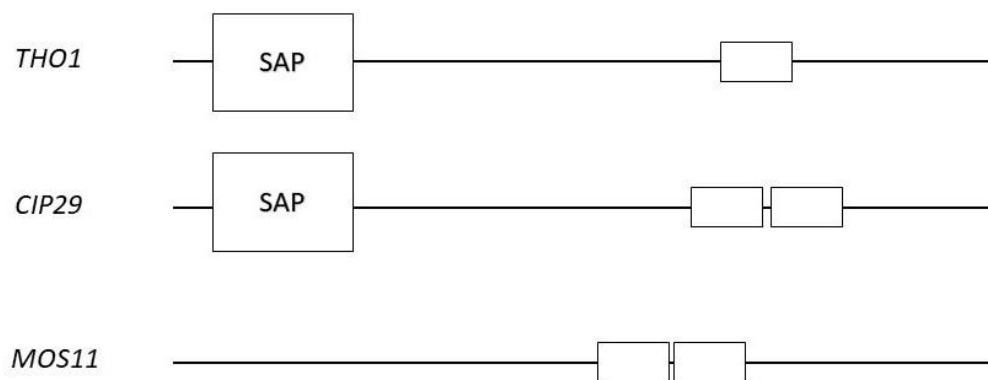


Figure 7. Schematic of domain organization comparison

Domain organization comparison of *S. cerevisiae* Tho1 with human CIP29 and *arabidopsis* MOS11 (based on Jacobsen *et al.* 2016).

1.8 linking miss regulated mRNP assembly to disease

As already explained, mRNP formation is an important step in gene expression and only functional mRNPs can leave the nucleus to be translated in the cytoplasm. The assembly of mRNPs in the nucleus is a multi-step process which can lead to various diseases and cell viability, if this mechanism is interrupted at certain time points (Carey and Wickramasinghe (2018), Corbett (2018), and Heath *et al.* (2016).

A large number of people suffering from various type of cancer developed from dysfunctional mRNP formation. One reason for genomic instability and cancer are R-loops (Aguilera and Garcia-Muse 2012, Dominguez-Sanchez *et al.* 2011, Gomez-Gonzalez *et al.* 2011, Santos-Pereira and Aguilera 2015 and

Huertas and Aguilera 2003). The THO and other mRNP components can prevent this process by binding to the nascent RNA (Castellano-Pozo *et al.* 2013 and Salas-Armenteros *et al.* 2017). On the other hand, R-loop formation can be introduced by the interaction of ORF57, a human gamma herpesvirus 8 (HHV-8), with the human TREX leading to DNA damage and tumorigenesis (Jackson *et al.* 2014).

It is known that cancer cells display dysfunctional mRNA export. ALY, a TREX component, directly interacts with human mRNA exporter NXF1-NXT1. Lung, ovarian and colon cancer cells show an upregulation of THOC1 (Chinnam *et al.* 2014, Dominguez-Sanchez *et al.* 2011b, Guo *et al.* 2005, 2012, Lapek *et al.* 2017, Li *et al.* 2007 and Liu *et al.* 2015) leading to the idea that fast growing tumours need a good mRNP biogenesis. However, another revealed that THOC1 down-regulation was observed in testis and skin cancers (Dominguez-Sanchez *et al.* 2011b). Also, in both types of myeloid leukemia, TREX proteins play an important role. Like the induced up regulation of an ALY adapter LUZP4 which is normally restricted to testis in a arrange of tumours (Viphakone *et al.* 2015). The depletion of UAP56 leads to reduced level of BRCA1 (Yamazaki *et al.* 2010) and CIP29 which is upregulated in leukemia with SARNP (Fukuda *et al.* 2002) is fused with the mixed lineage leukemia (MLL) protein (Hashii *et al.* 2004). Importantly, the proliferation and metastatic capacity of tumour cells can be inhibited by the depletion of ALY (Saito *et al.* 2013), LUZP4 (Viphakone *et al.* 2015) or THOC1 (Guo *et al.* 2005 and Li *et al.* 2005). The findings suggest an important role of TREX and other mRNP components in cancer, hence, could be used as targets in treatment strategies.

Some neurological diseases are connected to misregulation of mRNP assembly (Boehringer and Bowser 2018). The loss of THOC2, a protein which is important for neuronal development, leads to X-linked syndromic intellectual disability (ID) (Kumar *et al.* 2015, 2018). In mice dopaminergic neuronal cells, knockout of THOC5 could be linked to nuclear export defects causing degeneration of neurons (Maeder *et al.* 2018). The misallocation of proteins in the cytoplasm caused by a mutation on THOC6 was observed by patients with ID (Amos *et al.* 2017 and Beaulieu *et al.* 2013). In drosophila, dNab2 is needed for normal neuronal function by interacting with the Fragile X-Protein ortholog (Bienkowski *et al.* 2017 and Kelly *et al.* 2015). Mutation in the human ZC3H14 have been found in patients with non-syndromic form of autosomal recessive ID (Fasken and Corbett 2016). It is still unknown which function of Nab2 causes these ID phenotypes since in yeast, Nab2 functions in RNAP III transcription (Reuter *et al.* 2015).

The most prominent neuronal disease associated with TREX is amyotrophic lateral sclerosis (ALS). This neurodegenerative disease result in muscle atrophy, loss of motor neurons and progressive paralysis. The most common form of ALS (around 20%) is caused by the C9orf72 protein. In its normal form, the protein harbours around 30 copies of a GGGGCC repeat expansion motif. In a mutation state, this number increases to several hundred or thousand copies of this motifs. A G-quadruplex secondary is formed by the interaction of two proteins forming a toxic dipeptide of C9orf72 in the cytoplasm (Walsh *et al.* 2015). The export of the aberrant pre-mRNA from the nucleus is possible because ALY get sequestered by the GGGGCC repeats of the mRNA (Cooper-Knock *et al.* 2014; Hautbergue *et al.* 2017). The mRNP biogenesis and nuclear export might be important in the pathogenesis of ALS since a direct connection between TREX components and Matrin-3, a protein linked to ALS, was discovered. (Boehringer *et al.* 2017). The GGGGCC repeat expansion of C9orf72 was tested recently as the target for a small molecule drug (Simone *et al.* 2018).

1.9 Aim of this study

The Tho1 protein was discovered along with Tho2, one major component of the THO complex and an important part of TREX complex in yeast. Overexpression of Tho2 and Tho1 was able to suppress the deletion of Hpr1 in yeast. Moreover, only Δ tho2 shows a similar phenotype as Δ hpr1 (Piruat *et al.* 1998) indicating that Tho2 and Hpr1 have similar functions. Therefore, further investigations were done to define the role of Tho2 in the THO/TREX complex (Strasser *et al.* 2002). The recruitment of Tho1 to transcribed genes happens in a THO- and RNA- dependent manner, which has been described in yeast (Jimeno *et al.* 2006). Furthermore, the homolog, CIP29, interacts with the human TREX complex in an ATP-dependant manner (Dufu *et al.* 2010). Dominik Meinerl could show in his PhD thesis via metagenome analysis that Tho1 expression correlates more with the TREX components, Hpr1 and Yra1, as with the RNAP II (Rbp3). Interestingly, a mutation of the Spt5-CTR (S1A) leads to opposite correlation between the Tho1 occupancy (decrease) and TREX component Hpr1 (increase) in Chip analyses. Here, Tho1 shows similar changes in the occupancy levels as Paf1 (decrease), a component of the PAF complex. Overexpression of a plasmid with Tho1 lead to decreased levels of Hp1 and Sub2 but had no effect on Yra1 levels. These previous findings placing Tho1 in a “Y-relationship” (Figure 8).

Therefore, it is not yet clear which role Tho1 plays in transcription and mRNP biogenesis. Does it work together with TREX? Can Tho1 itself provide additional ways by interacting with Yra1, Mex67 or the PAF complex to support mRNP biogenesis?

To answer these questions, ChIP experiments have been performed to elucidate the interactions between Tho1, Spt5 and the TREX / PAF complex in yeast.

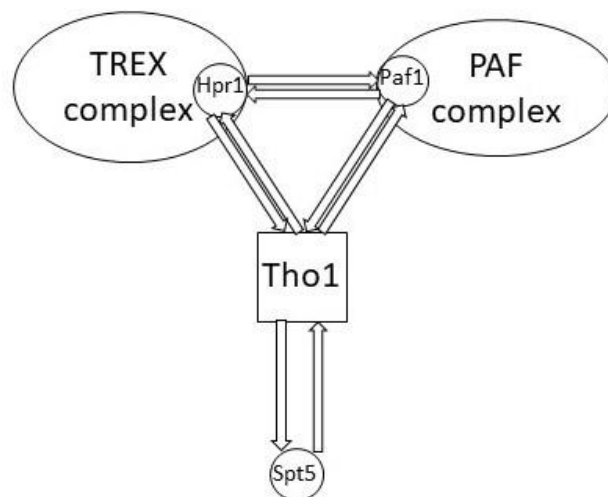


Figure 8. Schematic view of interaction (Y-relationship) between Tho1 and TREX / PAF complex
 CHIP experiments with Paf1(PAF complex), Hpr1(TREX), Spt5 and Tho1 are carried out to elucidate their interaction pattern and understanding the hierarchy in yeast during transcription.

The second part of the thesis focus more on the actual appearance of a single mRNP. Many diseases like neurodegenerative diseases and cancer are linked to defective nuclear packaging and export of mRNPs. Although nearly all RBPs in yeast are known, only partial structures are available. Furthermore, it is unclear how a specific nuclear mRNP looks like. The word specific describes here multiply identical copies of one single mRNA covered by all RBPs forming the nuclear mRNP.

Purification of Nab2-TAP protein revealed a correlation between the length of the mRNA and the particle size of the mRNP (Batisse *et al.* 2009). This study aims at purifying a specific nuclear mRNP from yeast. Nab2-TAP was not used for the purification; however, Cbc2-TAP was used to concentrate all nuclear mRNP. Downstream to select single specific mRNP, the principle of purification with anti-sense oligo nucleotide was used (2.2.2.9).

The first goal is the successful purification of a specific nuclear mRNP from yeast. The effect of different buffer compositions, incubation temperatures, centrifugation speed, ATP analogues, etc were investigated. Additionally, the effect of cross-linked cells vs non cross-linked cells for mRNP purification were analysed.

The second one is to establish a quality control pipeline to evaluate changes of the mRNP purification protocol. The target mRNP consist of the mRNA and the RBPs. The proteins have been detected on western blot while the mRNA has been quantified after reverse transcription with qPCR. The native elution of the purification was analysed under the TEM to screen for correct assembled nuclear mRNPs.

2 Materials and Methods

2.1 Materials

2.1.1 Consumables and Chemicals

Consumables and chemicals were purchased from the following companies: Applichem GmbH (Darmstadt, Germany), Applied Biosciences (Darmstadt, Germany), Fermentas (St. Leon- Rot, Germany), Bio-Rad (Hercules, USA), Eppendorf (Hamburg, Germany), Fermentas (St. LeonRot, Germany), GE Healthcare Europe (Freiburg, Germany), Invitrogen (Karlsruhe, Germany), Life Technologies (Carlsbad, USA), Macherey&Nagel (Düren, Germany), Millipore (Molsheim, France), Mobitec (Göttingen, Germany), Beckman Coulter (Krefeld, Germany), Open Biosystems (Huntsville, USA), Promega (Mannheim, Germany), Qiagen (Hilden, Germany), Roche (Mannheim, Germany), Sarstedt (Nümbrecht, Germany), Sigma (Taufkirchen, Germany), Thermo Scientific (Munich, Germany), Biozym (Hess. Oldendorf, Germany), Carl Roth (Karlsruhe, Germany), Diagenode (Liege, Belgium), Formedium (Norwich, UK), Fujifilm Corporation (Tokyo, Japan), Gilson (Bad Camberg, Germany), Hartmann Analytic GmbH (Braunschweig, Germany), Jena Bioscience GmbH (Jena, Germany), MembraPure (Bodenheim, Germany), Merck Biosciences (Darmstadt, Germany), NEB (Frankfurt, Germany), Neolab (Heidelberg, Germany), Stratagene (Amsterdam, Netherlands), VWR (Ismaning, Germany), Axon (Kaiserslautern, Germany), Biomol (Hamburg, Germany), Biorad (Munich, Germany), Chemicon (Temecula, Canada), MP Biomedical (Illkirch, France), Santa Cruz (Santa Cruz, USA), PSL (Heidelberg, Germany) and Serva (Heidelberg, Germany).

2.1.2 Equipment

Table 2. Equipment

Name	Supplier
Avanti JXN-26, JLA-8.1 Rotor	Beckman Coulter (Krefeld, Germany)
Beckman DU650 spectrophotometer	Beckman Coulter (Krefeld, Germany)
Beckman J2-HS, JA-20 Rotor	Beckman Coulter (Krefeld, Germany)
Beckman J6-HC, JS-4.2 Rotor	Beckman Coulter (Krefeld, Germany)
BIO-LINK 254	Vilber (Eberhardzell, Germany)
Bioruptor UCD-200 Diagenode	Diagenode SA (belgium)
ChemoCam Imager ECL HR 16-3200	Intas, (Göttingen, Germany)
CME microscope	Leica (Buffalo, USA)
CO8000 Cell Density Meter	WPA (Cambridge, UK)
Electrophoresis Power Supply Consort E835	Neolab (Heidelberg, Germany)
Eppendorf centrifuge FA-45-24-11 5424/5424R	Eppendorf (Hamburg, Germany)
Freezer/Mill™ 6870D	SPEX™ SamplePrep (Metuchen, USA)
Gel iX20	Intas, (Göttingen, Germany)
Heating oven	BINDER GmbH (Tuttlingen, Germany)
Heidolph Duomax 1030	Heidolph Instruments GmbH & Co. KG (Schwabach, Germany)
Incubator shaker ISF-1-V	Adolf Kühner AG (Basel, Switzerland)
Innova 44 shaking incubator	New Brunswick Scientific (Nürtingen, Germany)
L80 Ultracentrifuge	Beckman Coulter (Krefeld, Germany)
Megafuge 40R, 75003180 Rotor	Thermo Scientific (Munich, Germany)
Mini-Protean II system, Mini TransBlot Cell	Bio-Rad Laboratories (Hercules, USA)

MP Biomedicals™ FastPrep-24™ 5G Instrument	Thermo Scientific (Munich, Germany)
Optima™ L-90 K and L80 ultracentrifuge	Beckman Coulter (Krefeld, Germany)
Pipetboy acu	INTEGRA Biosciences AG (Zizers, Switzerland)
Planetary Mono Mill Pulverisette 6	Fritsch (Idar-Oberstein, Germany)
QuantStudio 3 Real-Time PCR System	Thermo Scientific (Munich, Germany)
Research Pipettes P2, P20, P200 P1000	Gilson (Bad Camberg, Germany)
Sonifier 250	Branson (Danbury, USA)
Spectrophotometer ND-1000	Thermo Scientific (Munich, Germany)
StepOnePlus™ Real Time PCR System	Thermo Scientific (Munich, Germany)
T3 Thermocycler	Biometra (Göttingen, Germany)
Thermomixer compact	Eppendorf (Hamburg, Germany)
Type 70 Ti Rotors	Beckman Coulter (Krefeld, Germany)
Universal Analytical Balance	Satorius (Göttingen, Germany)
VARI-X-LINK UV CROSS-LINKER	VARI-X-LINK (England)
Vortex Genie	Neolab (Heidelberg, Germany)

2.1.3 Yeast and *e.Coli* strains

Table 3. yeast strains

Strain name	Strain background	number	Genotype	Reference
RS453 wt	RS453	Y1	MAT a; ade2-1; his3-11,15; ura3-52; leu2-3,112; trp1-1; can1-100; GAL+	(Strasser and Hurt 2000)
W303 wt	W303	Y8	MAT a; ade2-1; his3-11, 15; ura3-1; leu2-3, 112; trp1-1; can1-100; rad5- 535	(Thomas and Rothstein 1989)
BY4741 wt	BY4741	Y2657	MAT a; his3Δ1; leu2Δ0; met15Δ0; ura3Δ0	Euroscarf
MEX67 shuffle	RS453	Y13	MAT a; MEX67-TAP::HIS3; ade2-1 ; ura3-52; leu2-3,112; trp1-1; can1-100; GAL+	Segref et al. 1997
HPR1-TAP	RS453	Y46	MAT a; HPR1-TAP::TRP1; ade2-1; his3-11,15; ura3-52; leu2-3,112; trp1- 1; can1-100; GAL+	(Strasser and Hurt 2000)
PAF1-TAP	RS453	Y432	MAT a; PAF1-TAP::TRP1; ade2-1; his3-11,15; ura3-52; leu2-3,112; trp1- 1; can1-100; GAL+	Wrong strain redone
SPT5 - TAP	RS453	Y533	MAT a; SPT5-TAP::TRP1; ade2-1; his3-11,15; ura3-52; leu2-3,112; trp1- 1; can1-100; GAL+	This study
RIX1-TAP	RS453	Y616	MAT α; RIX1-TAP::TRP1; ade2-1; his3-11,15; ura3-52; leu2-3,112; trp1- 1; can1-100; GAL+	Strässser Lab by Y. Kraus 2005
HPR1-TAP Mex67 shuffle	RS453	Y831	MAT α; MEX67-TAP::HIS3; HPR1-TAP::TRP1; ade2-1 ; ura3-52; leu2-3,112; can1-100; GAL+	Strässser Lab by S. German 2006
SUB2-GFP	RS453	Y1002	Mat a;SUB2-yeGFP::klTRP1 ade2-1; his3-11,15; ura3-52; leu2-3,112;can1-100; GAL+	Strässser Lab by K. Sträßer 2007
SPT5 shuffle PAF1-TAP	BY4741	Y2367	MAT a; shSPT5::HIS3; PAF1-TAP::URA3; leu2Δ0; met15Δ0;	Reference for new PAF1-TAP This study

PAF1-TAP	RS453	Y2751	PAF1-CBP-TEV-protA::TRP1;MAT a; ade2-1; his3-11,15; ura3-52; leu2-3,112;trp1-1 can1-100; GAL+	This study
Δ ilv5	BY4741	Y2757	Mat a/ α ; his3 Δ 1/his3 Δ 1;leu2 Δ 0/leu2 Δ 0;lys2 Δ 0/LYS2;MET15/ met15 Δ 0;ura3 Δ 0; YLR355c::kanMX4/YLR355c	Euroscarf
Δ ccw12	BY4741	Y2758	Mat a/ α ; his3 Δ 1/his3 Δ 1;leu2 Δ 0/leu2 Δ 0;lys2 Δ 0/LYS2;MET15/ met15 Δ 0;ura3 Δ 0; YLR110c::kanMX4/YLR110c	Euroscarf
Δ ccw12 + pRS314-CCW12	RS453	Y3238	MATa; ura3 Δ 0; leu2 Δ 0; his3 Δ 1; met15 Δ 0; YLR110c::kanMX4 + pRS314-CCW12	This study
Δ ilv5+ pRS314-ILV5	RS453	Y3239	MATa/MAT α ; ura3 Δ 0/ura3 Δ 0; leu2 Δ 0/leu2 Δ 0; his3 Δ 1/his3 Δ 1; met15 Δ 0/MET15; LYS2/lys2 Δ 0; YLR355c/YLR355c::kanMX4; pRS314-ILV5	This study

Table 4. *e. coli* strains

Strain	Genotype	Reference
<i>Escherichia coli</i> DH5 α	F - endA1 glnV44 thi-1 recA1 relA1 gyrA96 deoR nupG Φ 80dlacZ Δ M15 Δ (lacZYAargF) U169 hsdR17(rK - mK +) λ -	Woodcock et al. (1989)
<i>Escherichia coli</i> Rosetta TM (DE3) pLysS	F - ompT hsdSB(rB - mB -) gal dcm (DE3) pLysSRARE2 (CamR)	Novagen®

2.1.4 Plasmids

Table 5. plasmids used

Plasmid	Number	Description	Reference
pUN100	3	YC-type shuttle vector useful for the sectoring-shuffle mutagenesis assay	ATCC® 77270 TM
pRS426	12	pRS426 a yeast episomal vector with a URA3 marker derived from pBLUESCRIPT II plasmid with 20 copies per cell	(Sikorski and Hieter 1989)
pBS1479	84	Trp1 TAP tag amp integration cassette C terminal TAB	Puig <i>et al.</i> 2001
pBS1539	85	Ura1 TAP tag amp integration cassette C terminal TAB	Puig <i>et al.</i> 2001
pUN100-MEX67	142	pUN100 with MEX67 for shuffle mutagenesis assay	Segref <i>et al.</i> 1997
pUN100-mex67-5	152	pUN100 with mex67-5 for shuffle mutagenesis assay	Segref <i>et al.</i> 1997
pRS426-THO1	452	pRS426 with genomic THO1 app. 500 bp upstream and downstream, a sequence was	Meinel (Dissertation 2013)

		added to the 3' end of THO1 just before the stop codon, encoding an 6x HA-tag	
pBS1479	1330	His3 TAP tag amp integration cassette C terminal TAB	Puig <i>et al.</i> 2001
pBS1479	1332	Leu2 TAP tag amp integration cassette C terminal TAB	Puig <i>et al.</i> 2001
pRS316-CCW12		CCW12 was integrated in pRS316 for mRNA quantification	This study

2.1.5 Oligonucleotide sequences

Table 6. Oligonucleotides for genomic tagging

Name	Sequence (5'-3')
Hpr1-TAP fw	ATGCAGCTACTTCGAACATTTCTAATGGTTCATCTACCCAAGATATGAAA tccatgaaaagagaag
Hpr1-TAP rev	TAAAATCTATCTGAATTGTTTGGGACACTATGCATGAATTTCTTATCAGT tacgactcactataggg
Paf1-TAP fw	ACTGAACAAAAACCAGAGGAAGAAAAGGAACTTTACAAGAAGAA tccatgaaaagagaag
Paf1-TAP rev	AAGAACTACAGGTTTAAAATCAATCTCCCTTCACTTCTCAATATTCTA tacgactcactataggg
Tho1-TAP fw	AGAGTAAGTAAAAACAGGAGAGGCAACCGCTCTGGTTACAGAAGA tccatgaaaagagaag
Tho1-TAP rw	CCGAACTAGAAATGAAAACTCCACCAAACGGCTTGAGCCTTTA tccatgaaaagagaag

Table 7. Oligonucleotides for qPCR

Name	Sequence (5'-3')
YER fw	TGCGTACAAAAAGTGTCAAGAGATT
YER rv	ATGCGCAAGAAGGTGCCTAT
ADH1-5' fw	GTTGTTCGGCATGGGTGAAA
ADH1-5' rv	GGCGTAGTCACCGATCTTCC
ADH1-M fw	AGCCGCTCACATTCCTCAAG
ADH1-M rv	ACGGTGATACCAGCACACAAGA
ADH1-3' fw	TTGGACTTCTTCGCCAGAGG
ADH1-3' rv	GCCGACAACCTTGATTGGAG
CCW12-5' fw	ACTGTTCGCTTCTATCGCCGC
CCW12-5' rv	TTGGCTGACAGTAGCAGTGG
CCW12-M fw	CTGTCTCCCCAGCTTTGGTT
CCW12-M rv	GGCACCAGGTGGTGTATTGA
CCW12-3' fw	TGAAGCTCAAAGAACACCACC
CCW12-3' rv	AGCAGCAGCACCAGTGTAAG
ILV5-5' fw	AAGAGAACCTTTGCTTTGGC
ILV5-5' rv	TTGGCTTAACGAAACGGGCA

<i>ILV5</i> -M fw	TGCCGCTCAATCAGAAACCT
<i>ILV5</i> -M rv	GGGAGAAACCGTGGGAGAAG
<i>ILV5</i> -3' fw	TGGTACCCAATCTTCAAGAATGC
<i>ILV5</i> -3' rv	ACCGTTCTTGGTAGATTCGTACA
<i>PGK1</i> -5' fw	TTGCCAACCATCAAGTACGTTT
<i>PGK1</i> -5' rv	CCCAAGTGAGAAGCCAAGACA
<i>PGK1</i> -M fw	GGTAAGGCTTTGGAGAACCCAAC
<i>PGK1</i> -M rv	CGACCTTGTCCAACAAGTTGTC
<i>PGK1</i> -3' fw	TGACAAGATCTCCCATGTCTCTACTG
<i>PGK1</i> -3' rv	TGGCAATTCCTTACCTTCCAA
<i>PMA1</i> -5' fw	GTTTTTCGTCGGTCCAATTCA
<i>PMA1</i> -5' rv	AACCGGCAGCCAAAATAGC
<i>PMA1</i> -M fw	AAATCTTGGGTGTTATGCCATGT
<i>PMA1</i> -M rv	CCAAGTGTCTAGCTTCGCTAACAG
<i>PMA1</i> -3' fw	CAGAGCTGCTGGTCCATTCTG
<i>PMA1</i> -3' rv	GAAGACGGCACCAGCCAAT

Table 8. anti-sense oligonucleotides for mRNP purification

Name	Sequence (5'-3')
<i>CCW12</i> 1	gtgtttaagcgaatgacaga
<i>CCW12</i> 2	tagcagtggtaacgtagca
<i>CCW12</i> 3	aaagctggggagacagtttc
<i>CCW12</i> 4	ttggggcttcagtggtcaat
<i>CCW12</i> 5	gacagagtgagttggagcag
<i>CCW12</i> 6	tacaacaacaaagcagcggc
<i>CCW12</i> 7	taaaaaattagaatgtataaataataaaac
<i>CCW12</i> 8	gttaaatgccaaaaagttataaaaaatt
<i>ILV5</i> 1	ataactcctaggaataggtt
<i>ILV5</i> 2	gggagttgcagatcaatctg
<i>ILV5</i> 3	tggcttaacgaaacgggcag
<i>ILV5</i> 4	cttttctctggccagtcag
<i>ILV5</i> 5	gaaccaaccgtcttcgatg
<i>ILV5</i> 6	attgagcggcatcggacaac
<i>ILV5</i> 7	atctgacagttctaccggaa
<i>ILV5</i> 8	aacctcttcaccgtacaag
<i>ILV5</i> 9	agcatcgtacatgtaatcca
<i>ILV5</i> 10	ttctagcttttctctgtagt
<i>ILV5</i> 11	ttattggtttctggtctca
<i>ILV5</i> 12	gactatgacttgatgttgca
<i>ILV5</i> 13	aaaacagggcttcctagtgt

2.1.6 Growth media, Buffers and solutions

2.1.6.1 Growth Media

Table 9. Composition of growth media

Name	Composition
Yeast full medium (YPD)	2% (w/v) peptone; 2% (w/v) glucose; 1% (w/v) yeast extract; (2% (w/v) agar added for petri plates)
Yeast full medium (YPG)	2% (w/v) peptone; 2% (w/v) galactose; 1% (w/v) yeast extract; (2% (w/v) agar added for petri plates)

Luria-Bertani Broth (LB)	1% (w/v) tryptone; 0.5% (w/v) yeast extract; 0.5% (w/v) NaCl; (2% (w/v) agar added for petri plates)
Synthetic complete dropout medium (SDC)	0.67% (w/v) yeast nitrogen base; 0.06% (w/v) complete synthetic mix of amino acids; drop out as required; 2% (w/v) glucose; when required 0.1% (w/v) 5-FOA was added; (2% (w/v) agar added for petri plates)

2.1.6.2 Buffers and solutions

All the standard buffers and their compositions are listed below. Buffers related to some specific experiments are listed along with their protocols (in 'Methods' section).

Table 10. Buffers and solutions

Name	Composition
100x Protease inhibitors cocktail	8 ng/ml Leupeptin; 137 ng/ml Pepstatin A; 17 ng/ml PMSF; 0.33 mg/ml Benzamidine; dissolved in 100% EtOH (p.a.)
10x KNOP buffer	500 mM Tris-HCl (pH 9.2); 160 mM (NH ₄) ₂ SO ₄ ; 22.5 mM MgCl ₂
10x Phosphate-buffered saline (PBS) buffer	1.37 M NaCl; 27 mM KCl; 20 mM KH ₂ PO ₄ ; 10 mM Na ₂ HPO ₄ · 2 H ₂ O
10x TBE electrophoresis buffer	1 M Tris base; 1 M boric acid; 0.02 M EDTA (disodium salt)
10x TE buffer	100 mM Tris-HCl; 10 mM EDTA, pH 7.5
10x Tris-buffered saline (TBS) buffer	1.37 M NaCl; 27 mM KCl; 125 mM Tris-HCl, pH 7.4
1x High Salt FA Lysis Buffer (ChIP)	50 mM HEPES-KOH pH to 7.5; 0.5 M NaCl; 1 mM EDTA; 1% Triton X-100; 0.1% sodium deoxycholate
1x Low Salt FA Lysis Buffer (ChIP)	50 mM HEPES-KOH pH to 7.5; 150 mM NaCl; 1 mM EDTA; 1% Triton X-100; 0.1% sodium deoxycholate; 0.1% SDS
1x SDS-PAGE Running Buffer	25 mM Tris, 0.1% (w/v) SDS, 0.19 mM glycine
1x TAP Buffer	50 mM Tris-HCl pH 7.8; 100 mM NaCl; 1.5 mM MgCl ₂ ; 0.15% NP40
1x TLEND Buffer (ChIP)	10 mM Tris-HCl pH 8.0; 0.25 M LiCl; 1 mM EDTA; 0.5% Nonidet P-40; 0.5% SDS
1x Wet blotting buffer	25 mM Tris; 192 mM glycine; 10% methanol
20x SSC (pH 7.0)	300 mM sodium citrate (pH 7), 3M NaCl
4x SDS sample loading buffer	0.2 M Tris pH 6.8 at 25°C; 40% (v/v) glycerol; 8% (w/v) SDS; 0.2% (w/v) bromophenol blue; 0.1M DTT
4x separating SDS-gel buffer	3 M Tris, 0.4% (w/v) SDS, pH 8.8 (HCl)
4x stacking SDS-gel buffer	0.5 M Tris, 0.4% (w/v) SDS, pH 6.8 (HCl)
50x TAE buffer	2 M Tris; 1 M acetic acid; 100 mM EDTA, pH 8.0
5x Bradford reagent solution	0.05% (w/v) Coomassie Brilliant Blue G-250, 25% ethanol, 42.5% phosphoric acid
6x DNA loading dye	40% (w/v) sucrose; 0.25% bromphenol blue; 0.25% xylene cyanole FF
AE buffer	50 mM NaAc; 10 mM EDTA; 10 mM Tris/HCl pH 7.4
Coomassie destaining solution	30% (v/v) ethanol; 10% (v/v) acetic acid
Coomassie staining solution	0.25% (w/v) Coomassie Brilliant Blue R-250; 30% (v/v) ethanol; 10% (v/v) acetic acid
Elution buffer (ChIP)	50 mM Tris/HCl pH 7.5; 10 mM EDTA
Elution buffer (mRNP)	50 mM HEPES pH 7.8; 10 mM EDTA

Gerber wash buffer	10 mM Tris-HCl, pH 7.8, 150 mM NaCl, 0.5 mM EDTA, pH 8.0
Ponceau staining solution	0.1% (w/v) PonceauS; 5% acetic acid
Prehybridization buffer	50% formamide; 10% dextran sulphate; 125 µg/ml of <i>E. coli</i> tRNA; 500 µg/ml H.S. DNA + 4 ml SCC 20x SSC + 450 µl 50x Denhardt solution
50x Denhardt solution	Add 0,02% (0,02g) of BSA, Ficoll-400 and polyvinyl pyrrolodine (PVP) in 20 ml SSC
Spheroblasting buffer	0.1 M K-phosphate; 1.2 M sorbitol
Wash buffer mRNP (low salt)	20 mM HEPES, pH 7, 5; 100 mM KCl; 10 mM MgCl ₂ ; 0.01% Nonidet P-40 (NP-40); 1mM DTT
Wash buffer mRNP (high salt)	Wash buffer mRNP (low salt) + 300 mM KCl final conc.
Yeast Transformation Sol I	0.5 ml 10x TE; 0.5 ml 10x LiAc; 4 ml H ₂ O
Yeast Transformation Sol II	0.5 ml 10x TE; 0.5 ml 10x LiAc; 4 ml 50% PEG

2.1.7 Kits and Antibodies

List of commercially available kits

Table 11. Kits used

Kit name	Supplier
ECL Kit	Applichem GmbH (Darmstadt, Germany)
SuperSignal™ West Pico Plus	Thermo Fisher Scientific (Munich, Germany)
Nucleobond AX PC 100	Macherey&Nagel (Düren, Germany)
NucleoSpin® Gel and PCR Clean-up	Macherey&Nagel (Düren, Germany)
PureYield™ Plasmid Miniprep System	Promega (Mannheim, Germany)

Table 12. List of primary antibodies used for Western-blotting

Name	Source	Dilution	Supplier
Peroxidase αPeroxidase complex (PAP)	rabbit, monoclonal	1:5000	Sigma
α-Pgk1	mouse, monoclonal	1:10000	Invitrogen
α-Sub2	rabbit, polyclonal	1:10000	(Strässer et al. 2002)
α-Mex67	rabbit,	1:5000	(Strässer et al. 2002)
α-Npl3	rabbit, polyclonal	1:5000	Guthrie lab
α-Yra1	rabbit, polyclonal	1:2000	(Strässer et al. 2002)
clone 3F2 α-NAB2	mouse Ig G ₁ ,	1:7500	Swanson lab
α-8WG16	mouse, monoclonal	1:1000 for WB and 4 µl for each CHIP exp.	Covance
α-Tho1 (animal2)	rabbit	1:5000	Pineda lab
α-Cbp80	rabbit, polyclonal	1:20000	Görlich lab

Table 13 List of secondary antibodies used for Western blotting

Name	Source	Dilution	Supplier
α -mouse HRPO	goat, monoclonal	1:3000	Bio Rad
α -rabbit HRPO	goat, monoclonal	1:3000	Bio Rad

2.2 Methods

2.2.1 Standard technics

2.2.1.1 Molecular cloning

Standard molecular cloning techniques such as restriction digestion, dephosphorylation of DNA, DNA separation using agarose gel electrophoresis, DNA ligation and transformation in *E. coli*. were performed according to Sambrook and Russell (2001). All commercially available kits were used according to instructions mentioned by the manufacturer. The restriction enzymes used were from Fermentas or New England Biolabs. For DNA preparations from *E. Coli* the following kits were used: Nucleobond AX PC100 Macherey&Nagel (Düren), Nucleospin Mini Macherey&Nagel (Düren). Agarose Gel electrophoresis was performed in 1% Agarose gels buffered with 1x TAE at 180 V for 10-20 min, with SybrGreen™ stain (VWR, Ismaning). The Nucleospin extract Macherey&Nagel (Düren) Kit was used for extraction of DNA from PCR reactions or Agarose gels. All plasmids were verified by sequencing at Microsynth (Balgach, Switzerland).

2.2.1.2 Polymerase chain reaction (PCR)

For the purpose of TAP tagging, two different enzymes have been used according to Table 14 and Table 15. The KNOP polymerase mix (a mixture of Taq-DNA Polymerase and Vent Polymerase) was more frequently used compared to the Phusion PCR mixture (more expensive and for more difficult cloning reactions). Target DNA was purified from a 300 μ l sample (2.2.1.3) and transformed into yeast cells.

Table 14 KNOP PCR

100 μ l PCR reaction mix	PCR program used
0.5 μ M forward primer and 0.5 μ M reverse primer	94 °C 2 min
0.2 mM of each dNTP	94 °C 1 min
1x KNOP buffer (50 mM Tris-HCl pH 9,2, 16 mM (NH ₄) ₂ SO ₄ , 2,25 mM MgCl ₂)	55 °C 30 sec
100-300 ng template DNA	68 °C 1 min/1000bp 35x
1 μ l KNOP polymerase (2 U Taq and 0.56 U Vent),	68 °C 10 min
ddH ₂ O added till 100 μ l final volume	

Table 15 Fusion PCR

20 μ l PCR reaction mix	PCR program used
0.5 μ l template DNA (100-250 ng)	98 °C 1 min
0.25 μ l fwd primer (10 pmol/ml)	98 °C 30 sec
0.25 μ l rev primer (10 pmol/ml)	45-55 °C 30 sec
10 μ l 2x Phusion PCR Master Mix	72 °C 15 sec /1000bp 35x
9 μ l ddH ₂ O	72 °C 5 min

For cloning purposes, high-fidelity amplification of DNA was performed using Phusion® HighFidelity PCR Master Mix with HF Buffer (NEB) according to manufacturer's protocol.

For confirmation of genomic integration, freshly growing yeast cells were picked up with a yellow tip and transferred to an eppendorf tube containing 25 μ L of a PCR reaction mix (Table 16) on ice. The cells were lysed for 20 min at 98 °C and spinned down at 13,000 rpm for 1 min. after the addition of 0.5 μ l Phire II the colony PCR was performed according to following reaction program (Table 16):

Table 16 colony PCR in yeast

25 μ l PCR reaction mix	PCR program used
1 scratch template DNA (white loop)	98 °C 30 sec
1.25 μ l fwd primer (10 pmol/ml)	98 °C 10 sec
1.25 μ l rev primer (10 pmol/ml)	64 °C 20sec
2.5 μ l dNTP mix	77 °C 30 sec 35x
5 μ l 5x Puffer	72 °C 20 min
14.5 μ l ddH ₂ O +	
0.5 μ l Phire II (later)	

For yeast colony PCR, high-fidelity amplification of DNA was performed using Phire™ Hot start II polymerase (Thermo scientific) according to manufacturer's protocol.

For the colony PCR from *E. coli.*, the same program as mentioned above was used except that the initial denaturation was carried out for 2 min (to lyse the cells within the reaction tube).

2.2.1.3 Phenol-Chloroform extraction of DNA/RNA

PCR products for yeast transformation were purified by standard phenol-chloroform extraction procedure. One volume of phenol:chloroform:isoamyl (PCI) alcohol (25:24:1, pH 7.5-8.0) was added to the DNA solution, which was then vortexed and centrifuged at RT for 5 min at top speed. The upper aqueous phase was transferred to a fresh tube and the above step was repeated. For total RNA extraction from yeast cells, the cell pellet was resuspended in 500ul AE buffer and 55ul of 10% SDS was added. An equal volume of aquaphenol:chloroform:isoamyl alcohol (25:24:1, pH 4.5-5) was then added. The cell mixture was vortexed vigorously and incubated at 65 °C for 30 min (vortexed 2-3-times in between). The sample was then centrifuged at top speed for 5 min and the upper phase containing RNA was transferred to a new tube. To increase the amount and quality of RNA, this step was repeated twice, first with aqua-phenol:chloroform:isoamyl alcohol and then with only chloroform. The aqueous phase thus obtained was collected in the fresh tube.

To precipitate the purified DNA or RNA, 1/10 of the volume of 3 M sodium acetate (pH 5.2) and 2.5 volumes of 100 % ethanol were added to the extracted aqueous phase. After incubating the tubes at -20 °C for 20 min (or longer), DNA was precipitated for 20 min at 4 °C at top speed and the pellet was washed with 80 % ethanol. The pellet was dried, resuspended in 20 µl of 1x TE buffer and used subsequently.

2.2.1.4 SDS PAGE

Sodium dodecylsulfate polyacrylamide gel electrophoresis (SDS-PAGE) was performed according to (Laemmli 1970). Mini-PROTEAN II Electrophoresis Apparatus from Biorad was used for casting the gels. The samples for SDS-PAGE were prepared by adding SDS sample loading buffer to the final concentration of 1x and boiling the samples at 95 °C for 3 min. Unless mentioned, 10 % of polyacrylamide mini gels were used for most of the purposes. The protein samples were loaded and resolved in 1x SDS-PAGE running buffer at 200 V until the bromophenol blue dye runs out of the separating gel (around 45 min to 1 h). After running the gel, the apparatus was dismantled and the separated proteins on the gel were either stained with Coomassie Blue or transferred to a membrane for specific detection with Western Blotting. For Coomassie staining, the gel was incubated in hot Coomassie staining solution for 15 min RT while shaking under the hood. Afterwards destained in hot Coomassie destaining solution till desired bands were obtained.

Unstained Protein Ladder, Broad Range or Color Prestained Protein Standard, Broad Range (both NEB) were used as a marker for gels to be analyzed with Coomassie staining. For gels meant to be used for Western Blotting only the Color Prestained Protein Standard, Broad Range was used as a marker. The protocol for preparing 10% SDS polyacrylamide (PAA) gel is described in Table 17.

Table 17 SDS polyacrylamide (PAA) gel preparation

Component (per 1 gel)	Separating Gel (10%)	Stacking gel (4.5%)
4x separating SDS-gel buffer	2.5 ml	-
4x stacking SDS-gel buffer	-	2 ml
30% Acrylamide/Bis-acrylamide (29:1)	3.33 ml	1.2 ml
ddH ₂ O	4.17 ml	4.8 ml
TEMED (100 %)	10 µl	50µl
APS 10 %	50 µl	50 µl

2.2.1.5 Western Blot

For specific detection of a protein of interest, Western Blotting technique was used. The protein samples were separated on a SDS gel as described in the previous section and the resolved proteins on the gel were electrophoretically transferred onto a nitrocellulose membrane (Porablot, Macherey&Nagel) using a standard wet blotting apparatus (Biorad). A sandwich assembly comprising of 2 layers of sponge material, 3 layers of Whatman paper, the gel, the membrane, 3 layers of Whatman paper and 2 layers of sponge material (all of them were pre-soaked in Wet Blotting buffer) was assembled. During the assembly, care was taken that no bubbles were trapped inside the sandwich. The prepared sandwich cassette was placed in the transfer tank containing an ice block. The transfer was done at 150 V for 1 h and 10 min in precooled 1x Wet Blotting buffer. After transfer, the membrane was stained with Ponceau S solution to confirm the transfer of proteins. Ponceau S stain was rinsed off by washing the membrane with ddH₂O. The membrane was blocked for 1 h in the blocking buffer – 2.5 % (w/v) milk in 1x PBS buffer - to prevent non-specific signal due to the background binding of antibodies. Afterwards, the blocking buffer was removed, and the membrane was incubated in primary antibody solution (prepared in the blocking buffer with recommended dilution) for 2.5 h at RT with mild shaking. After incubation, the excess antibody was removed by washing the membrane 3 times with the blocking buffer, each time for 10 min. The membrane was then incubated for 1 h with the secondary antibody conjugated to horseradish peroxidase. The membrane was finally washed three times with 1x PBS buffer, each time for 10 min. The signal from the blot was detected with chemiluminescence, using CheLuminate-HRP PicoDetect ECL kit (Applichem) according to manufacturer's instructions. The bands were imaged on the ChemoCam Imager (Intas).

2.2.1.6 Bradford Assay

Bradford assay was performed according to Bradford (1976) in order to determine the protein concentration in the nucleic extracts for the transcription assay. A standard curve was prepared using Bovine serum albumin (BSA) as a standard. The unknown protein samples were diluted and mixed with 5x Bradford reagent solution to the final concentration of 1x. The absorbance was measured at 595 nm in a microplate reader (Tecan Sunrise).

2.2.1.7 Negative stain with uranyl acetate sample preparation for electron microscopy (EM)

The samples been prepared on copper grids. For high quality EM pictures, the concentration of the target should be in the mg/ml range. The grids carbon surfaces were activated for 40 sec in the glow discharge unit (40-50 % power)

A drop 5 µl sample was added on the grid with a silicon tip. After 3 min of incubation the excess sample was wipe away with a whatman paper. The grid was moved with a tweezer and dipped 3 times for 3-10 sec in into a fresh drop of contrast solution (NanoW or uranyl acetate 2%) and the excess was also removed with a what man paper. In the last step the sample was washed in a drop of water for 10 sec and the sample was dried on air and afterwards put in grid box 184695.

2.2.1.8 Transmission electron microscopy (TEM)

The sample was analysed after staining with uranyl acetate (2.2.1.7) using an EM912a/b TEM (Carl Zeiss, Oberkochen, Germany) at 120 kV under zero-loss conditions. The pictures were taken in different magnifications to check for abundance of the nuclear mRNP (higher magnification levels) and for the abundance of aggregation and other impurities (at lower magnifications). Two meshes (per grid) were chosen to make a series of picture which always start with an overview of the whole mesh at 2500 magnification. After finding a suitable spot the samples were analysed further and pictures were taken at 10.000, 20.000 and 31.500 magnification. On the two highest magnifications the mRNPs of *CCW12* from the purification (5.2.2.7) have been detected. All images were recorded with slight underfocus using a cooled $2k \times 2k$ slow-scan charge-coupled device camera and the iTEM package (Olympus Soft Imaging Solutions, Münster, Germany).

2.2.2 Yeast technics

2.2.2.1 Culture of *Saccharomyces cerevisiae*

Yeast strains were cultivated either in full-media (YPD) or synthetic complete (SC) media (composition in Table 9) at 30 °C (if not stated otherwise) in motion. For solid agar plates, 2% (w/v) agar was added to the media. Cell optical densities (OD) were determined at 600 nm using a spectrophotometer (one optical density unit or 1 OD corresponds to approximately 2.5×10^7 cells).

2.2.2.2 Transformation of yeast cells

50 ml of a yeast culture were grown to log phase (0.6-0.8 OD 600) and harvested by centrifugation (3600 rpm, 3 min). Cells were washed with 10 ml of H₂O and with 500 µl of solution I and then resuspended in 200 µl solution I. 1-5 µg of DNA were mixed with 5 µl single stranded carrier DNA (DNA of salmon or herring testis, 2 mg/ml). 50 µl cell suspension and 300 µl of solution II were added. After 30 min incubation at room temperature, cells were heat shocked (42 °C, 10 min) and incubated 3 min on ice. After addition of 1 ml H₂O, cells were pelleted. When plasmids were transformed, yeast was immediately plated on the selective plates in 100 µl H₂O. For genomic integration, cells were resuspended in 1 ml of YPD and incubated 1-5 h at room temperature on a turning wheel and then plated on selective media and stored at 30 °C till colonies appeared (3-5 days).

Whole cell extracts (WCE)

For testing integration of tags, WCE were prepared from yeast restreaked and freshly grown on plates: one blue inoculation loop of cells was resuspended in 100 µl of 1x SDS-sample buffer and approx. 50 µl of glass beads were added. Samples were incubated 1 min at 95 °C, and vortexed for 1 min. This was repeated twice and then samples were again incubated 1 min at 95 °C and loaded on a SDS PAGE after 3 min centrifugation at 12.000 rpm.

WCE have been also prepared with the MP Biomedicals™ FastPrep-24™ 5G Instrument using the program yeast one time (1x shake for 45 sec). The sample preparation was identical, but no heating was necessary after adding the beads.

2.2.2.3 Dot Spot Assay

Dot spot assay was used to compare the growth phenotypes of different yeast strains. Briefly, a loop of freshly growing yeast cells was resuspended in 1 ml of ddH₂O and four times another 10x dilution was made (serial dilutions starting with similar OD). 5 µl of each dilution (5 per sample) was spotted on a desired media plates and incubated for 3-5 days at required temperatures.

2.2.2.4 Glycerol stocks

For long term storage of yeast cells, glycerol stocks were prepared. The yeast cells were freshly grown on agar plate for 2 days, scrapped off from the plate and resuspended in 1ml of 50% sterile glycerol. The cell suspension was flash frozen in liquid nitrogen and stored at -80° C.

2.2.2.5 Genomic deletion in *Saccharomyces cerevisiae*

The ORF of the gene was replaced with an auxotrophic marker or an antibiotic resistance gene via homologous recombination. To achieve this, either the disruption cassette was amplified from a commercially available deletion strain (Euroscarf), or primers were made containing flanking regions (50-70 nucleotides) homologous to the promoter and terminator of the targeted gene and sequence complementary to the both sides of a marker cassette (for example, HIS3 cassette from plasmid YDp-H). In both the cases, the amplified PCR product was purified and transformed into yeast cells. Cells were plated on appropriate selective media plates. The positive colonies were verified by Colony PCR using one primer binding outside of the amplified region (in 5' or 3' UTR of the targeted gene) and other primer binding within the selection marker.

2.2.2.6 Genomic integration of tandem affinity (TAP) tag

To achieve the genomic integration of C TAP tag to the desired protein, primers were designed as described in (Puig *et al.* 2001). 3x KNOP PCR reaction (300 µL) was prepared (2.2.1.2) and the PCR product was purified by phenol chloroform extraction (2.2.1.3). The purified DNA was transformed into yeast cells (2.2.2.2) to integrate the tag into the yeast genome by homologous recombination. The correct integration of the tag was confirmed either by Western Blotting (2.2.1.5) or Colony PCR (2.2.1.2).

2.2.2.7 UV Cross-linking in *Saccharomyces cerevisiae*

2 l of yeast cells were inoculated using an overnight saturated preculture of the required strain. The cells were grown overnight at 30 °C in YPD medium to an OD₆₀₀ of 3-3.5 and harvested by centrifugation at 5000 rpm for 5 min ^{*1}. The pellet of 2 l cells was resuspended in 750 ml 1x Tap buffer and added to the VARI-X-LINK UV CROSS-LINKER. A dose of 1200 mJ was applied and the cells were washed once with water and once with 1x TBS buffer, and frozen in liquid N₂.

^{*1} Since the 254-Biolinker can only take 20 ml as input sample the cells from 2l culture were resuspended after 5 min and transferred to a falcon tube, washed once with water and centrifugation at 3600 rpm for 3 min. The pellet was resuspended with 20 ml 1x Tap buffer on a plastic petri dish. The petri dish was inserted with a water/ice bath into the 254-Biolinker for a dose of 1200 mJ. This was repeated two more times and after each dose the sample was removed and shaken for 5 min in the ice bath to prevent the yeast cells from sedimentation Afterwards the cells were washed once with water and once with 1x TBS buffer, and frozen in liquid N₂.

2.2.2.8 Tandem affinity (TAP) Purification

TAP-tagged proteins were purified from *S. cerevisiae* using tandem affinity purification technique as described previously (Puig *et al.* 2001, Strasser *et al.* 2002). 2 l of yeast cells were inoculated using an overnight saturated preculture of the required strain. The cells were grown overnight at 30 °C in YPD medium to an OD₆₀₀ of 3-3.5 and harvested by centrifugation at 5000 rpm for 5 min. The cells were washed once with water and once with 1x TBS buffer, and frozen in liquid N₂.

For mRNP purification the pellet was not lysed in the bead beater (Pulverisette, Fritsch) instead a SPEX SamplePrep 6875 D Reezer/Mill® was used. The frozen droplets of the yeast culture been grinded 8 times for 3min with 2 min break in between. The powder was stored at -80 °C.

10 ml of cold TAP buffer (Table 10) containing 1x Protease inhibitor cocktail and 1 mM DTT is added to the frozen powder. The crude lysate was precleared first with centrifugation at 4000 rpm for 10 min, 4°C and then with ultra-centrifugation at 35 k rpm for 1 h, 4 °C (later 25 min at 25 k rpm). The top fatty phase was removed with a vacuum pump and the clear upper phase was incubated for 1.5 h (or overnight) with 400 µl of pre-equilibrated IgG-coupled Sepharose 6 Fast Flow slurry (GE Healthcare) at 4 °C. After IgG binding, the IgG beads slurry was centrifuged down and transferred to a mobicol with a 35µm filter. The beads were then washed by gravity with 10 ml of TAP buffer containing freshly added 0.5 mM DTT. For TAP purification under high salt conditions, buffer containing high salt concentration (250 mM to 1000 mM of NaCl) was used during the washing step. After washing, 120 µl of TAP buffer (+0.5 mM DTT) was added to the mobicol and the beads were treated with 5 µl of Tobacco-etch-virus protease (TEV protease) (4 mg/ml) for 1 h at 16 °C. Afterwards, the bound protein of interest was eluted by spinning at 2000 rpm for 2 min at 4 °C.

The protein was further purified with a second affinity step by incubating the TEV eluate with 500 µl of calmodulin-coated beads for 1 h at 4 °C in the presence of calcium. Calmodulin Sepharose beads (Agilent Technologies) were prewashed 3 times with 10 ml of TAP buffer containing 1mM DTT and 2 mM CaCl₂ and two times with 10 ml of TAP buffer containing 1 mM DTT and 4 mM CaCl₂. After incubation, beads were washed in mobicol column with 5 ml of TAP buffer (+1 mM DTT and 2 mM CaCl₂). The protein of interest was eluted by adding 600 µl of elution buffer (10 mM Tris-HCl pH 8.0, 5 mM EGTA). The elution was carried out at 37 °C for 15 min in a thermomixer with shaking so that the beads do not settle down. The eluted protein was precipitated by adding TCA to a final concentration of 10% (v/v) and incubating for 20 min on ice followed by 20 min centrifugation top speed at 4°C. The pellet was dried and resuspended in 50 µl of 1x SDS-sample buffer and 2-3 µl of 1 M TRIS base was added to neutralize the pH. The purified protein was boiled at 95 °C for 3 min, centrifuged and subjected to SDS-PAGE (2.2.1.4).

For mRNP purification the sample was further purified like described in 2.2.2.10 after the TEV elution.

2.2.2.9 Anti-sense oligo design for nuclear mRNP purification

To design the oligos complementary to the sequences of the target genes *CCW12* and *ILV5* the sequence of those two genes was downloaded from the yeast database (<https://www.yeastgenome.org>) 22-nt long DNA sequences spanning the whole body of genes were randomly chosen and reverse complementary sequence was generated using an internet tool http://www.bioinformatics.org/sms/rev_comp.html). We designed 8 anti-sense oligos for *CCW12* and 11 for *ILV5* (Table 8).

Before ordering we investigated the property of forming hairpins or self-annealing of the sequences with Oligocalc (<http://biotools.nubic.northwestern.edu/OligoCalc.html>).

2.2.2.10 Nuclear mRNP purification with 2'-O-methylated anti-sense oligonucleotides

The mRNP purification was performed from the crude lysate (1 ml samples) or from the TEV eluate of the TAP purification (2.2.2.8). 12 µl of one 2'-O-methylated anti-sense oligonucleotide (200 pmol, Table 8) for *CCW12* or *ILV5* was added and incubated at 4 °C for 2h in the cold room. One sample without any anti-sense Oligo served as Mock control in each experiment. In the last 30 min of incubation M280 dynabeads have been washed 4x with wash mRNP wash buffer on at RT on the turning wheel. The buffer exchange was done using MPC to collect the beads. 100 µl of washed M280 beads have been added to each sample including the mock control and incubated for 30 min at 37 °C. The beads being afterwards washed 6x times in total. The first four times with 1ml low salt buffer and two times with 1 ml high salt buffer (the 2x high salt been replaced by 2x low salt buffer in the final protocol). Each incubation between the buffer changes on MPC was 5 min. After the washing 100 µl low salt buffer was added and the sample was split in 20 µl beads for RNA analysis and 80 µl for protein analysis on SDS PAGE (2.2.1.4). The 80 µl removed on the MPC and 10 µl 1 SDS was added. The sample was boiled for 5 min at 95 °C and stored for SDS PAGE. For the RNA sample the beads been cooked 10 min at 65 °C or 95 °C for 2 min with 50 µl elution buffe and used for RNA extraction (2.2.1.3).

Changing buffers, temperatures and incubation times are the focus of the second part of the study and can be found in the results section. Important to mention is that adding NP40 to the elution buffer prevents the rapid wear of the M280 beads.

2.2.2.11 Fluorescence-In-Situ-Hybridization (FISH) in *Saccharomyces cerevisiae*

10 ml of yeast cells were grown till OD₆₀₀ 0.5-1.0 (mid-log phase) and 1.25 ml of formaldehyde was added to cross link the cells for 90 min at RT on a turning wheel. For mex67-5 cells, the cells were grown till mid-log phase at 30 °C and shifted for 15 min to 37 °C before adding formaldehyde. The cells were spinned down for 5 min at 3000 rpm. The cells were washed with 5 ml of 0.1 M KPO₄ buffer (pH 6.4) and again with 1 ml 0.1 M KPO₄ (pH 6.4) and transferred to the eppendorf tube. Then cells were spinned again and resuspended in 1 ml of 0.1 M KPO₄ plus 1.2 M sorbitol buffer (called spheroblasting buffer). The cells were spinned again, resuspended in 200 µl of spheroblasting buffer with 100 µg of Zymolyase 100T powder and incubated for 30 min at 30 °C. To stop the Zymolyase 100T treatment, the cells were spinned for 4 min at 2,000 rpm. The cells were washed with 1 ml of spheroblasting buffer, and the pellet was resuspended in >10x volume of the pellet. The spheroplasts were then attached to the glass slide pre-coated with polylysine and allowed to sit undisturbed for 5 min. Afterwards, the nonadherent cells were removed by aspiration. The cells dry at RT for around 1 h. The dried cells were incubated first with 100 µl 2x SSC solution for 10 min at RT and then with 12 µl of prehybridization buffer in a humid chamber for 1 h at 37 °C. For hybridization with Cy3-labelled oligo d(T)₅₀ probe, 0.75 µl of 1 pmol/µl of probe was added and the slide was incubated at 37 °C overnight in a humid chamber. After incubation, cells were washed with 100 ml of 0.5x SSC solution in staining jar (100 ml) at RT for 30 min. For staining of the nuclei, 2 µl of 4',6- diamidino-2-phenylindole (DAPI, 2.5 mg/ml stock solution) was added to the 100 ml of 0.5x SSC solution in the staining jar and the slide was incubated inside it for 3 min. Afterwards, the slide was washed again in fresh 0.5x SSC solution for 5 min at RT. The slide could dry at RT in the dark. The dried slides were finally covered with 5 µl moviol. Olympus BX60 fluorescence microscope was used for analysing the results.

2.2.2.12 Chromatin Immuno Precipitation (ChIP)

Chromatin immunoprecipitation (ChIP) assays were performed according to (Röther *et al.* 2010) with some modifications. 100 ml of yeast cell culture was grown till the mid-log phase (OD₆₀₀ of 0.7-0.8). The growing cells were crosslinked with 1% formaldehyde with mild shaking for 20 min at RT. The reaction was quenched with 0.25 M glycine for 5 min. The cross-linked cells were centrifuged, and the pellet was washed two times with 1x TBS buffer, frozen in liquid nitrogen and stored at -80 °C.

The crosslinked cells were resuspended in 800 µl of low salt FA lysis buffer (Table 10) and lysed by vortexing with an equal volume of glass beads for 7 x 3 min and 3 min on ice in between. The lysate was sonicated using Bioruptor UCD-200 (Diagenode) for 3 x 15 min (30 sec. ON/30 sec. OFF) at 'HIGH' power setting with intermittent cooling in between (5 min). The average size of resulting chromatin fragments was between 200-250 bp. The sheared lysate was cleared by two centrifugations for 5 and 10 min 14000 rpm at 4 °C. The concentration of supernatant was measured in Spectrophotometer ND1000 at 280 nm. 10 µl of lysate was reserved as 'INPUT'. For each ChIP same amount of sample was used of lysate was used in a total volume of 1200 µl low salt FA lysis buffer. For immunoprecipitation (IP) of TAP-tagged proteins, the lysate was incubated with IgG-coupled dynabeads tosylactivated M280 (Thermo Scientific) for 2.5 h at 20 °C. For RNAPII ChIP, 4 µl of anti-RNA Polymerase II Rpb1 8WG16 monoclonal antibody (Biolegend) was added for 1.5 h at 20 °C followed by 1 h incubation with Protein G dynabeads. The immunoprecipitated (IP) samples were washed two times with 800 µl of low salt FA lysis buffer, two times with high salt FA lysis buffer, one time with 1x TLEND buffer and one time with 1x TE buffer and afterwards eluted in ChIP elution buffer (Table 10). Both INPUT and eluted IP samples were treated with Proteinase K (P4850; Sigma) at 37 °C for 2 h and incubated at 65 °C overnight for reversal of crosslinks. INPUT and IP DNA was purified using NucleoSpin® Gel and PCR Clean-up Kit (Macherey-Nagel) and quantified using Real Time PCR cycler Quant Studio 3 (Thermo Fischer). At least three biological replications of each ChIP experiment were performed and analysed.

2.2.2.13 real-time quantitative PCR (qPCR)

To analyse the DNA from ChIP experiments, 1:20 dilutions of 'INPUT' and 'IP' DNA were used as a template for a 10 µl PCR reaction (Table 18). SYBR Green based 2x PCR Master Mix (Applied Biosystems) was used as recommended by the manufacturer and PCR reactions were carried out on MicroAmp Fast Optical 96-Well Reaction Plate (Applied Biosystems). QuantStudio 3 Real-Time PCR System (Thermo Fischer) along with its recommended software was used for the qPCR and data analysis.

Table 18 Working scheme for qPCR analysis

1x qPCR Reaction Mix:	qPCR program:
2.5 µL of diluted DNA	95 °C 10 min (Initial Denaturation)
0.1 µL (100 pmol/µL) of each primer	95 °C 15 sec (Denaturation)
5 µL 2x Power Sybr Green PCR Master Mix	60 °C 1 min (Annealing and Elongation) for 45 cycles
2.3 µL of ddH ₂ O	Melting curve program:
= 10 µL total volume	95 °C 15 sec
	60 °C 60 sec
	60 °C – 95 °C continuously 0.3 °C
	95 °C 15 sec

A yeast non-transcribed gene region (Yer or NTR1, 174131–174200 on chromosome V) served as a negative control to account for nonspecific DNA binding of the target protein and H₂O instead of DNA served as a NTC (non-template control) for the PCR. Several highly expressed genes like *ADHI*, *PGK1*, *PMA1*, *ILV5* and *CCW12* were analysed for the occupancy of the protein of interest. The occupancy of the target protein at a particular gene was calculated as its enrichment at that gene relative to its presence at the non-transcribed region (NTR). The sequence of this primers belonging to the 5', mid or 3' region of the specific genes can be found in Table 7. Standard curves were plotted to calculate PCR efficiencies and to ensure that the detected signal lies in the linear range. Melting curve analysis of the amplicons was done to verify the specificity of primers. Three technical replications of each PCR reaction were performed, and the average values were considered for further analysis. All qPCR data are presented as average \pm Standard Deviation (SD) of at least three biologically independent experiments. Asterisks indicate the statistical significance (Student's t-test (1908); * P < 0.05 and ** P < 0.01).

2.2.2.14 Quality control PCR for *CCW12* and *ILV5* amount in Nuclear mRNP purification

To compare the amount of purified *CCW12* and *ILV5* mRNA in the nuclear mRNP purification the RNA was analysed using the same qPCR Program as Table 18. As negative control served the high abundant mRNA of *PGK1*. RNA samples haven been transcribed to DNA with the MuLV enzyme (Thermo Scientific) according to the manual. The 20 μ l sample (containing 2 μ l 10x MuLV buffer and 7 μ l RNA) was adjusted 5 min to RT before it was heated for 1h at 42 °C. The enzyme was inactivated for 20 min at 65 °C and DNA extraction was performed (2.2.1.3)

The calculation was done by the comparison of the ct-values for *ILV5* or *CCW12* and *PGK1* in the purification the mock sample. According to the following equation three quality parameters were used to compare different purifications.

Equation 1 Quality criteria for nuclear mRNP purification by qPCR

Specificity	$\frac{ct(ASO)}{ct(MOCK)}$	$\frac{ct(PGK1)}{ct(MOCK)}$	$\frac{ct(ASO)}{ct(PGK1)}$
Relative amount	Relat. Amount = Ct-value		
Enrichment	$\frac{ct(ASO)}{ct(Flow)}$	$\frac{ct(PGK1)}{ct(Flow)}$	

2.2.2.15 RNase H assay

A Tap purification (2.2.2.8) was performed to the TEV eluate. The 150 μ l sample was adjusted to 1ml with 100 μ l 10x RNaseH-Buffer (NEB), NaCl (final con. 60 mM) and water. An input sample for qPCR was taken and the sample was split in two 500 μ l samples. In one sample 100 pmol 2'-O-methylated anti-sense oligonucleotide was added. After 2 h incubation in the cold room 2,5 μ l RNaseH (NEB) have been added to each tube. The sample have been digested for 20 min and at 37 °C. After adding 500 μ l PCI as RNA extraction was performed as described (2.2.1.3). The reverse transcription reaction was performed with 200 ng RNA and the mRNA values have been analysed by qPCR.

2.2.2.16 Copy number calculation of CCW12 molecules in mRNA purification.

The *CCW12* was inserted into a pRS316 vector. The pRS316-*CCW12* was expressed in *e. Coli* DH5 α cells and the purified DNA was measured with the nanodrop. A dilution series was made and analysed with qPCR among the other *CCW12* samples. From the ct-values of the dilution series a standard curve was calculated in excel. The amount of DNA (ng) of the samples have been calculated from the standard curve. Knowing the amount of input DNA (in ng) and the total number of base pairs for pRS316-*CCW12* one can calculate the copy number of the plasmid using following page on the internet.: <https://scienceprimer.com/copy-number-calculator-for-realtime-pcr> or <http://cels.uri.edu/gsc/cndna.html> for only dsDNA.

The calculator on that site is using this formula:

Equation 2 copy number calculation for qPCR

$$\text{Number of copies} = \frac{\text{Amount (ng)} \times 6.022 \times 10^{23}}{\text{Length (bp)} \times 1 \times 10^9 \times \text{Mass of DNA bp}}$$

Mass of DNA bp is 660 g/mol for dsDNA and 330 g / mol for ssDNA

Amount (ng) is the DNA (ng) Length (bp) bp of template x 6,022 x10²³ (Avogadro's constant) 1x 10⁹ conversion factor to ng

3 Results

3.1 Role of Tho1 in Transcription

Chromatin immunoprecipitation (ChIP) experiments have been performed to elucidate the interaction of Tho1 with Paf1 and Spt5. In the experimental setup, endogenous TAP-tagged Paf1 and Spt5 strains have been analysed in a RS453 wt background versus an RS453 Δ tho1 background. In Another experiment, RS453 background strain with endogenously TAP-tagged Paf1 was transformed with an empty plasmid (pRS426) or the same plasmid expressing THO1(pRS426-THO1). The Paf1 and Spt5 occupancy have been determined by Real Time PCR at different positions in highly transcribed yeast genes which includes *ADH1*, *PMA1* and *PGK1*.

To make sure all tested strains were healthy and have no defects in transcription, the occupancy of RNAPII was determined using the same set of genes.

3.1.1 Tho1 overexpression does not influence the occupancy of Paf1 on transcribed genes

A connection between Paf1 and Tho1 seemed obvious since Tho1 overexpression can suppress the transcriptional defects of HPR1 deletion (Fasken and Corbett 2016), which have similar phenotype as Δ paf1 (Chang *et al.* 1999). Also, Dominik Meinel showed in his PhD thesis that Paf1 has the same occupancy pattern as Tho1 in a Spt5-CTR mutant ChIP (Figure 9). Based on this established finding the Paf1-TAP strain was modified with a high copy plasmid pRS426 (20 copies per cell) with and without THO1 (Figure 10). ChIP was performed as described in (2.2.2.12), however, there was no significant change in the occupancy of Paf1 over the genes *ADH1*, *PMA1* and *PGK1* (Figure 11 and Figure 12).

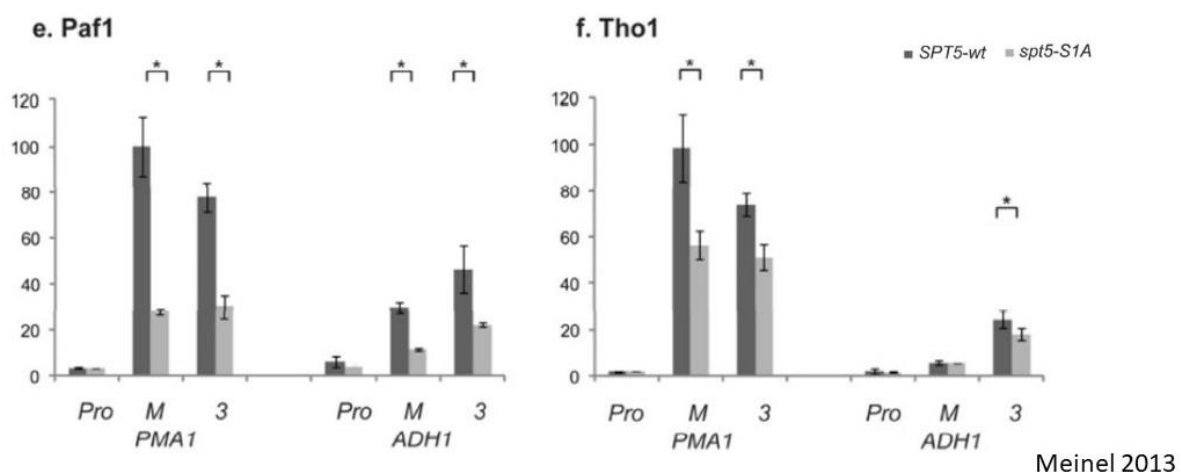


Figure 9. Spt5-CTR S1A mutations lead to decreased Tho1 and Paf1 occupancies

The two graphs show the fold enrichment over Yer for PAF1 and Tho1 in a ChIP experiment comparing the SPT5-CTR with the S1A mutation. Both proteins showed the same patterns of decreased occupancy in the S1A mutation (Meinel 2013).

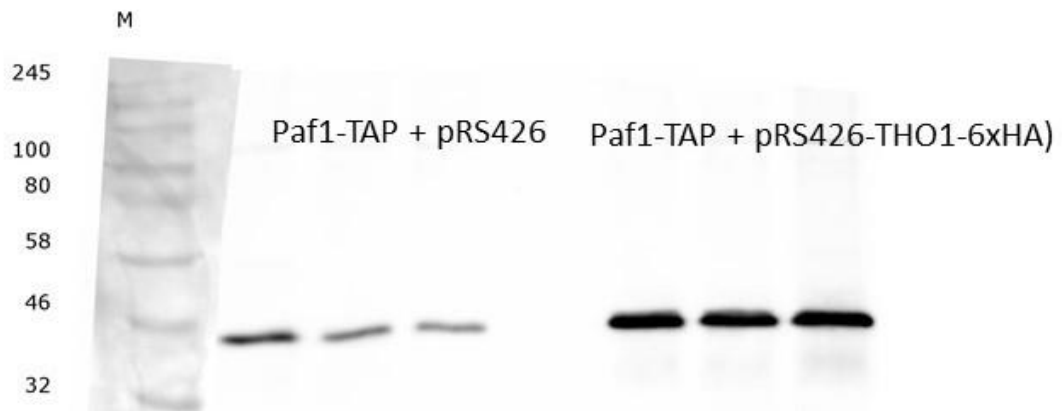


Figure 10. Western blot of PAF1-TAP with and without overexpression of Tho1
Before each ChIP experiment the overexpression of Tho1 was checked in all strains using Western blotting.

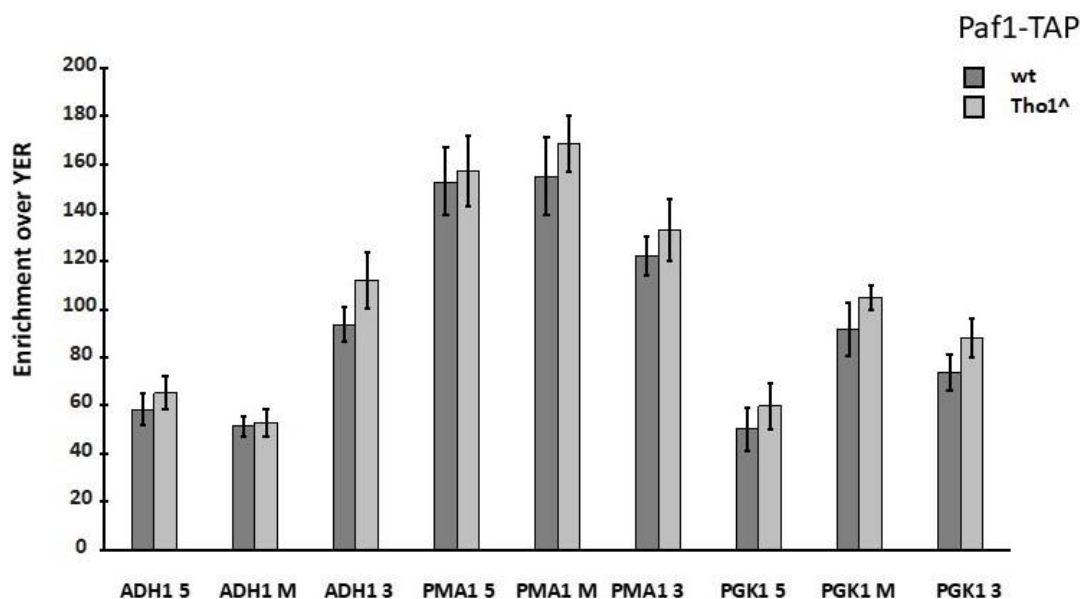


Figure 11. ChIP of Paf1-TAP with and without THO1 overexpression

The bar graph shows the enrichment of Paf1-TAP and the 5' and 3' ends of the gene body of the highly transcribed *ADH1*, *PMA1* and *PGK1*. The wt strain carries only the empty plasmid pRS426. Overexpression of Tho1 incurred no changes. This experiment was carried out 2 times (n=2)

In this experiment no influence on Paf1 recruitment to the active transcription site by overexpression of Tho1 was detected. Both strains grew normal in media as well on petri dishes. To rule out the possibility that the tested strains are influenced by the inserted by the empty plasmid or the Tho1 overexpressing plasmid further experiments have been performed. The occupancy of RNAP II has been determined in both strains using the RNAP II specific antibody 8WG16 to assess difference in transcription levels of the genes mentioned above.

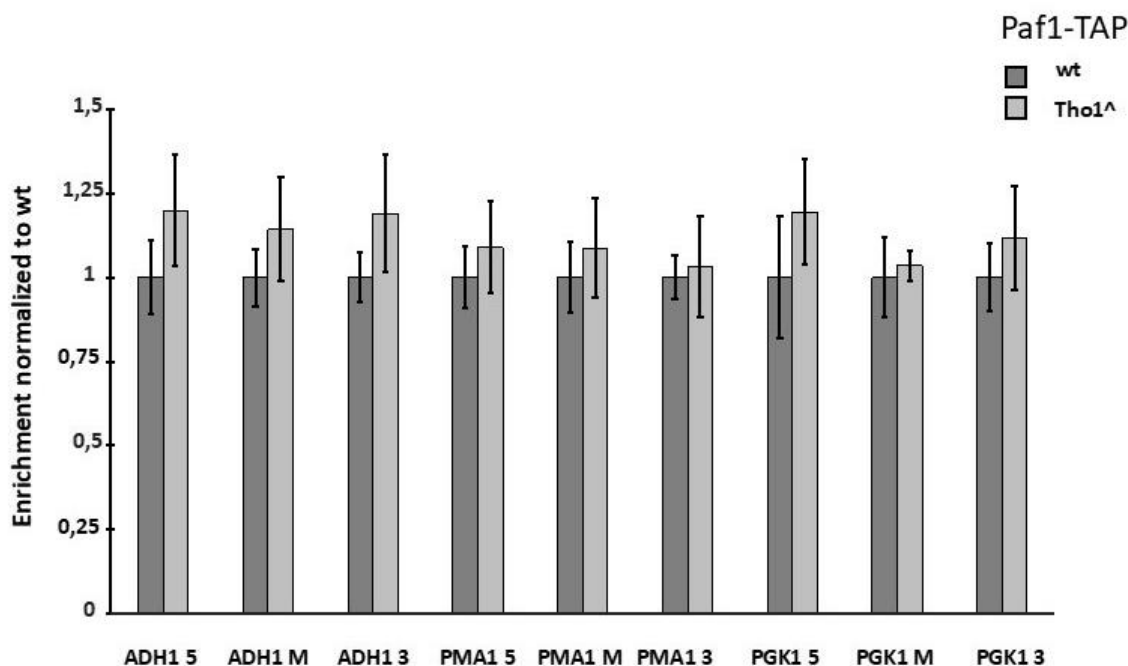


Figure 12. ChIP of Paf1-TAP with and without THO1

The data set of Figure 3 was normalized to 1. The occupancy level was the same however, the error bars were bigger due to the differences in scales (n=2).

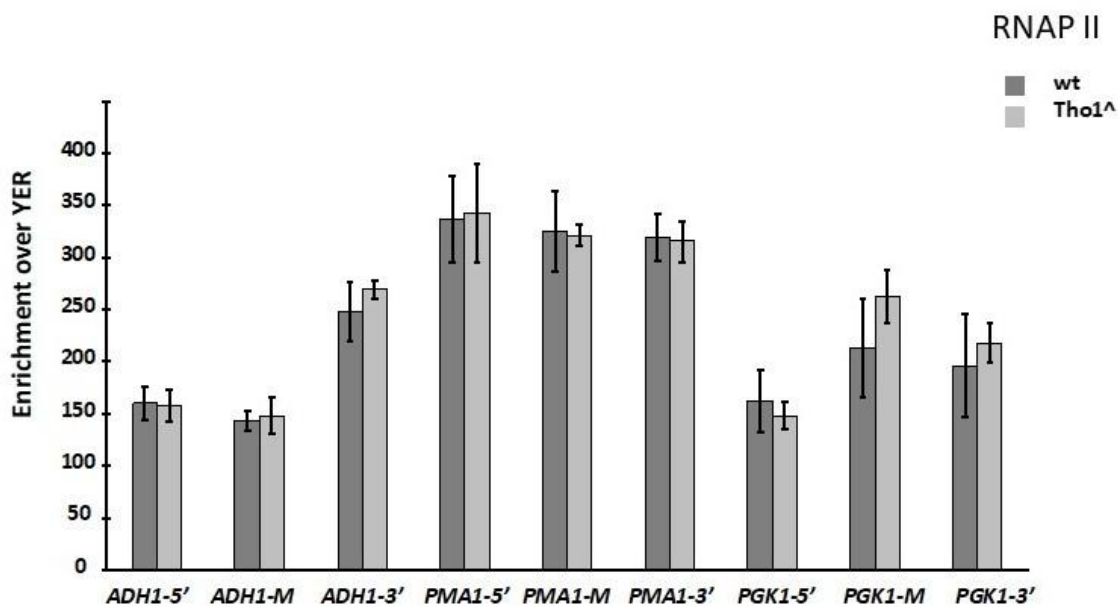


Figure 13. RNAPII ChIP THO1 overexpression

The bars show the occupancy of RNAP II over the 5' and 3' end of the gene body of the highly transcribed genes, *ADH1*, *PMA1* and *PGK1*. The wt strain carries only the empty plasmid, pRS426. There were no significant changes between the wt and the Tho1 overexpression strains. The polymerase II was abundant on the transcribed genes compared to other proteins, for example, Paf1. (n=4)

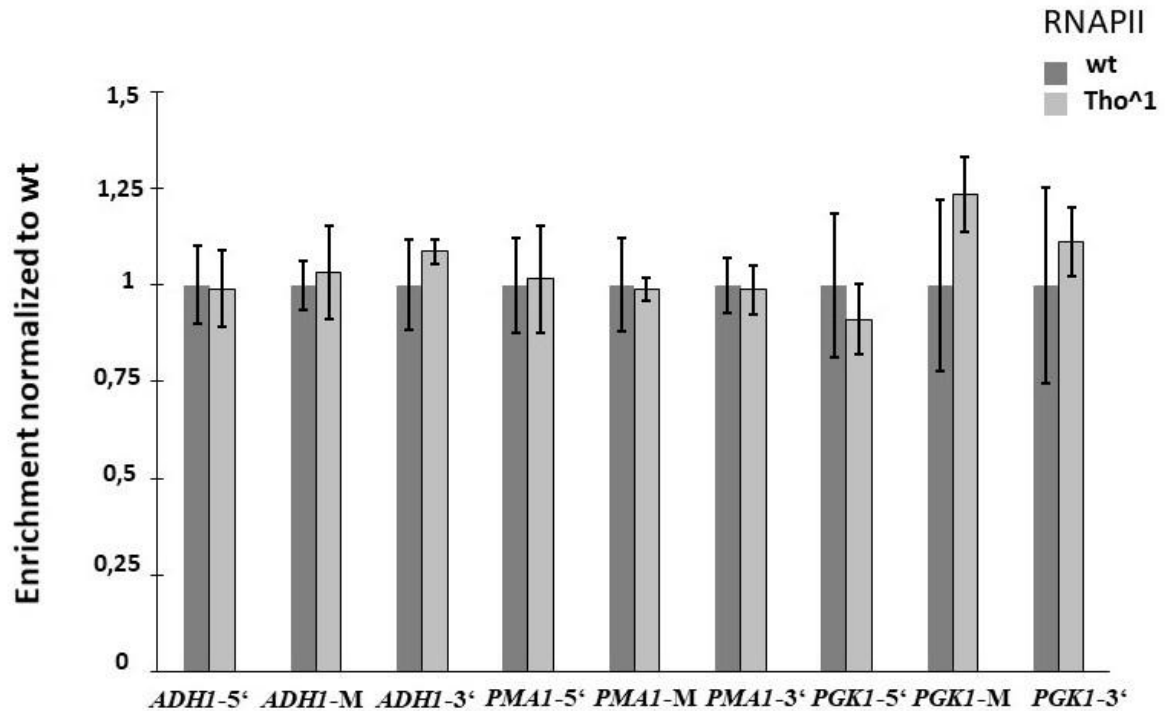


Figure 14. RNAPII ChIP THO1 overexpression

The data set of (Figure 13) was normalized to 1. The occupancy level was the same however, the error bars were bigger due to the differences in scales (n=2).

3.1.2 Tho1 deletion does not influence the occupancy of Spt5 on transcribed genes

The Spt5-CTR is an important recruitment platform which interacts with various transcription factors and protein with various functions (1.1.4.3). The connection between Tho1 and Spt5 was first established by a pull-down experiment of Spt5-TAP (Lindstrom *et al.* 2003), and additionally, S1A mutation of Spt5-CTR leads to decreased occupancy of Tho1 at transcribed genes (Meinel 2013).

Therefore, a C-terminally TAP-tagged Spt5 in a Δ tho1 RS453 strain (2.2.2.6) was created and further compared to the Spt5-TAP RS453 strain in a ChIP to elucidate the effect of THO1 on the occupancy of Spt5 assessed at the genes *ADHI*, *PMA1* and *PGK1*.

As already observed in the Paf1-TAP strain (3.1.1) overexpression with Tho1, there was no influence of the mutant for the occupancy of Spt5 on the transcribed genes.

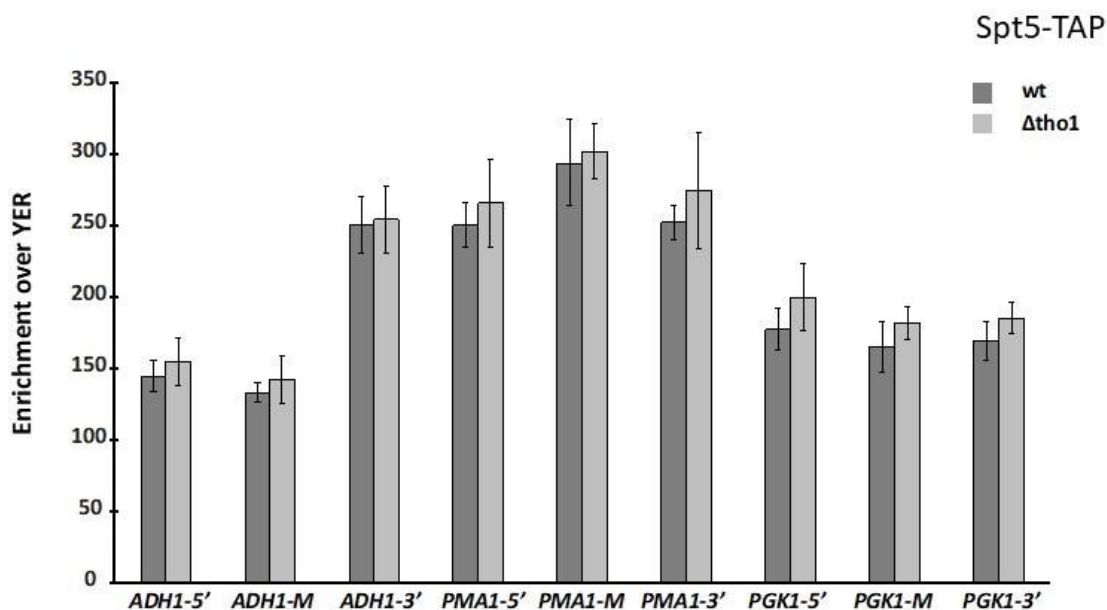


Figure 15. Spt5-TAP ChIP in RS453 strain ± Δtho1

The figure shows the enrichment of Paf1-TAP over the whole gene body of the highly transcribed genes *ADH1*, *PMA1* and *PGK1*. The Spt5-TAP expressed in a strain of RS453 devoid of the protein, Tho1. No effect on the occupancy of SPT5 was observed. (n=3)

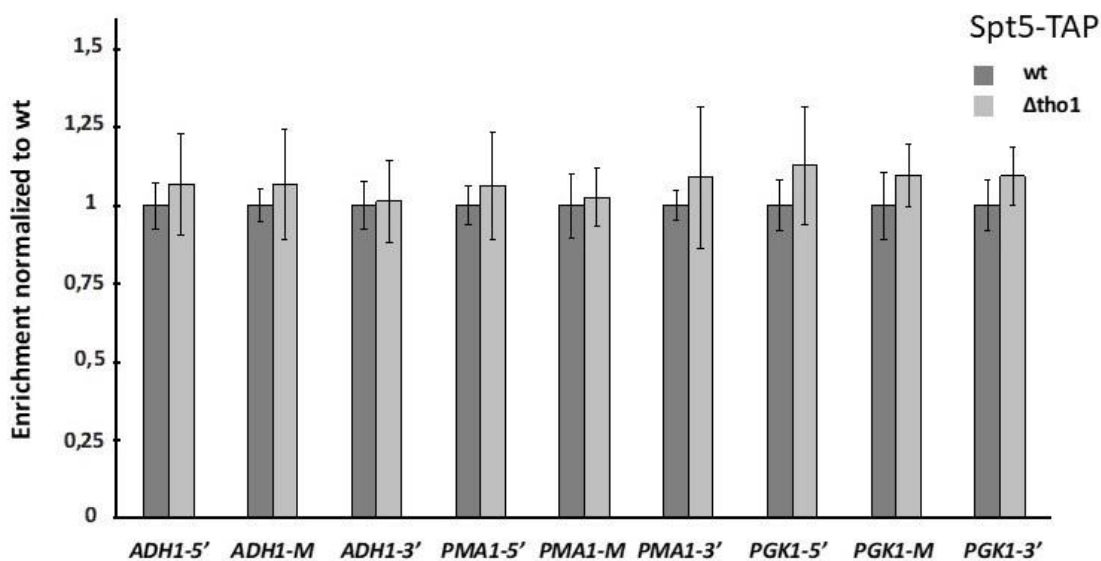


Figure 16. Spt5-TAP ChIP in a ± Tho1 deletion RS453 strain

This graph indicates the Data set of Figure 7 normalized to 1. (n=3)

It was previously shown that *THO1* deletion complements a temperature sensitive *nab2-1* mutant (Jimeno *et al.* 2006). Therefore, the transcription levels of RNAP II were ascertained in those cells via ChIP experiments.

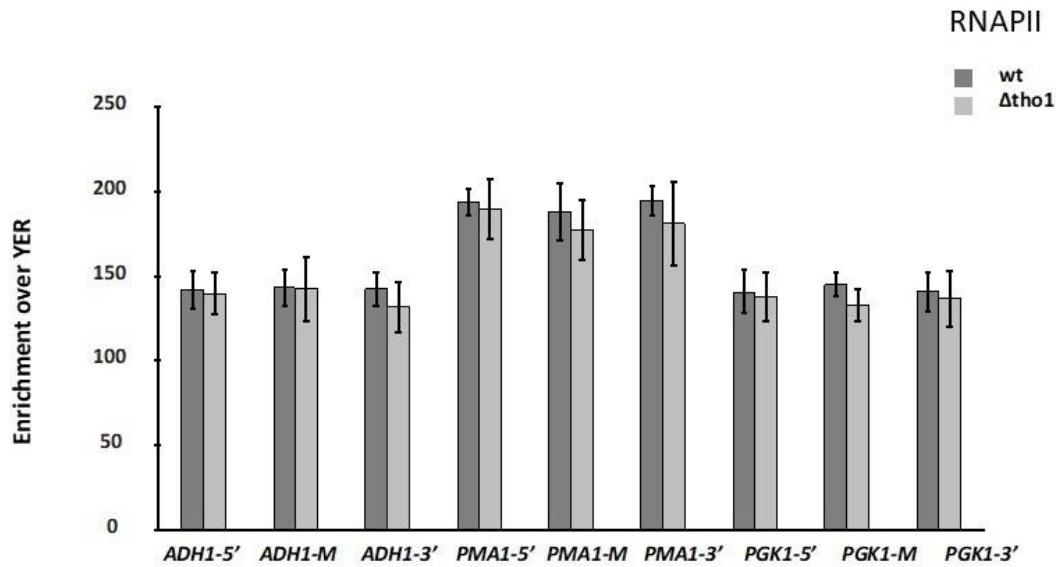


Figure 17. RNAPII ChIP in a RS453 strain \pm Δ tho1

Experiments for this Figure was done as explained for Figure 13 and Figure 14. No change was observed in the Tho1 deleted strain compared to those overexpressing THO1. (n=2)

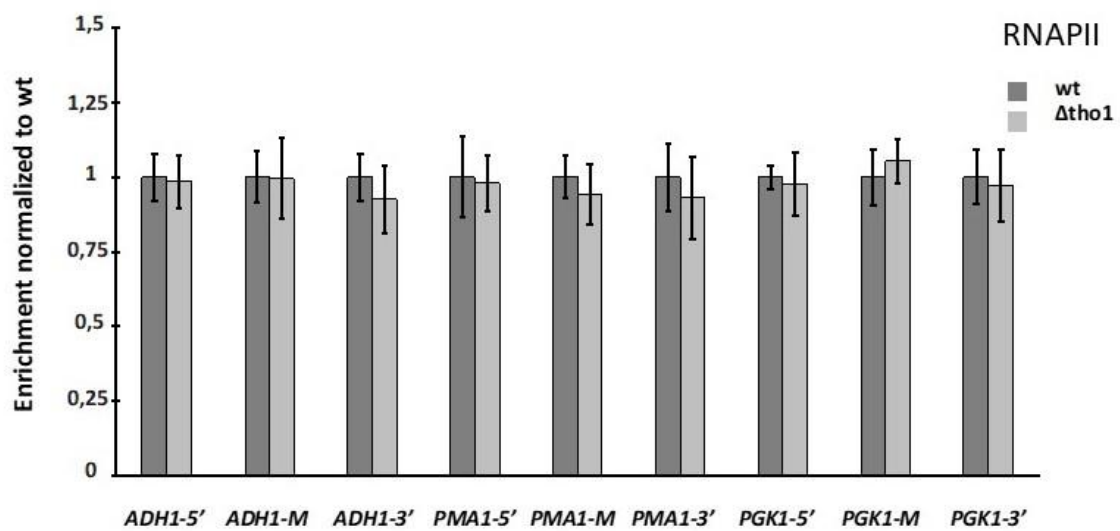


Figure 18. RNAPII ChIP in a \pm Tho1 deletion RS453 strain

Here, the normalized Data of Figure 17 showed no observed changes (n=2).

In this part of the study, there was no indication of transcriptional defects since the occupancy levels of RNAPII on the actively transcribed genes did not change in the deletion mutant compared to the wt Spt5-TAP strain. These results match observations in the Tho1 overexpression experiment. Taken together, overexpression or deletion of Tho1 does not affect RNAPII during transcription.

3.1.3 A Δ tho1 deletion increases the Paf1-TAP occupancy on transcribed genes

Since overexpression of Tho1 did not exhibit much impact, Tho1 was deleted in a Paf1-Tap Rs453 strain. Although there was no effect on Spt5 when THO1 was deleted, a significant decrease in the occupancy of Paf1-TAP was observed after a ChIP experiment (Fig 11 and 12). Quantitatively, the reduction was shown to be between 15 and 25 % in the deletion strains compared to the wt Paf1-TAP strain. Although the decrease was not significant at the 3' end of PGK1, the occupancy dropped in the range of one to three asterisks for all other parts of the genes, *ADH1*, *PMA1* and *PGK1*. The calculation was done using a student's *t*-test according to (2.2.2.13) Interestingly, results for RNAPII levels resembled findings of the Spt5-TAP Δ tho1 strain (Figure 17 and Figure 18). Altogether, there was no change, and therefore, no indications that the strains used might have impaired transcription.

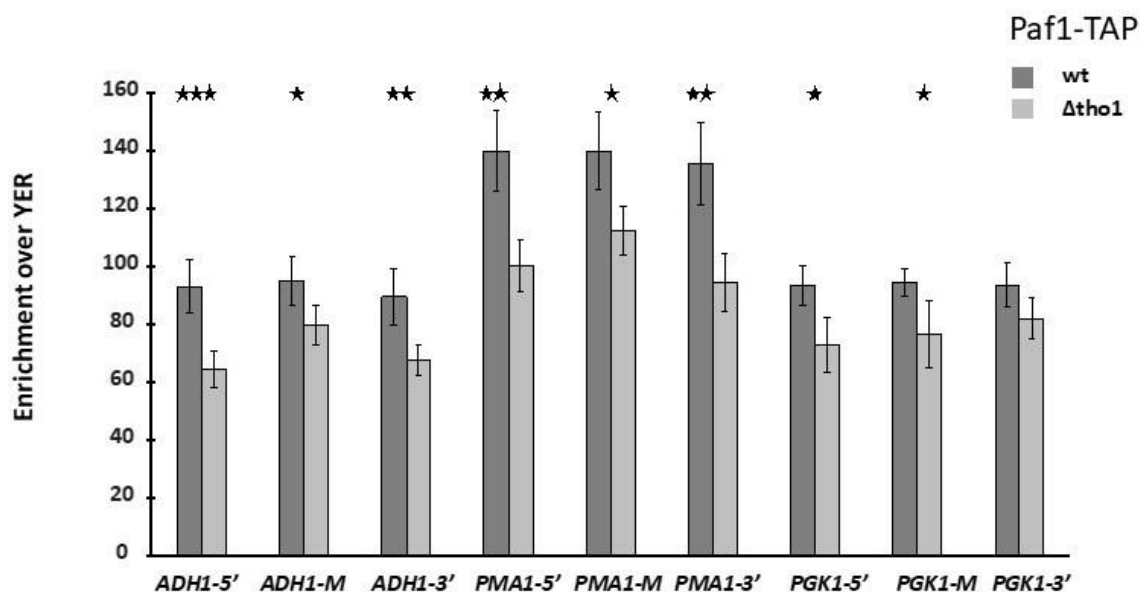


Figure 19. Paf1-TAP ChIP in RS453 strain \pm Δ tho1

The graph shows decreased occupancy of Paf1-TAP at the three control genes. The values for wt were significantly higher in Δ tho1 and the asterisks represent significance after analysing with a Student's *t*-test (* $P < 0.05$, ** $P < 0.01$ and *** $P < 0.001$) ($n=4$).

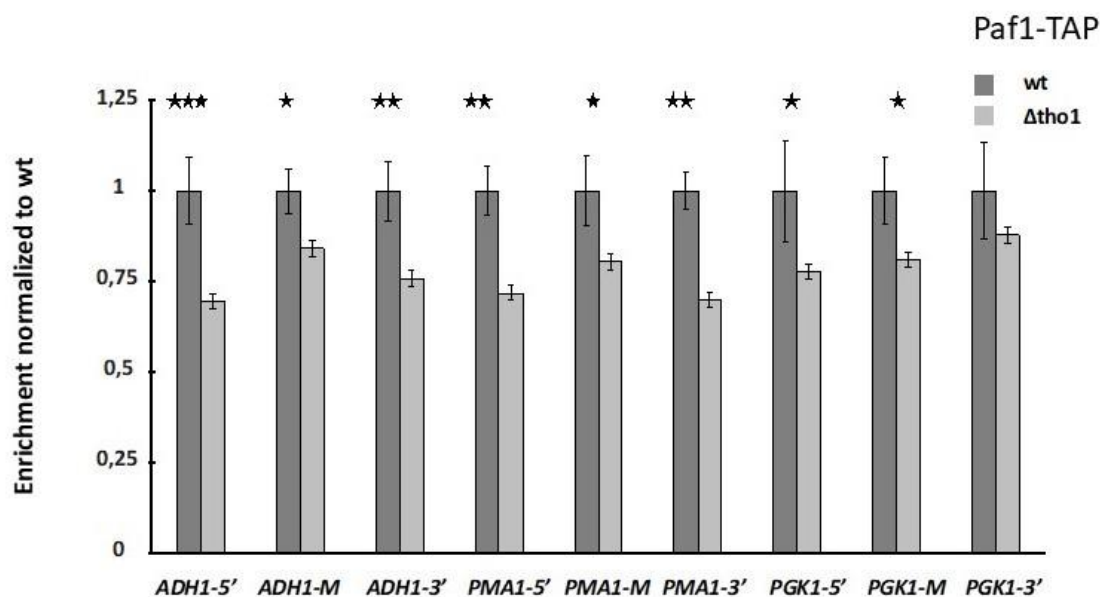


Figure 20. Paf1-TAP ChIP in a \pm Tho1 deletion RS453 strain

Here, Chip data was normalized to 1. Decrease in the Δ tho1 was clearly visible and reproducible (n=4).

3.1.4 Additional ChIP experiments to study Tho1 function in yeast

As seen in the aim of the thesis, the interaction of Tho1 with TREX, Spt5 and Paf1 was to be ascertained. Results from a separate set of experiments in our laboratory however showed the interactions. There was a complex interplay of protein interaction in various backgrounds. Nonetheless, these interactions in a severe growth impaired phenotype like Δ hpr1 and Δ paf1 makes interpretation of the results very laborious as the change in occupancy of RNAPII had to be considered. To study those interactions further, TAP Purification and pull-down experiment of the TAP tagged proteins in the different backgrounds had to be done.

Table 19. Summary of Tho1 interaction results by ChIP

strains	RNAPII	Hpr1	Tho1	Paf1	Spt5
spt5-S1A	no ch.	increase	decrease	decrease	no ch.
spt5-S1D	no ch.	decrease	slightly decrease	slightly decrease	no ch.
Tho1 overexpression	no ch. ©	decrease	(decrease)	no ch. ©	X
Δ hpr1	decrease	X	decrease, decrease normalized to RNAPII	no ch., increase normalized to RNAPII	X
Δ tho1	no ch. ©	increase	X	Decrease ©	no ch. ©
Δ paf1	decrease	no ch., increase normalized to RNAPII	no ch., increase normalized to RNAPII	X	X

Δ hpr1 and Δ paf1 had decreased RNAPII occupancy therefore, normalization to RNAPII had to be done for TAP strain tested in that background. © marked experiments are from this study. All other experiments carried out in the laboratory by Birte Keil. No ch. = no change and X = not done.

3.2 Purification of a specific nuclear mRNP in *saccharomyces cerevisiae*

As described in the introduction, mRNP components in yeast are well studied in terms of function and structure of most of the protein. The formation is essential for the survival of the cells though the assembly process (chronological order, building blocks) and the 3-D structure remains unclear. Recently, it was indicated that misregulation in mRNP formation could be linked to diseases like cancer or ALS, and therefore, the desire to understand those fundamental processes are essential. In the following part of this thesis, the establishment and modification of a protocol to purify a single species of mRNP and how samples were prepared for electron microscopy and cross-linking mass spectrometry (XL-MS) are shown in a chronological manner.

The first blueprint of the mRNP purification with anti-sense oligonucleotides was taken from the Handbook of RNA Biochemistry 1 (Hartmann, Bindereif and Schön, 2005), in which an article described the purification of the human spliceosome. Earlier, another article proposed the use of biotinylated antisense 2'-OMe RNA oligonucleotides for purifying human U4U& snRNPs from HeLa cells (Blencowe *et al.* 1989).

3.2.1 Selecting *CCW12* and *ILV5* as targets for specific nuclear mRNP in yeast

To purify a specific nuclear mRNP, one requires a highly transcribed nuclear mRNA. In a RNAPII screen done in our lab, the mRNA of *CCW12* and *ILV5* were identified as candidates with extremely high polymerase II occupancy. Thus, it is most likely that those mRNAs will be highly abundant in the nucleus during transcription. Moreover, another advantage of the two intron-less genes is that the genomic DNA of *ILV5* (1180 bp) is about two times longer as the *CCW12* (around 500 bp). It is known that the length of a nuclear mRNPs increases with the number of base pairs (Batisse *et al.* 2009). Under the EM, the particles of *ILV5* shall be twice longer compared to the *CCW12* mRNPs. In the same study, the mRNA of *CCW12* was described as highly abundant in a Nab2-TAP purification. In the present study, the total RNA of yeast was analysed in a RT-qPCR comparing the two candidates, *CCW12* and *ILV5* to our standard genes for ChIP experiments (*ADH1*, *PMA1* and *PGK1*) (Figure 21). Indeed, *CCW12* had the highest abundance of all mRNAs whereas *ILV5* had the lowest copy number (Table 20) in yeast total RNA. So, anti-sense oligonucleotides for the mRNA of *CCW12* and *ILV5* were designed, and the first experiments have been performed targeting the *CCW12* mRNA.

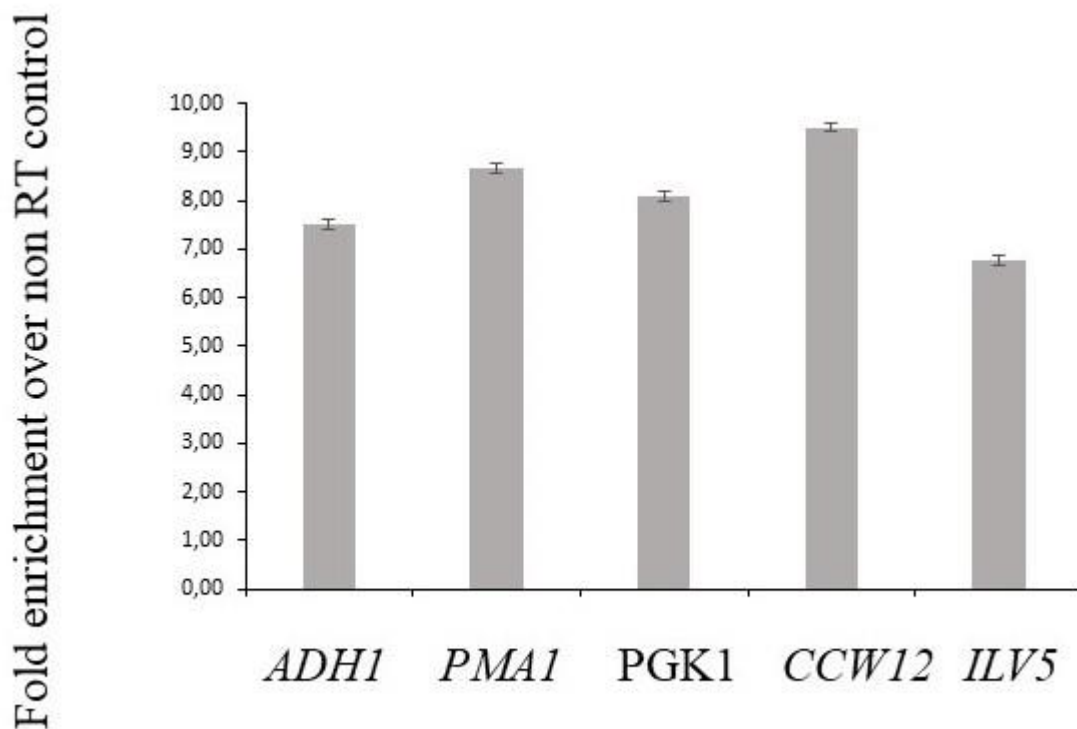


Figure 21. RT-qPCR experiment in yeast WCE

The abundance of *CCW12* and *ILV5* was analysed compared to the control genes of the ChIP experiments.

Table 20. Copy number of genes in yeast WCE

Gene	Enrichment over non-RT = Δ ct	Copy number ($=2^{\Delta}$ ct) per cell
<i>ADH1</i>	7,52	183
<i>CCW12</i>	9,51	729
<i>ILV5</i>	6,77	109
<i>PMA1</i>	8,66	404
<i>PGK1</i>	8,10	275

3.2.2 mRNP purification from RS 453 WCE

To start the purification of a specific nuclear mRNP from yeast, a fast and simple approach was employed using the anti-sense oligos (ASOs) of *CCW12* and *ILV5* in the crude yeast lysate.

From the international literature, it is known that some proteins could be extracted directly from HeLa whole cell extracts (WCE) (Blencowe *et al.* 1989) without any other preclearance. Therefore, 4x 2 l RS 453 from an overnight culture was harvested with an OD600 around 0.8. After the ultracentrifugation, 1ml of the lysate was frozen with 15 % glycerol. To the thawed sample, 12 μ l of a single anti-sense oligonucleotide of *CCW12* or *ILV5* (Table 8) was added, followed by mRNP purification (2.2.2.10). The qPCR results were calculated according to our laboratory's quality criteria (2.2.2.14). To compare the mRNA level of *CCW12* with that of *ILV5*, the mRNA was pulled down with the different ASOs. All enrichments were calculated over a mock control, and as a purity control, the *PGK1* mRNA in the samples were analysed. Before starting with the western blot analysis of the RBP components of the nuclear specific mRNP (Figure 22), the eight designed ASOs for *CCW12* have been tested with qPCR.

All the CCW12 oligos were able to purify CCW12 mRNA in higher amounts compared to their mock control (Figure 17). Only samples 5 to 7 had higher contamination of *PGK1* mRNA. Therefore, samples ASO 1-4 and 8 were used for further experiments.

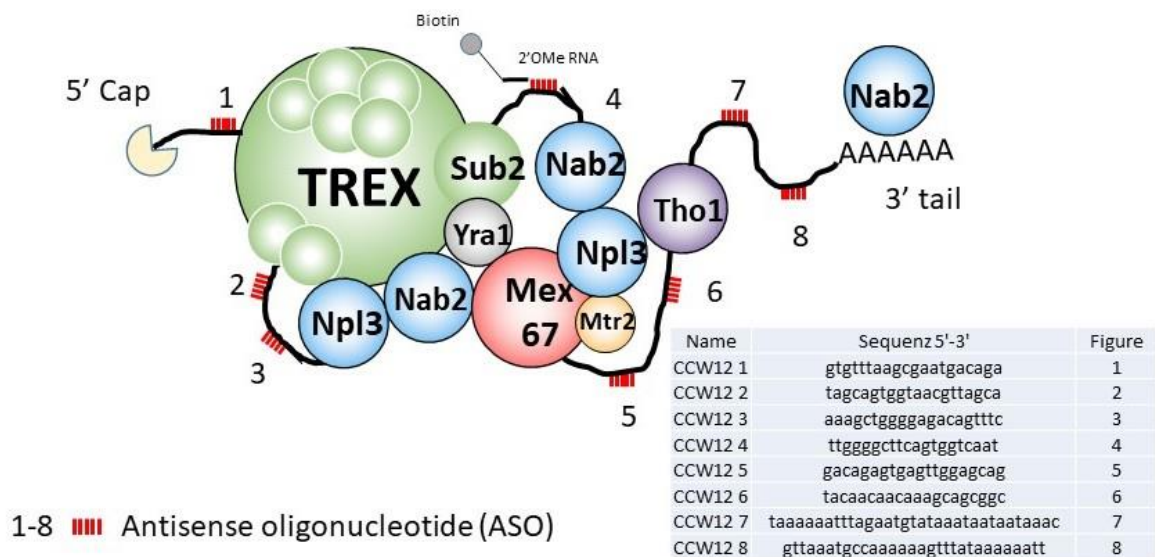


Figure 22. Schematic view of a nuclear specific CCW12 mRNP

The scheme shows TREX and other RBPs binding to the 5' capped and 3' tail polyadenylated mRNA of CCW12. The 2'-O-Me RNA antisense oligos (red) are bound to their complementary sequences among the mRNA body. In the box shows the 5'-3' sequence of the used oligos.

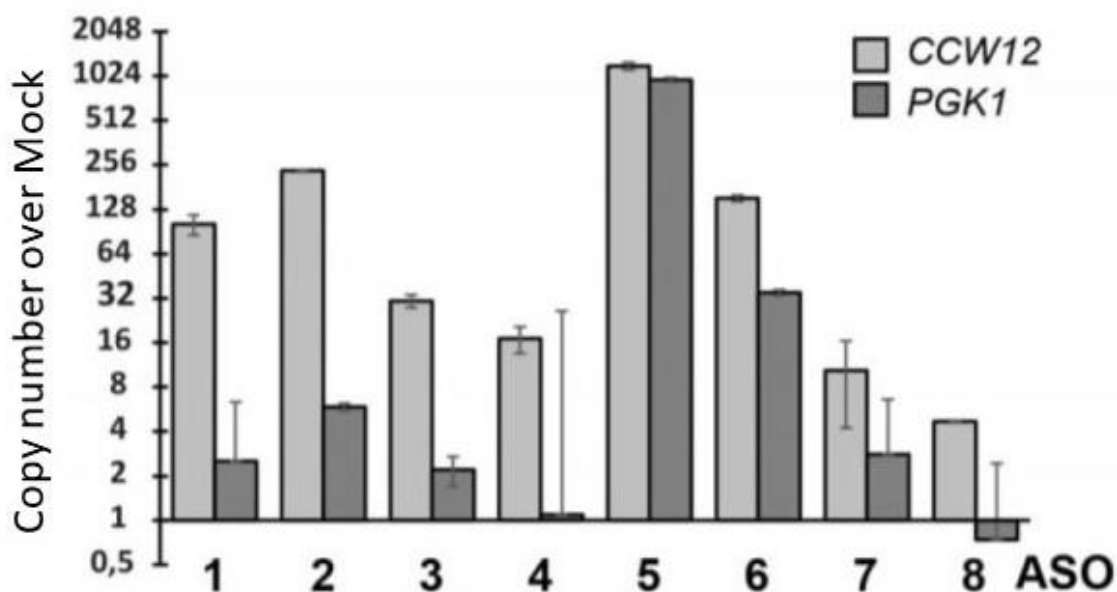


Figure 23. CCW12 Aso purification in RS453 WCE

The graph shows the enrichment of purified *CCW12* mRNA over mock using ASO 1 to 8. ASO 5 was not specific to purify *CCW12* mRNA. ($n = 4$), copy number = $2^{\Delta CCW12}$ or $\Delta PGK1$ (Table 21)

Table 21. Overview of CCW12 Aso purification in RS453 WCE for Figure 17.

<i>CCW12</i> ASO	$\Delta CCW12$	$\Delta PGK1$
1	6,8	1,4
2	7,9	2,3
3	4,7	1,2
4	4	0,5
5	10	9,9
6	6,9	4,9
7	3	1,5
8	2	-1

3.2.3 Optimization the pull-down for nuclear mRNP purification

The most important step apart from the binding of the 2'-OMe RNA oligonucleotides to the target mRNA in the purification process is the capture and pull down of the target mRNP from the input sample (lysate or later TEV-lysate). Therefore, streptavidin coated magnetic M280 Dynabeads™ (Thermo scientific) were used. The streptavidin biotin interaction is one of the strongest known with a $K_D = 10^{-15}$. The M280 which been used in the lab for other purification were compared with the three other streptavidin coated beads. In parallel four magnetic beads were used for the purification from RS lysate using ASO 2 and another time ASO 8. The M280 performed the best while the M270 (and its next Generation T1) were not so well suited for the ASO purification (Figure 24).



Beads	ASO	CCW12-Mock	PGK1-Mock	Relative amount
M280	2	-2,1	1,6	27,7
M270	2	2,1	4,7	28
C1	2	-3,3	-0,1	25,1
T1	2	-1,6	0,5	19
M280	8	-3,3	-1,6	25,4
M270	8	-2,2	-2	24,8
C1	8	-0,44	0,8	25,3
T1	8	0,87	1	22,7

Figure 24. Dynabeads Test with CCW12 ASO 2 and 8

The table shows the qPCR results for the mRNP purification of *CCW12* with Aso2 and 8 using four different beads. C1 beads are like M280 but with a lower nearly three times smaller diameter (1 μm to 2,8 μm).

3.2.4 Optimization of the input culture in terms of strain and optical density

The sample preparation for an mRNP experiment is not so easy because one must harvest the pellet of eight litre culture with an OD600 around 0.8. The same pellet preparation is used as done for TAP experiments. The new culture was labelled 2 l with an OD600 of roughly 3.5. The sample was cross-linked as described in (2.2.2.7). The mRNP purification with *CCW12* ASO 2 showed that the samples were equally suited for mRNP purification (Table 22). Therefore, for the next experiments, cultures of 2 l with an OD600 of roughly 3.5 were harvested. In the qPCR results, there was no observed change for UV crosslinked samples.

Nab2-Tap is known to be suitable for purifying many nuclear mRNPs from yeast (Batisse *et al.* 2009) thus, TEV eluates from TAP purifications were used as starting material for the anti-sense purification. Hpr1-TAP and Cbc2-TAP strains were used to purify *CCW12* mRNP with ASO2 (Table 23).

Comparison of TEV eluate and input samples on Western blot after mRNP purification revealed the presence of Pab1 in the mock control of the WCE (Figure 25) but not in the mock of the TEV eluates. The total amount of PAB1 in the lysate samples was only slightly higher than in TEV eluates. It is known that Pab1 is not only localized in the nucleus but also in the cytoplasm in a higher amount. Therefore, Pab1 was eliminated as one of the western blot controls since it seems not be specific for the nuclear pool of proteins.

While purifying from TEV eluates it was observed that using high salt buffer leads to a decreased presence of Yra1 on western blot (Figure 26). So, the last high salt washing step during the mRNP purification was replaced by another wash with low salt buffer.

Table 22. Testing different OD600 and UV cross-linking for mRNP purification

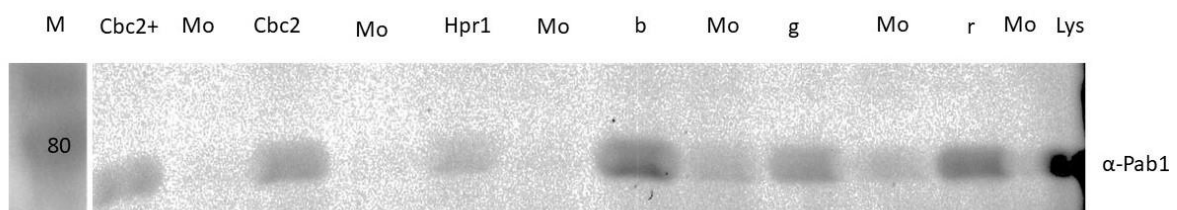
sample	ct <i>CCW12</i>	ct <i>PGK1</i>	<i>CCW12</i> -Mock	<i>PGK1</i> -Mock	<i>CCW12</i> - <i>PGK1</i>
r Aso2	24	29,1	-6	-4,3	-6,2
r mock	30	34			
r Input	14	18,3			
g Aso2	24,4	30,8	-5,7	-1,5	-6,4
g mock	30	32,3			
g Input	15,5	18,8			
b Aso2	23,9	28	-5,8	-2	-4
b mock	29,7	30			
b Input	15	18,1			

r = 4x 2 l OD600:0,8 g = 2 l OD600:3,5 b = g + cross-linking at 254 nm with 1,2 mJ

Table 23. Testing different TAP strains and UV cross-linking for mRNP purification

sample	ct <i>CCW12</i>	ct <i>PGK1</i>	<i>CCW12</i> -Mock	<i>PGK1</i> -Mock	<i>CCW12</i> - <i>PGK1</i>
Hpr1 ASO	27,7	34,4	-3,2	2,9	2,9
Hpr1 Mock	30,8	31,6			
Hpr1 Input	23,4	23,3			
Cbc2 ASO	23,7	25,5	-5,1	-1,8	-1,8
Cbc2 Mock	28,8	27,3			
Cbc2 Input	20,9	19,7			
Cbc2 ⁺ ASO	25,2	28,3	-4,8	-0,8	-3,1
Cbc2 ⁺ Mock	30,2	29,1			
Cbc2 ⁺ Input	20,6	20,7			

Cbc2⁺ cross-linked sample Cbc2TAP

**Figure 25. nuclear mRNP purification with TEV and WCE in WB comparison**

The Western blot (WB) shows the enrichment of Pab1 in the purification from various starting materials compared to their Mocks (Mo). In the mock of the lysate samples b, g and r the amount of Pab1 was detected, but the Mock controls of the TAP strains are empty. The samples are indicated and described in Table 22 and Table 23. M stands for marker.

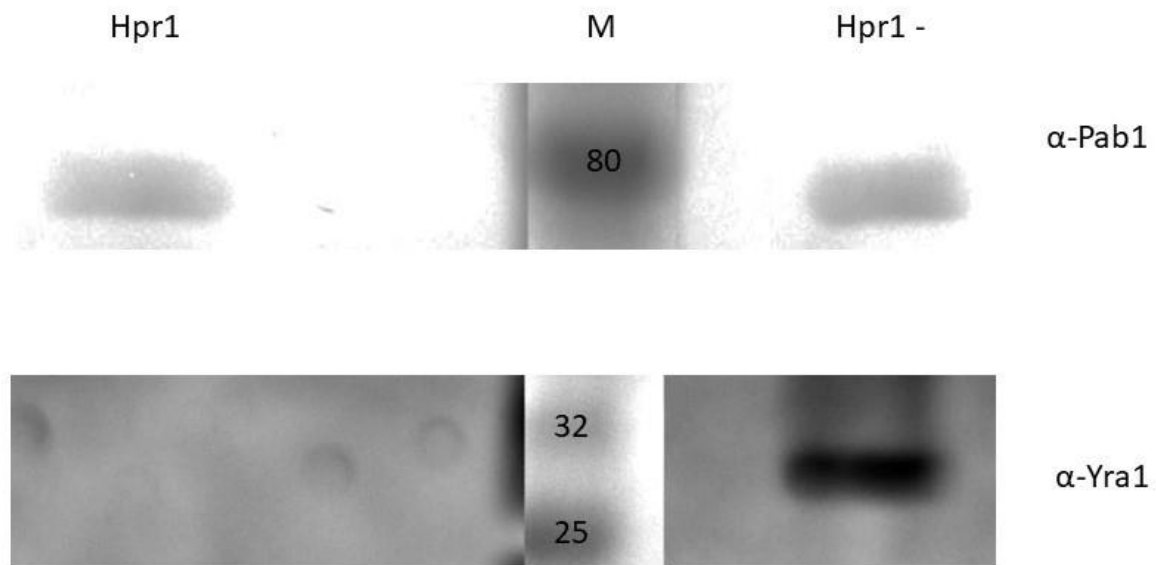


Figure 26. mRNP purification in a Hpr1-TAP strain with or without high salt buffer

On the left side, the high salt Hpr1 sample shows one band in the Pab1. The Yra1 signal is missing compared to the preparation without high salt (Hpr1-).

In the mRNP purification six RBPs were detected on WB and in the qPCR the mRNA was enriched. Work with Cbc2-TAP was continued for two reasons. First, each specific nuclear mRNP should have a 5' cap for correct maturation and folding. The second reason is that TAP purification of Cbc2 is easier to handle and at least on the SDS PAGE the yield of the target protein was higher compared to Hpr1. All mRNP purification optimization experiments using a pellet from Cbc2-TAP with or without UV cross-linking from a 2 l culture with OD600: 3,5 The TAP purification was always performed to the TEV eluate which was used as input for the anti-sense purification of the nuclear *CCW12* mRNP.

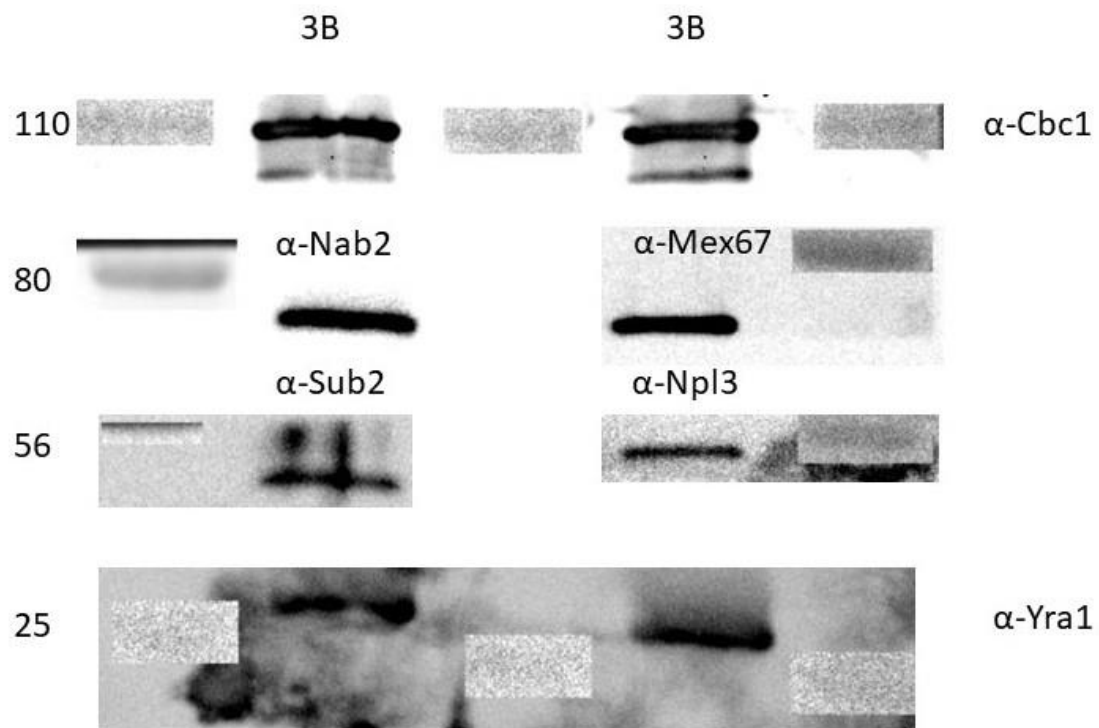


Figure 27. WB set for mRNA purification experiments in a Cbc2-TAP strain

The panel shows six of the eight antibodies analysed on WB in the *CCW12* mRNP purification. Only Pgl1 and Tho1 are missing. The marker band for Tho1 is 32 kDa and that for Pgl1 46 kDa. Pgl1 as negative control is only visible in TEV eluates if it contains impurities of cytoplasmic proteins. The qPCR results can be found in Table 24.

Table 24. qPCR of Cbc2-TAP *CCW12* mRNP purification from Figure 27

Sample	<i>CCW12</i>	<i>PGK1</i>	<i>CCW12-PGK1</i>
TEV	17,8	20,8	-3
ASO 3	22	26,8	-4,8

3.2.5 Comparing a mixture of good *CCW12* ASOs with ASO 2 from *CCW12* and modifying the ultracentrifugation step (UZ)

For some targets like the Xist RNA (Minajigi et al. 2015 and McHugh et al. 2015), purification with a mixture of anti-sense oligonucleotides have been shown to be successful. Therefore, the oligos were tested as mixtures compared to ASO 2 which performed the best in the qPCR studies. Four mixtures and ASO 2 were tested on WB for five proteins (Table 25). Unfortunately, no Yra1 or Nab2 were detected in any of the samples. Sub2 was present as a 58 kDa signal for the full-length protein and as a 46 kDa indicating a degradation product signal (Figure 28). Compared to the Sub2 signals Npl3 was only barely visible. A modification of the ultracentrifugation step (UZ) was further done. However, instead of 35k rpm for 45 min, the samples were either run for 30 min at 10k rpm or the pre centrifugation in a falcon tube was extended to 20 min. The lysate after 30 min ultracentrifugation at 10 k rpm was most of the time clear, just like the one at 35 k rpm. The pellet was smaller, but the detection of the target RBPs signals on WB (Table 26) have been visible. Nab2, Npl3 and Yra1 were found in those experiments (Figure 29 and Figure 30). Surprisingly, for Sub2, most of the degradation product at around

46 kDa (Figure 29) was detected. Since in the ASO2 purifications less proteins were detected on WB compared to the mixtures, CCW12 ASOs (except ASO5 because it was not specific enough) were tested with the new centrifuged samples. Four Proteins, Nab2, Sub3, Npl3 and Yra1 were detected in nearly all mRNP purifications with 10k rpm centrifugation step (Figure 31). In ASO 2 samples, the highest amount of mRNA was found but not all the proteins were detected.

The samples without UZ were not clear and dense before going through the mRNP purifications step. Although a lot of proteins for the different ASOs were found, it was still surprising that the Mock control had such a high signal for Sub2 and Npl3 (Figure 32). After calculating copy numbers from the qPCR results as described (2.2.2.16) for all experiments, with the different centrifugation step (Table 29), the purification was modified to 25 k rpm for 25 min at the lysate preparation step because the UV cross-linked were not clear after the 10 k rpm UZ.

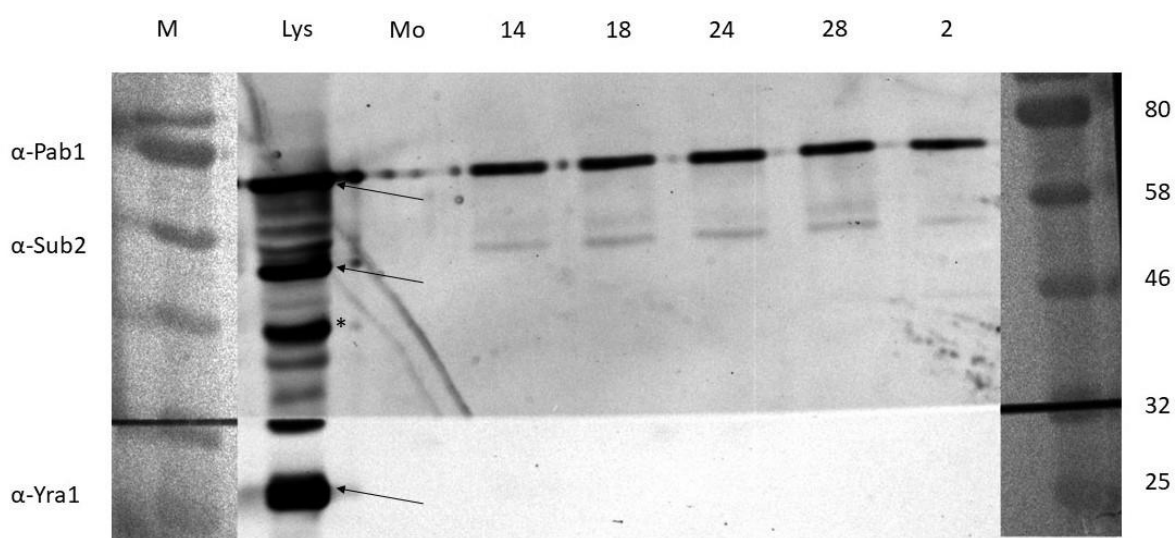


Figure 28. WB analysis of various CCW12 ASO mix compared to ASO 2 and lysate

In the lysate sample, the target proteins Pab1, Sub2 and Yra1 are marked with an arrow. The signal at 46 kDa marked with an asterisk is the degradation product of Sub2 which was found in some mRNP purification. A faint Pab1 signal was also found in the Mock control while the Sub2 signal was only visible in the lysate and all ASO purifications. For Yra1, only a strong signal in the lysate was detected. Mixture 14 contained 3 μ l of each CCW12 ASO from 1 to 4, Mixture 18 contained 2.4 μ l μ l of each CCW12 ASO from 1 to 4 plus 8, Mixture 24 contained 6 μ l of each CCW12 ASO from 2 and 4, and Mixture 28 contained 4 μ l of each CCW12 ASO from 1.4 and 8. The evaluation for each protein have been shown in Table 25.

Table 25. WB pattern comparison of CCW12 ASO 2 with ASO mixes at 35k rpm

sample	Nab2	Npl3	Pab1	Sub2	Yra1
ASO 2	--	-	++	-/-	--
14	--	-	++	-/-	--
18	--	--	++	-/-	--
24	--	-	++	-/-	--
28	--	-	++	-/-	--

-- Not detectable; - faint; x/x two bands; + visible; ++ strong

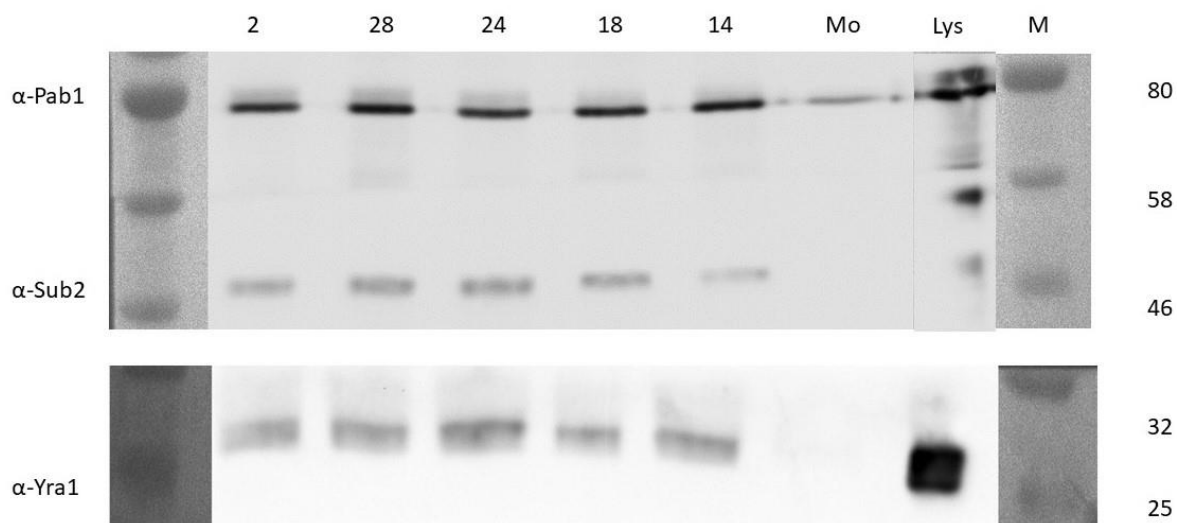


Figure 29. WB of various *CCW12* ASO mix compared to ASO 2 and lysate at 10 k rpm part I

At 10 k rpm ultracentrifugation speed, the western blot for Pab1, Sub1 and Yra1 showed more signals for the same set of samples as in Figure 28. Yra1 was present in all samples except the mock. For Sub2, the degradation band at 46 k Da was detected. The evaluation for each protein can be seen in Table 26.

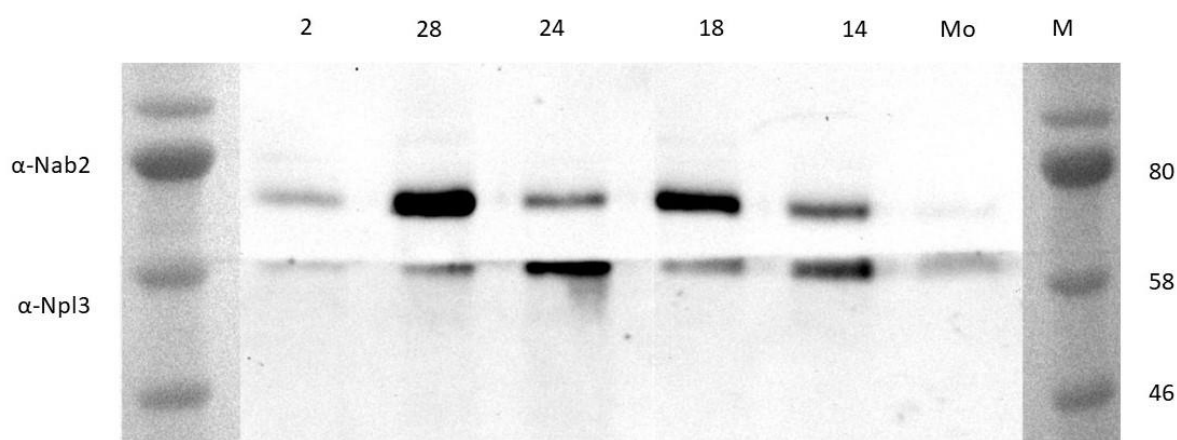


Figure 30. WB of various *CCW12* ASO mix compared to ASO 2 and lysate at 10 k rpm part II

In the sample with 10 1 rpm UZ Nab2 was detected in all samples except the mock. Also, Npl3 was more enriched in the purifications of the mock compared to the ASO 2. The evaluation for each protein can be seen in Table 25.

Table 26. WB pattern comparison of *CCW12* ASO 2 with ASO mixes at 10k rpm

sample	Nab2	Npl3	Pab1	Sub2	Yra1
ASO 2	-	-	++	-	+
14	+	++	++	-	+
18	++	+	++	-	+
24	+	++	++	-	+
28	++	+	++	-	+

-- Not detectable; - faint; + visible; ++ strong

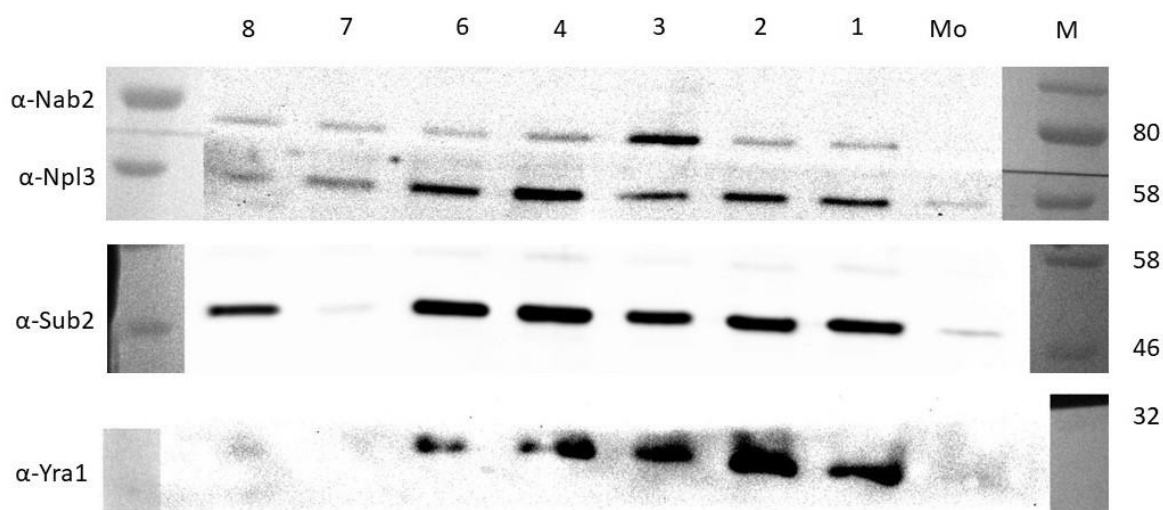


Figure 31. WB analysis of CCW12 ASO 1-8 at 10 k rpm UZ

Protein distribution of Nab2, Npl3, Sub2 and Yra1 in CCW12 ASO 1-8 purification. In the mock, faint signals for Npl3 and Sub2 were observed. Sub2 signals were present, but the degradation product was more prominent. The evaluation for each protein is illustrated in Table 27 (no ASO 5).

Table 27. WB pattern comparison of CCW12 ASO 1 to 8 at 10k rpm

sample	Nab2	Npl3	Sub2	Yra1
ASO 1	+	+	+/-	++
ASO 2	+	+	+/-	++
ASO 3	+	++	+/-	++
ASO 4	++	+	++/-	+
ASO 6	++	+	++/-	+
ASO 7	-	+	-/-	-
ASO 8	-	+	+/-	-

-- Not detectable; - faint; x/x two bands; + visible; ++ strong no ASO5

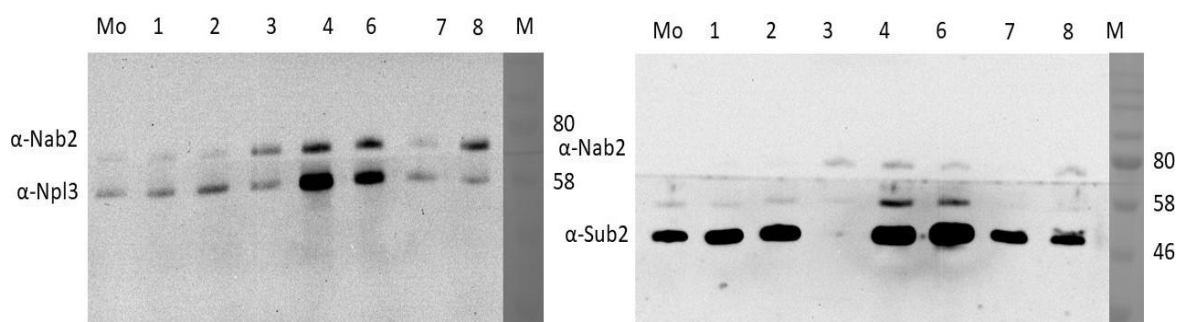


Figure 32. WB analysis of CCW12 ASO 1-8 without UZ

Protein distribution of Nab2, Npl3, and Sub2 in CCW12 ASO 1-8 purification without ultracentrifugation. In the mock high signals for Npl3 and Sub2 were detected. Sub2 signals are present, but the degradation signal is more prominent at 10 k rpm (Figure 31). The evaluation for each protein can be seen in Table 28 (no ASO 5).

Table 28. WB protein pattern comparison of CCW12 ASO 1 to 8 without UZ

sample	Nab2	Npl3	Sub2
ASO 1	-	+	+/-
ASO 2	-	+	+/-
ASO 3	+	+	-/-
ASO 4	++	++	+/>++
ASO 6	++	++	+/>++
ASO 7	-	+	+/-
ASO 8	+	+	+/-

-- Not detectable; - faint; x/x two bands; + visible; ++ strong no ASO 5

Table 29. copy number calculation for ASO 2 and 3 with different centrifugations

CCW12 ASO	ct old	ct 10 k rpm	ct no UZ	Copy number old	Copy number 10 k rpm	Copy number no UZ
2	22,1	21,6	26,7	650000	1940000	58150
3	23,8	22,9	27,1	472000	895000	46230

ct: ct value UZ: ultracentrifugation steps

3.2.6 Cross-linking of Hpr1-TAP with formaldehyde and glutaraldehyde

Formaldehyde is a chemical long known in biology for being able to modify biological molecules to allow their physical interaction, for example, protein-protein interactions or DNA-protein interactions. The molecules are so small that they can travel through the cell membrane and enter the nucleus to cross link with their DNA and proteins, which are used in ChIP experiments (2.2.2.12). To stop the reaction and stabilize the complexes, a quencher is added after a certain incubation time. Instead of formaldehyde another substance called glutaraldehyde can be used too. Both crosslinkers are widely used in literature and their concentrations range from 1 % to 0,0001 % with various incubation times. Five samples of Hpr1-TAP were cross-linked with formaldehyde (number 2 to 6), and two samples with glutaraldehyde (samples 7 and 8) (Figure 33). Only sample 5, 6 and 8 showed the typical SDS PAGE purification pattern of Hpr1-TAP. The options with low amounts of cross-linker (0,1% and 0,001%) and short incubation period of 5 min could be implemented in further mRNP purifications.

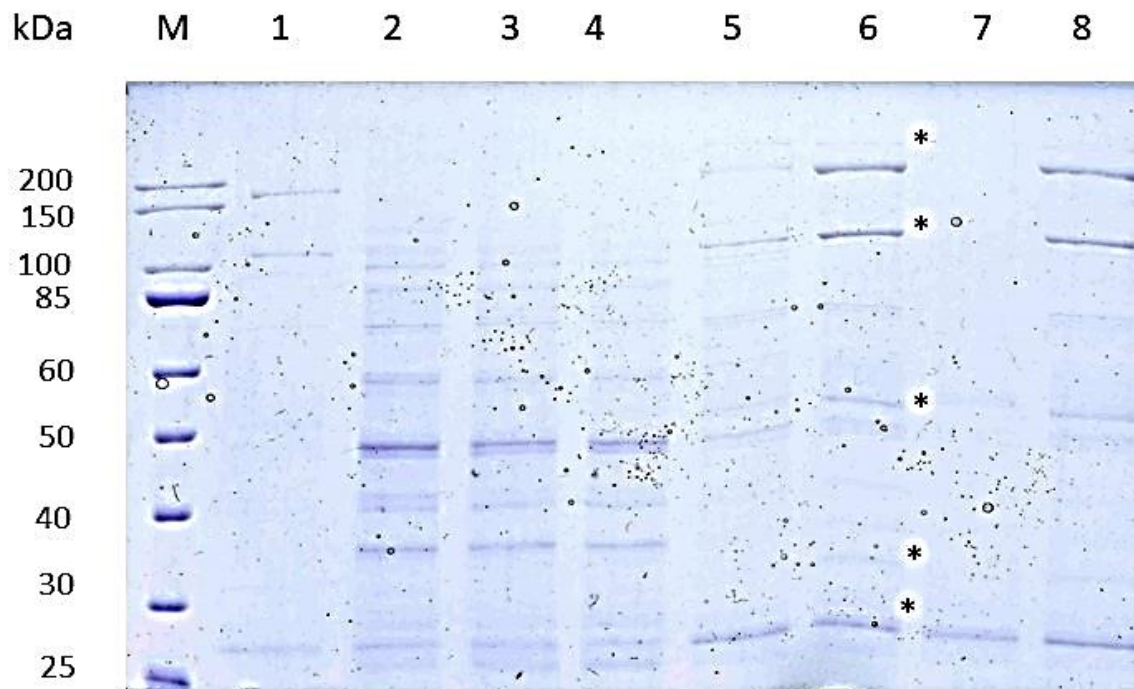


Figure 33. Cross-linking of Hpr1-TAP with formaldehyde and glutaraldehyde

The SDS PAGE shows the purification results of Hpr1-TAPs with different concentrations of formaldehyde ranging from 1% (lane 2-4), 0,1 % (lane 5) to 0,01 % (lane 6), and for glutaraldehyde, 1% (lane7) to 0,01 % (lane 8). Lane 2 to 4 differ in their incubation times thus,5, 10 and 20 min, respectively. The control Hpr1-TAP in lane 1 did not work well and had too less materials for the visualization of the characteristic TREX pattern as seen in lane 6 (with the asterisks). On the top are Tho2 (184 kDa) and Hpr1 (110 kDa). Around 50 kDa the protein bands of Sub2, Mft1, Tex1 and Gbp2 are clearly visible. Over 30 kDa is the Thp2 protein and around 27 kDa, there are Yra1 with the TEV protease in each lane. Only lanes 5, 6 and 8 resemble the control pattern in lane 1.

3.2.7 ATP- γ -S a trap for Sub2 in TAP purification with or without MgCl₂

The helicase Sub2 was present in the mRNP purification in two characteristic signals on western blot (Figure 31). A signal around 56 kDa belongs to the active enzyme while the lower band around 46 kDa is most likely a degradation product. Since Sub2 is active in formation of nuclear mRNPs, is not yet clear if the protein is part of the target mRNP structure. In this experiment, the changes in Sub2 on western blot was evaluated after using the ATP analogue, ATP- γ -S, in order to prevent the ATPase activity of Sub2. Therefore, 4 mM of ATP- γ -S were added to the lyses buffer and TAP purification was further performed (Figure 34). In the same approach the MgCl₂ concentration of the TAP buffer was modified. MgCl₂ is known to be important for enzymes like DNase, however, high concentrations are needed for isolating polyribosomes. Mg²⁺ is the most important ion to stabilize RNA-protein interactions.

The standard buffer (wt) contained 1.5 mM MgCl₂, and increased amounts of the salt was added to a final concentration of 3 mM (+). The buffer, without MgCl₂ (-), was tested with ATP- γ -S (y) in a TAP purification (-y). Interestingly, most of proteins were not somewhat affected by the changes. In both experiments, the Sub2 signal was detected on the right, high under 56 kDa. Pgk1, a plasmatic protein, served as a negative control. The exposure time of this extremely sensitive antibody was set to 1 min and the faint bands on the left side were very weak compared to the lysate signal (Figure 34). Therefore, the second purification was not as clean as the first one. In the first experiment, the detection of Npl3 and Nab2 signals were done under overexposed conditions in the WB, as seen in the brighter filled signals (left site Figure 34). From the two WB, it is hard, without consistent pattern, to draw a conclusion

on the presence of Sub2. A few years ago, the crystal structure of a UAP56 (human Sub2) mutant was crystallized with Mg-ADP (Shi *et al.* 2004). Therefore, using ATP analogues or MgCl₂ might be a good avenue to study the helicase Sub2. Only Tho1 seemed to be increased the absence of MgCl₂. Experiments changing only the MgCl₂ concentration had a high impact on the purified *CCW12* mRNA (see Table 30). Therefore, the purification buffer contains MgCl₂.

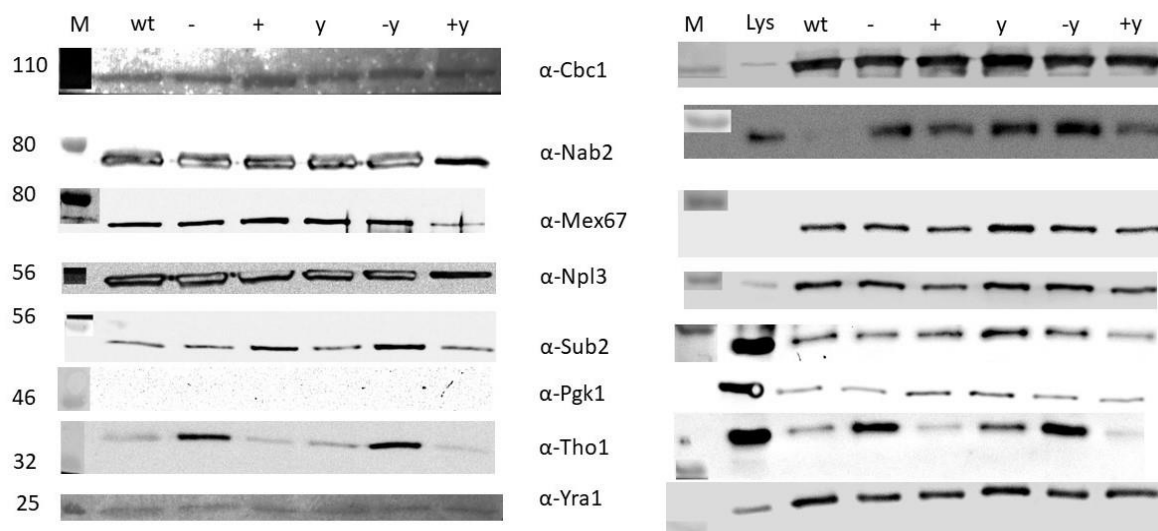


Figure 34. Cbc2-TAP with or without ATP- γ -S and three different concentrations of MgCl₂
Comparison of two Cbc2-TAP purifications with ATP- γ -S(y) in TAP buffer without the ATP analogue (wt). The two samples were purified in addition with higher MgCl₂ concentration (+y or x) or without MgCl₂ (-y or -). All WB control proteins were visible in the purifications except Pgk1, the negative control which indicates the purity of the TEV eluate. Only Tho1 seems to be directly affected by the MgCl₂ concentration.

Table 30. qPCR of three *CCW12* ASO 3 purifications with different concentrations of MgCl₂

Sample	<i>CCW12</i>	<i>PGK1</i>	<i>CCW12-PGK1</i>
TEV	17,3 ± 0,3	19 ± 0,8	-2,7
0	24 ± 0,3	27,7 ± 1,8	-3,5
1.5 mM	22 ± 0,4	28,8 ± 1,3	-6,8
3 mM	22,5 ± 0,4	29,6 ± 1,1	-7,05

3.2.8 Anti-sense oligo optimization: biotin vs desthiobiotin

The modification of commercial oligos is endless and for each scientific question optimized. One can add molecules like GFP or YFP on 5' or 3' ends of proteins for localization experiments, or other fluorescent dyes such as FAM™ are used in qPCR experiments. The anti-sense methylated RNA oligos are 5' labelled with biotin or desthiobiotin for purification of a specific nuclear mRNPs. Since biotin streptavidin is the strongest interaction known in science, the binding of the target to the magnetic beads should be extraordinarily strong. It is impossible to analyse the target further on beads therefore, the mRNP must be removed. Furthermore, this could be done in two ways. First, by adding free biotin to substitute the bound mRNP, and second, by the addition of a displacement oligonucleotide. A modified

version of biotin, the so called desthiobiotin, can also be used. Moreover, it does not bind so strong to the beads and can be exchange easier by the two elution methods. The TAP purification as starting point of the mRNP purification can enrich a lot of RBPs. Only Sub2, Tho1 and Pgc1 are exceptions (Figure 35, right side). When purifying Cbc2-TAP with *CCW12* ASO 3 biotinylated (B as first letter) vs desthiobiotinylated (D as first letter) using both elution methods (B for biotin elution and D for the displacement of elution as second letter), one can observe that the elution in the samples with the desthiobiotin ASO3 yields higher signals in the western blot. The Biotin elution DB has the strongest Nab2 signal and other proteins like Npl3, Sub2 Cbc1 and Yra1 are also visible. The Biotin ASO 3 samples have the lower yield, so it is right to assume that if a lot of target mRNPs bind due to the strong interaction of streptavidin and biotin, it is extremely hard to recover them (Figure 35, left side).

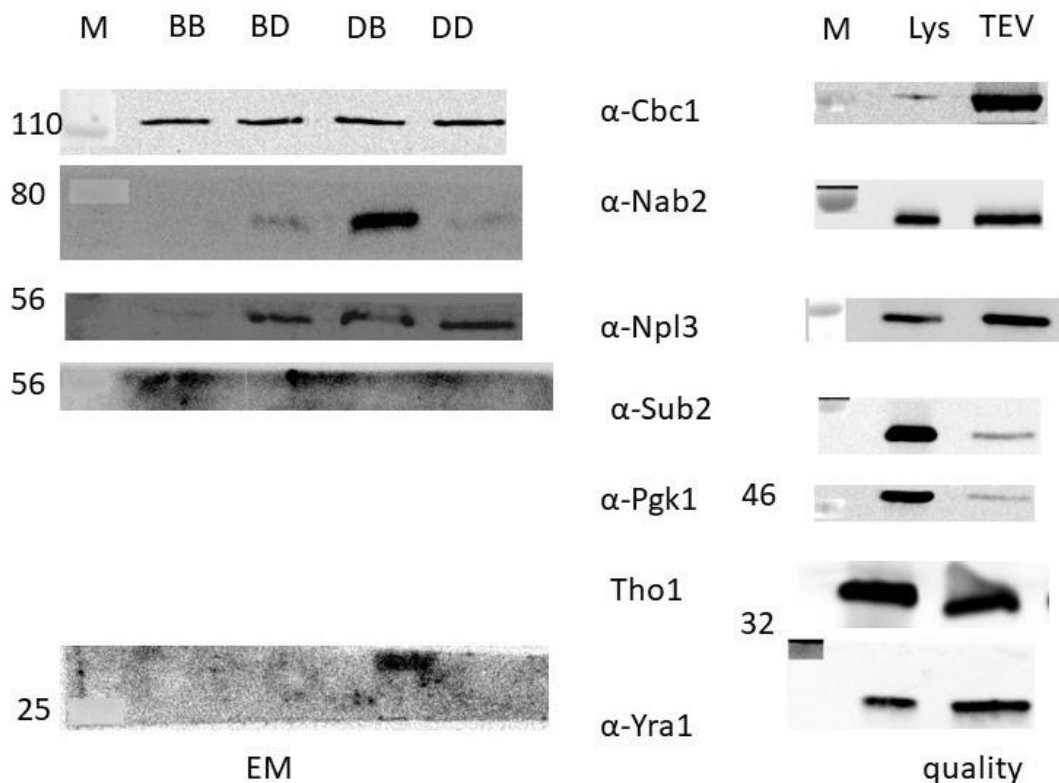


Figure 35. WB analysis of biotin and desthiobiotin eluted samples for EM

On the right is the quality control, the comparison of lysate and TEV eluate for the control set of proteins (Cbc1, Nab2, Npl3, Sub2, Pgc1, Tho1 and Yra1). In TEV eluate, all these proteins are enriched compared to the input except for Sub2, Tho1 and PGK1 (an indicator for cytoplasmic impurities in the TAP purification). Usually not the whole set is visible after the elution from the M280 beads. On the left side is the WB for the EM samples. *CCW12* ASO 3 biotin (B first letter, BX) was added in two samples of ASO 3 desthiobiotin (D first letter, DX), and eluted with biotin (B second letter, XB) or desthiobiotin (D second letter, XD). The sample DB showed the most protein signals on WB while the BB showed the least signals.

When comparing negative stains of the biotin elution with the displacement elution of *CCW12* desthiobiotin ASO 3, many aggregates were observed on the grid in the lowest zoom (Figure 36) under the EM. Those aggregates are non-specific accumulation of proteins and it's known from literature that a lot of displacement oligos form primer dimer, which can promote aggregation. Therefore, the purification with displacement oligos was abandoned. While analysing the biotin elution samples of both *CCW12* ASO 3's particles of the expected seize, for a specific nuclear *CCW12* mRNP were found (Figure 37). Based on available literature (Batisse *et al.* 2009), the particles are around 8 nm x 20 nm. Still, a lot of optimization must be done to also purify *ILV5* specific mRNPs (Figure 38 Figure 39 and Figure 39). The amount of *ILV5* is still low compared to the *CCW12* (compare Table 29 and Table 31).

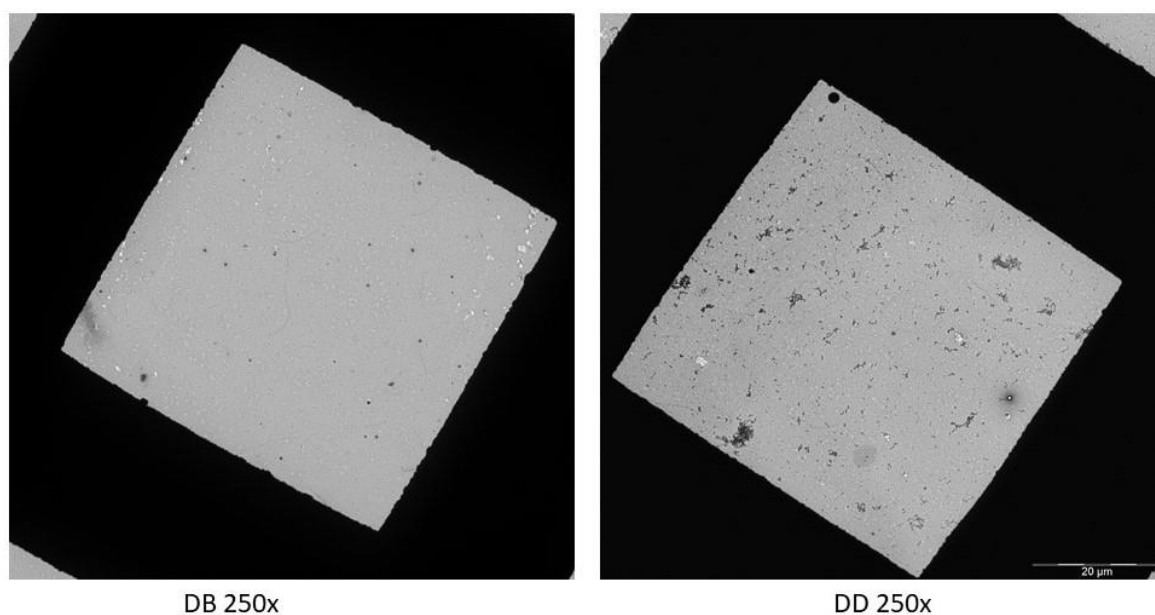


Figure 36. Negative stains from *CCW12* biotin elution and displacement oligonucleotide elution
The picture shows the comparison of a sample *CCW12* desthiobiotinylated ASO 3 eluted with biotin (on the left side, DB) with a sample, DD (on the right side), which was eluted with displacement oligo at a low EM magnification of 250. In the DD sample, there are too many aggregates compared to the clean sample on the left side. Zooming into the DB samples, the specific *CCW12* mRNPs were detected (Fig31).

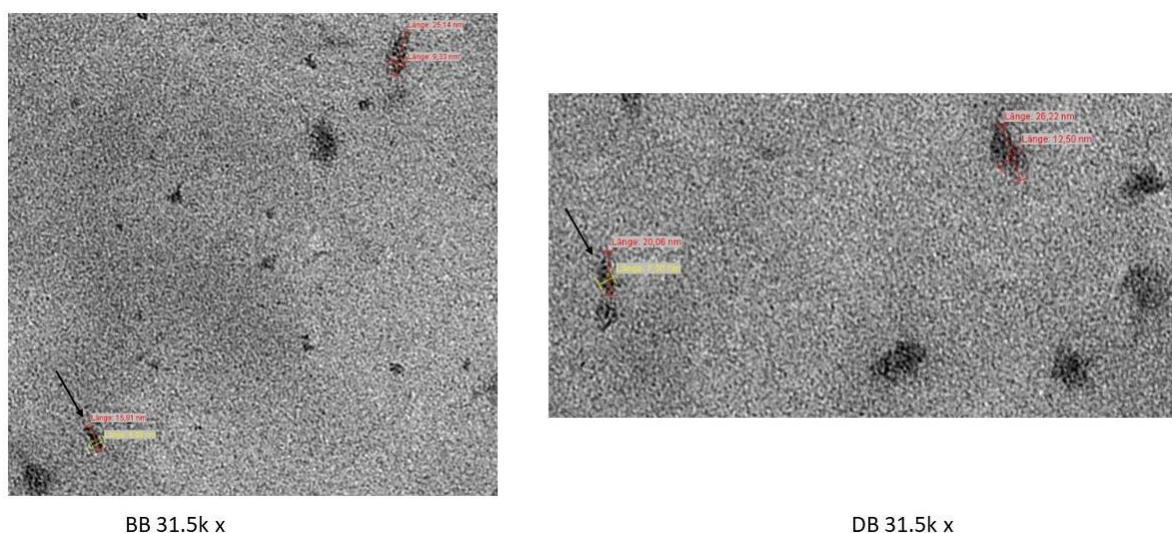


Figure 37. Biotin elution samples of (desthio)biotinylated *CCW12* ASO 3 under the EM
The images show the uranyl stain of the mRNP purification of the biotinylated *CCW12* ASO 3 (BB, on left side) and the desthiobiotinylated ASO 3 (DB, on right side). The two arrows mark the detected *CCW12* mRNPs in the sample. The elution in both cases were done with biotin. Both particles fit the 8 nm x 20 nm predicted size. The pictures were taken at a magnification of 31.5k.

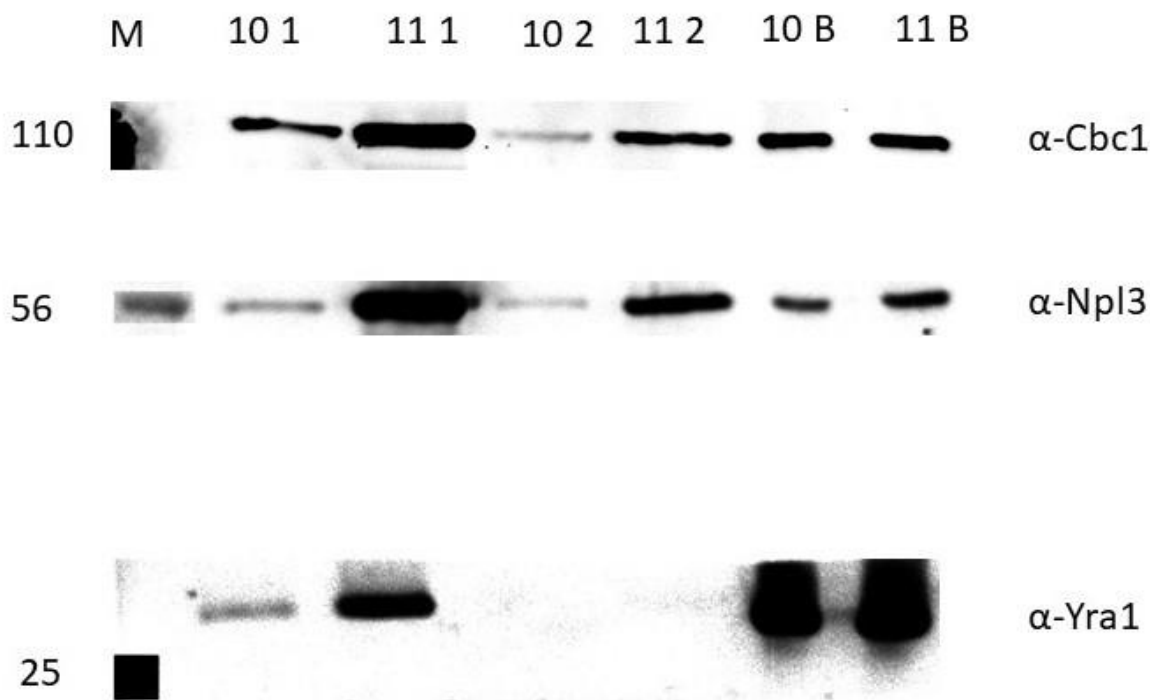


Figure 38. *ILV5* 11 and 10 mRNP elution with biotin from magnetic beads

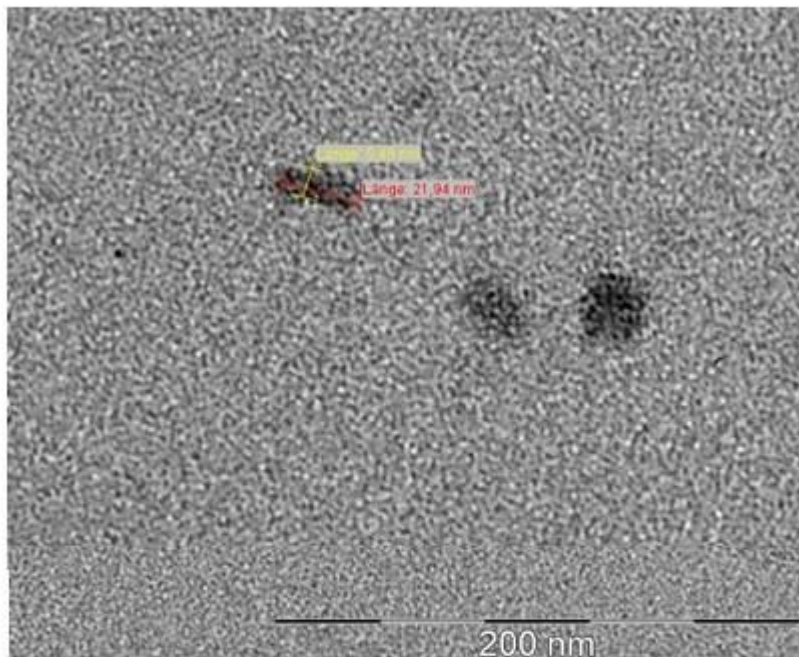
The first elution of *ILV5* ASO10 (10 1) contains less Cbc1, Npl3 and Yra1 compared to ASO11 (11 1). The same beads were incubated with fresh elution buffer + 5 mM biotin and incubated for another 30 min before the elution was collected. In the second elution step ASO 11 (11 2), still had more protein signals for Cbc1 and Npl3 as ASO 10 (10 2). The second elution did not have Yra1 in detectable range. Some proteins stayed bound to the beads even after the second elution of ASO 10 (10 B) and 11 (11 B). The qPCR results are listed in Table 31.

Table 31. qPCR results of *ILV5* mRNP purification with ASOs 10 and 11

Sample	<i>ILV5</i>	<i>PGK1</i>	<i>ILV5-PGK1</i>
10 1	28,9	30,5	-1,6
11 1	27,5	27	0,5
10 2	31,9	33,3	-1,4
11 2	29,9	31,4	-1,5
10 B	27,6	30,7	-3,1
11 B	27,8	29,3	-1,5

10 /11 1: first elution with biotin 10 /11 2: second elution with biotin
fraction after 2x elution

10/11 B: beads



11 1 B 31.5k

Figure 39. First biotin elution of *ILV5* ASO 11 under the EM

The image shows the uranyl stain of the mRNP purification of the biotinylated *ILV5* ASO 11 (11 1 from Table 31). The elution was done with biotin (B). All three visible particles in the picture do not fit the expected size of 8 nm x 40 nm. The picture was taken at a magnification of 31.5k.

3.2.9 Purification of nuclear mRNPs using a temperature sensitive yeast mutant

It has been shown that a *mex67-5* mutation results in an mRNA export defect at 37 °C (Segref *et al.* 1997). As observed, nuclear accumulation could be used to enrich specific nuclear mRNP in the nucleus to make the mRNP purification easier. Therefore, Hpr1 and Cbc2 were tagged in a *Mex67*-shuffle strain (2.2.2.6). From each strain, two clones were taken and the control plasmid pUN100 *Mex67* was added to one clone, and the pUN100 *mex-67-5* plasmid, into the other. Since the defect in mRNA export for Hpr1-TAP *mex67-5* was already shown, this strain was used as a control for the Cbc2-TAP experiment. Indeed, the Cbc2-TAP tagged strain showed an accumulation of mRNA labeled with Cy3 against poly (A) which colocalized with DAPI signal of the nucleus (Figure 41). This was observed in the experiment with the Hpr1 as well (Figure 40). Taken together, using the export mutant of *Mex67* might help to purify and enrich nuclear mRNPs for antisense purification.

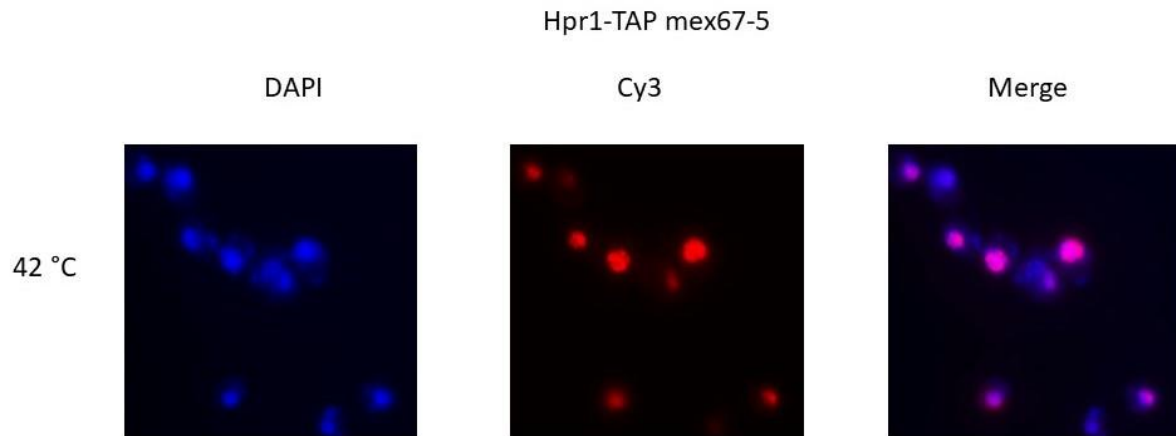


Figure 40. mRNA export defect in a Hpr1-TAP mex67-5 strain

The FISH experiment was done as described. The Hpr1-TAP mex67-5 cells were shifted for 15 min to 42 °C. The nuclei were stained with DAPI while the poly(A)-tail of bulk mRNA was detected by hybridization with a Cy3-labelled oligo d(T)50 probe. The red dots show mRNA colocalized with the DAPI signal of the yeast nuclei, and the pink dots indicate the merged images. The mRNA export defect is clearly visible in the merged picture.

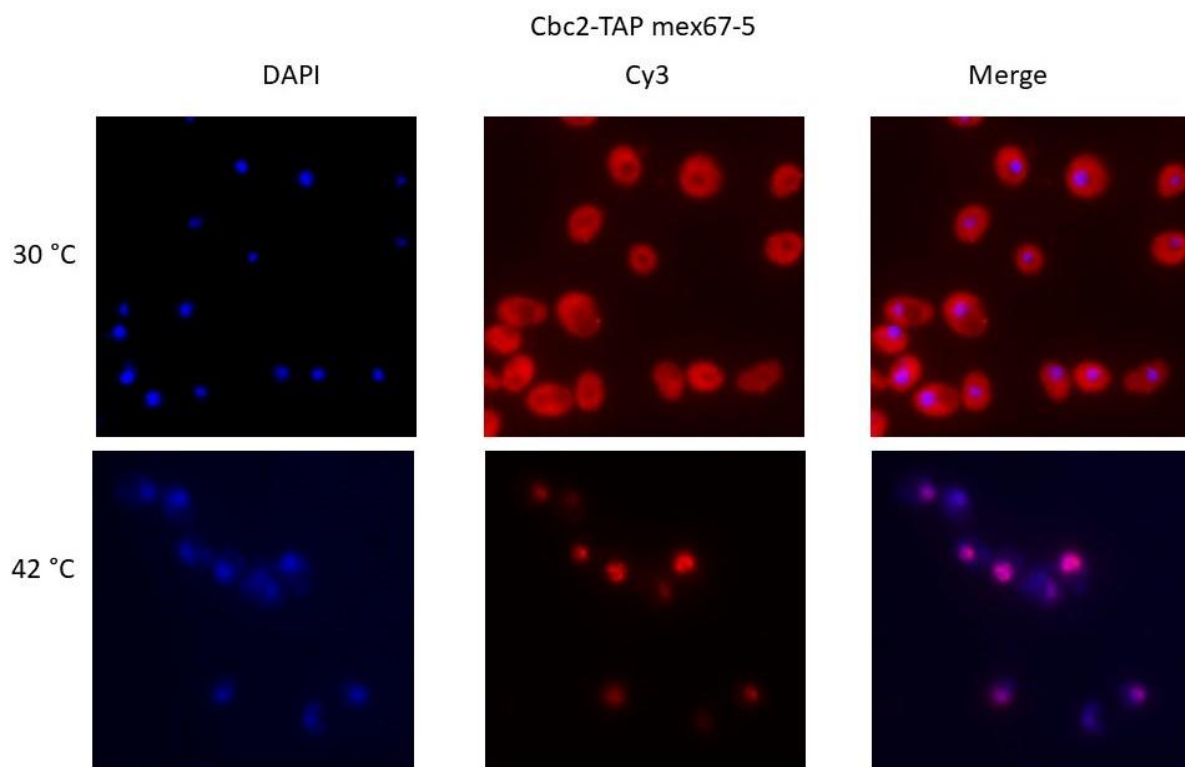


Figure 41. mRNA export defect in a Cbc2-TAP mex67-5 strain

The FISH experiment was done as described. One culture Cbc2-TAP mex67-5 was shifted for 15 min to 42 °C while the other stayed at 30 °C. The nuclei were stained with DAPI while the poly(A)-tail of the bulk mRNA was detected by hybridization with a Cy3-labelled oligo d(T)50 probe. At 30 °C the signals of the nuclei and the mRNA are separated and did not overlap (upper panel). At a higher temperature, the diffuse mRNA signal is concentrating at certain spots (red dots, lower panel) and is co-localized with the blue yeast nuclei. The merged pictures of Cbc2-TAP indicate the same export defect as the Hpr1-TAP mutant strain in Figure 40.

3.2.10 Testing the good buffers HEPES and TRIS in *CCW12* mRNP purification and dilution of TEV eluate

Tris is among the 20 so-called Good-Buffer (Good and Izawa 1972 and Ferguson *et al.* 1980) which have been tested for various properties like pH range, toxicity, solubility, interaction with proteins and UV, solubility and price. It is worldwide used for purification of proteins. TRIS featured buffers at pH 7.8 have been used for TAP purification in most protocols. Apart from the disadvantage that pH changes with temperature, the TRIS buffer cannot be used in cross linking experiments. Since cross-linking mass spectrometry (XL-MS) could be a follow up experiment to analyse nuclear mRNPs (see Discussion) the TRIS has been replaced by HEPES buffer. Changing this component does not lead to any observable differences during *CCW12* mRNP purification and detection on WB (Figure 42). In this study, the enrichment of *CCW12* over *PGK1* was higher in HEPES upon using Tris (Table 32). Therefore, Tris was replaced with HEPES pH 7.8 as standard purification buffer.

The TEV eluate of Cbc2-TAP is a concentrate of nuclear mRNAs having a 5' cap and their interacting proteins. A TEV sample was compared with a 1:1 diluted sample (200 μ l wash buffer + 0,5 mM DTT) to study the effect of molecular crowding on the mRNP purification. Further, *CCW12* ASO 3 was used to purify a specific nuclear mRNP. The qPCR results however showed that, according to the quality criteria (Equation 1), there is no advantage in diluting the TEV elute since the specificity for *CCW12*-*PGK1* was nearly identical (Table 33).

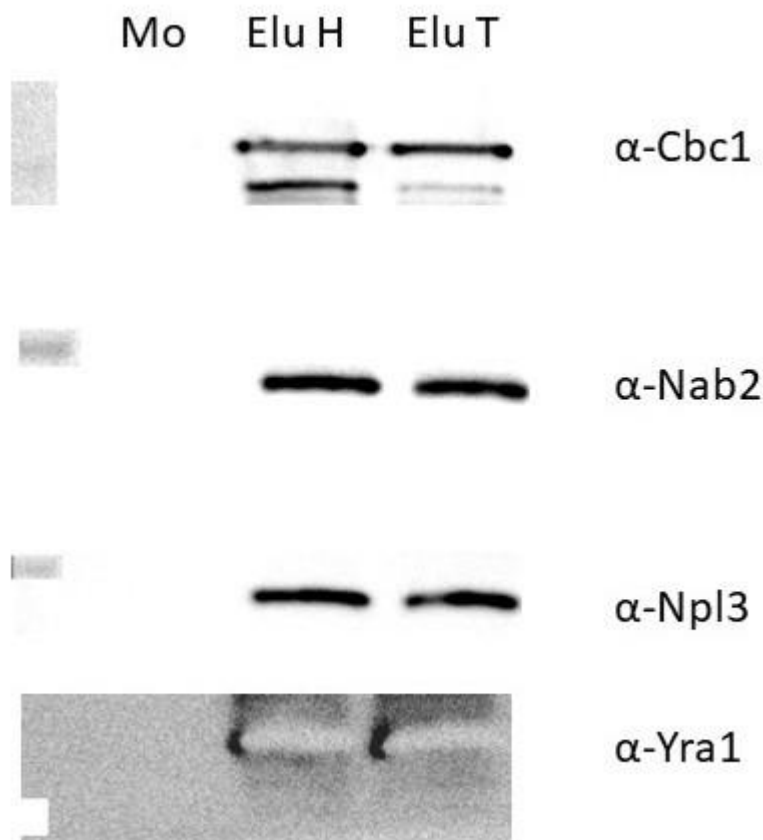


Figure 42. WB comparison of TRIS and HEPES buffer purified mRNP samples from Cbc2-TAP
The signals of the four proteins Cbc1, Nab2, Npl3 and Yra1 after using HEPES compared to TRIS. In the mock, there is no detection of any protein compared to the other samples.

Table 32. qPCR results of *CCW12* mRNP purification with TRIS and HEPES buffer

Sample	<i>CCW12</i>	<i>PGK1</i>	<i>CCW12- PGK1</i>
TEV HEPES	18,5	21,1	-2,6
TEV TRIS	19,1	22,2	-3,1
Eluate HEPES	22,7	25,9	-3,2
Eluate TRIS	21,9	23,5	-1,6
Mock	28,8	31	

Table 33. qPCR results of *CCW12* mRNP purification with diluted TEV eluate

Sample	<i>CCW12</i>	<i>PGK1</i>	<i>CCW12- PGK1</i>
TEV 1	17,4	20	
TEV2	19,9	22,8	
Mock 1	27,3	31,4	
Mock2	32,6	34	
ASO 3 1	22,2	25,6	-3,4
ASO 3 2	25,9	29,1	-3,2
Dilution 1	21,1	24,4	-3,3
Dilution 2	25	28,4	-3,4

3.2.11 Testing three annealing temperatures of *CCW12* ASO 3 in mRNP purification

A method called TRIP in the literature has been described to purify mRNA-protein complexes (Iadevaia *et al.* 2018). The protocol using high temperature to anneal a 3'-biotinylated 2'-O-methylated antisense RNA oligonucleotide to the mRNA of interest. However, in this study, instead of 70 °C, 50 °C, RT and 4 °C were used as annealing temperatures. The TEV eluate was incubated with 12 µl *CCW12* for 30 min at 4 °C and RT. The incubation time for the 50 °C sample was 5 min. After 30 min incubation with M280 beads at RT, a 37 °C pre-heated wash buffer was further used for the high temperature sample while the other two samples were treated with a wash buffer stored at RT. In the 50 °C sample, many of the control proteins were detected on the Western blot. An ASO 3 ordered by another company (€ from Eurogentec purified at RT) did not purify Nab2 and Sub2 as good as the old ASO3 (Biomers) (Figure 43).

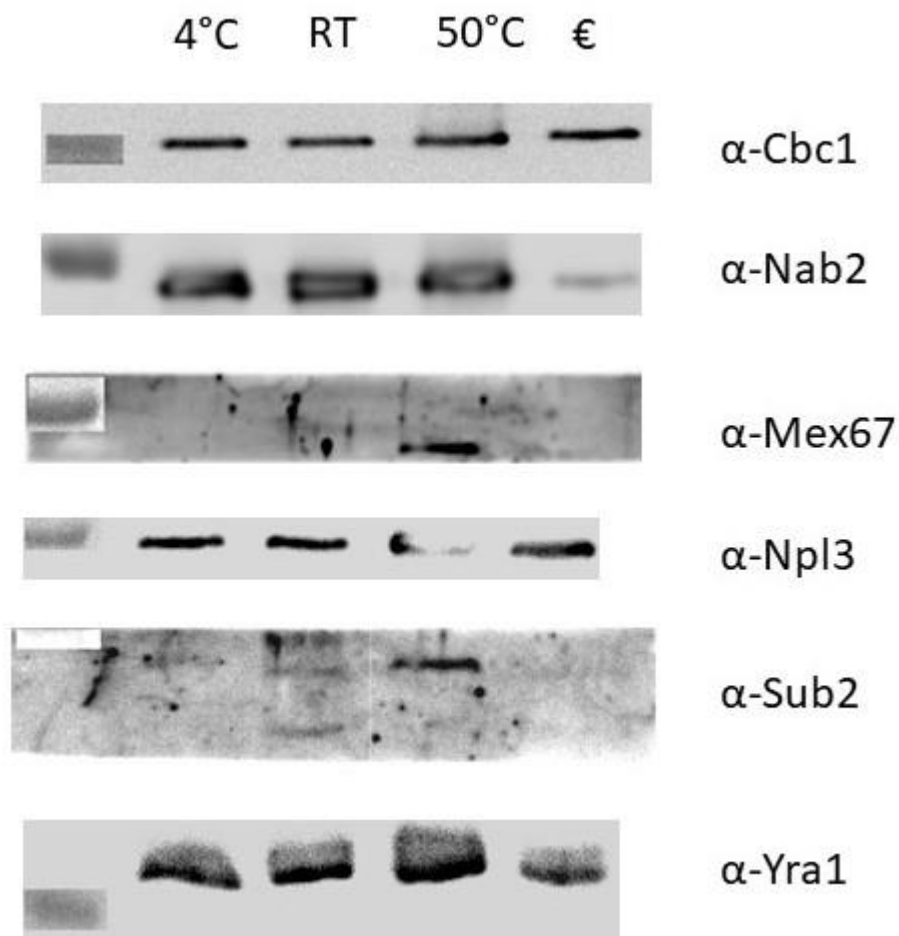


Figure 43. Comparison of *CCW12* ASO 3 annealing at 4°C, RT and 50°C

The 50 °C sample contains the strongest Signal for each protein. The RT sample (from Biomers) and the ASO 3 from Eurogentec (€) were all given the same treatment. The oligonucleotide from Biomers purify more proteins in the mRNP purification step.

Table 34. qPCR of *CCW12* mRNP purification with different annealing temperatures

sample	<i>CCW12</i>	<i>PGK1</i>	<i>CCW12-PGK1</i>
TEV	16,7	19,9	-3,2
Cbc2 4°C	21,3	23,8	-2,5
Cbc2 RT	19,1	22,6	-3,5
Cbc2 50°C	27,5	30,5	-3
€	20,7	23,2	-2,5
Mock	33,6	35,5	

€: ASO 3 *CCW12* from Eurogentec

The qPCR data show that the elution of mRNPs at 50 °C has extremely low amount of target compared to the 4°C and RT samples. The qPCR data from the Eurogentec ASO 3 are comparable with the one from Biomers (Table 34). Based on these results, the annealing of ASO 3 was done for 30 min at RT.

3.2.12 Introducing the “Gerber wash buffer” in mRNP purification

As already mentioned, another group tried to purify protein complexes with a 3'-biotinylated 2'-O-methylated antisense RNA oligonucleotide in their TRIP method (Matia-González *et al.* 2017). The “Gerber wash buffer” was included in the mRNP purification. The qPCR showed earlier, indicate quite a high amount of *PGK1* in the biotin elution of the specific nuclear mRNP for *CCW12*. The TRIS based “Gerber wash buffer” used by the group contains 0.5 mM EDTA pH 8 and had no detergent like the 1x TAP Buffer used in this study (Table 10). In this experiment the same conditions as mentioned 3.2.11 have been tested but this time a HEPES based Gerber buffer was compared to the regular HEPES based mRNP wash buffer. The Yra1 signals were not observed in the purification with the old buffer as in the purification before (Figure 43 and Figure 44). Altogether, on the WB level, the 50 °C purification seems to yield the most protein amount compared to RT and 4°C (38).

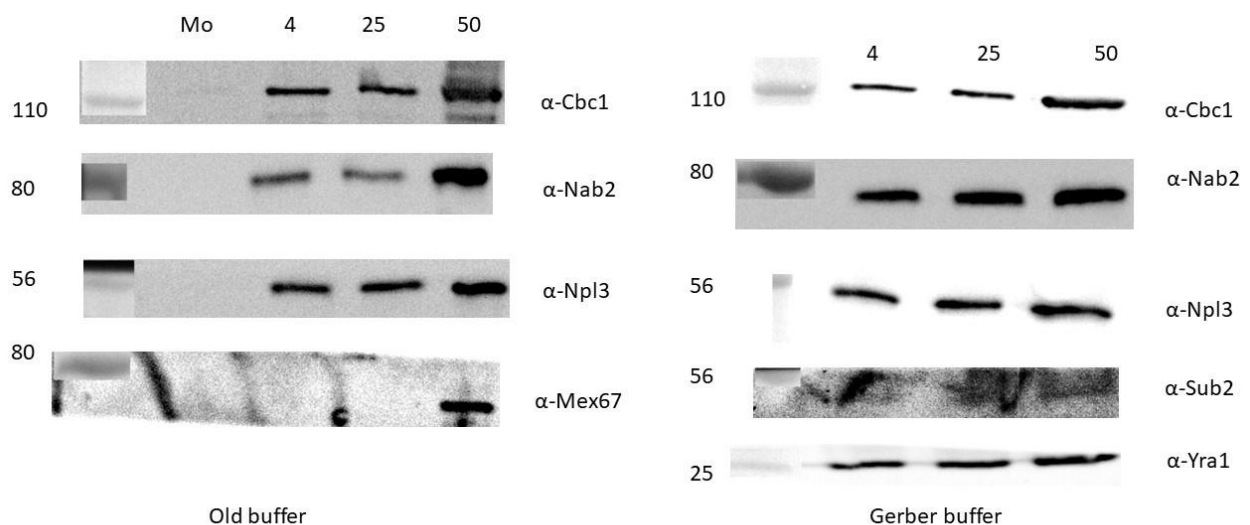


Figure 44. Old wash buffer and Gerber buffer at three different annealing temperatures

On the left site is the WB pattern with the old wash buffer. As seen before, most of the proteins are present in the 50 °C purification. Sub2 and Yra1 were not detected as in the previous experiment (Figure 43). On the right site is the WB result for the Gerber buffer purification. Sub 2 shows a faint signal in all three tested conditions, but Mex67 was not detected like on the left side. Also, with the Gerber buffer, the most proteins were found in the 50 °C fraction. The samples were eluted in a denaturing condition from the beads, which means the protein was cooked from the beads with SDS buffer.

Table 35. Buffer comparison at three different temperatures

Sample	<i>CCW12</i>	<i>PGK1</i>	<i>CCW12-PGK1</i>
TEV old	18,5	21,2	-2,7
TEV Gerber	18,4	20,5	-2,1
4 °C old	22,5	25,2	-2,7
4 °C Gerber	24,5	29	-4,5
RT old	20,2	22,9	-2,6
RT Gerber	24,7	29,2	-4,5
50 °C old	23	25,7	-2,7
50 °C Gerber	22,4	27,6	-5,2
Mock old	29,8	31,3	
Mock Gerber	33	33	

Old: old wash buffer Gerber: Gerber wash buffer RT: room temperature

The qPCR results show a decrease in the amount of *PGK1* in the Gerber buffer compared to the old buffer. The specificity for *CCW12* over *PGK1* increases by twofold (Table 35). In each purification was the relative amount of *CCW12* mRNA comparable with the values in the other samples (Table 35). The purification before shows compared to that lower relative amount of *CCW12* at 50 °C (Table 34). Still, there are questions on how viable a specific nuclear mRNP at 50 °C and its look compared to a more native one at RT or 4°C. Therefore, the mRNPs purification was done at 4°C or RT.

3.2.13 Testing biotin and desthiobiotin *CCW12* ASO 3 at 4 °C vs RT annealing temperature and performing the whole mRNP purification at 4 °C vs RT

In 3.2.8 the purification properties of desthiobiotinylated and biotinylated *CCW12* ASO 3 were analysed in terms of elution with biotin vs elution with the displacement oligo. Now two different annealing temperatures for *CCW12* ASO 3 were investigated and analysed on WB and qPCR. The samples were denatured, which means, the amount of mRNA and protein which is bound on the beads before elution were detected. On WB, the desthiobiotin samples (D) contain a bit less protein as the biotin (B) samples at each temperature (Figure 45). At RT, it seems that there was more Npl3 in sample D compared to the others tested. At 4 °C, more Npl3 and Cbc1 were in the D sample. More proteins were expected for the B samples because the interaction of the oligo with the beads is stronger as for the D samples. In Figure 35, more proteins were eluted from the desthiobiotinylated samples (DB and DD) since here the interaction between the beads and the mRNA is weaker. Both mock controls are empty except for Sub2 signal at 4 °C.

The CT values for *CCW12* in the samples D were nearly equal at 4°C and RT. Also, the difference between both B samples were less than one ct-value (Table 36). Performing the whole purification at 4 °C or RT leading to similar western blot pattern as seen in Figure 45. Inferring to the qPCR results, the *CCW12* biotin ASO 3 bind higher amounts of target mRNA compared to the desthiobiotin ASO 3 in most cases (Table 37). The purification at 4 °C led to empty WB and extremely low amount of *CCW12* mRNA on the beads. A short incubation time of 30 min with M280 beads at 4°C was not sufficient for capturing the target mRNPs. Either the incubation with M280 beads was shifted to RT for 30 min or the incubation time in the cold room was increased (to 1.5 h- 2 h at 4 °C) (Table 37). Performing the whole mRNP purification at 4 °C increased the duration of the experiment by hours and slowed down the interaction of samples with the 2'-OMe RNA anti-sense oligos or the M280 beads. On the other hand, low temperatures slow down the activity of enzymes like DNAses or RNAses which can destroy specific nuclear mRNP.

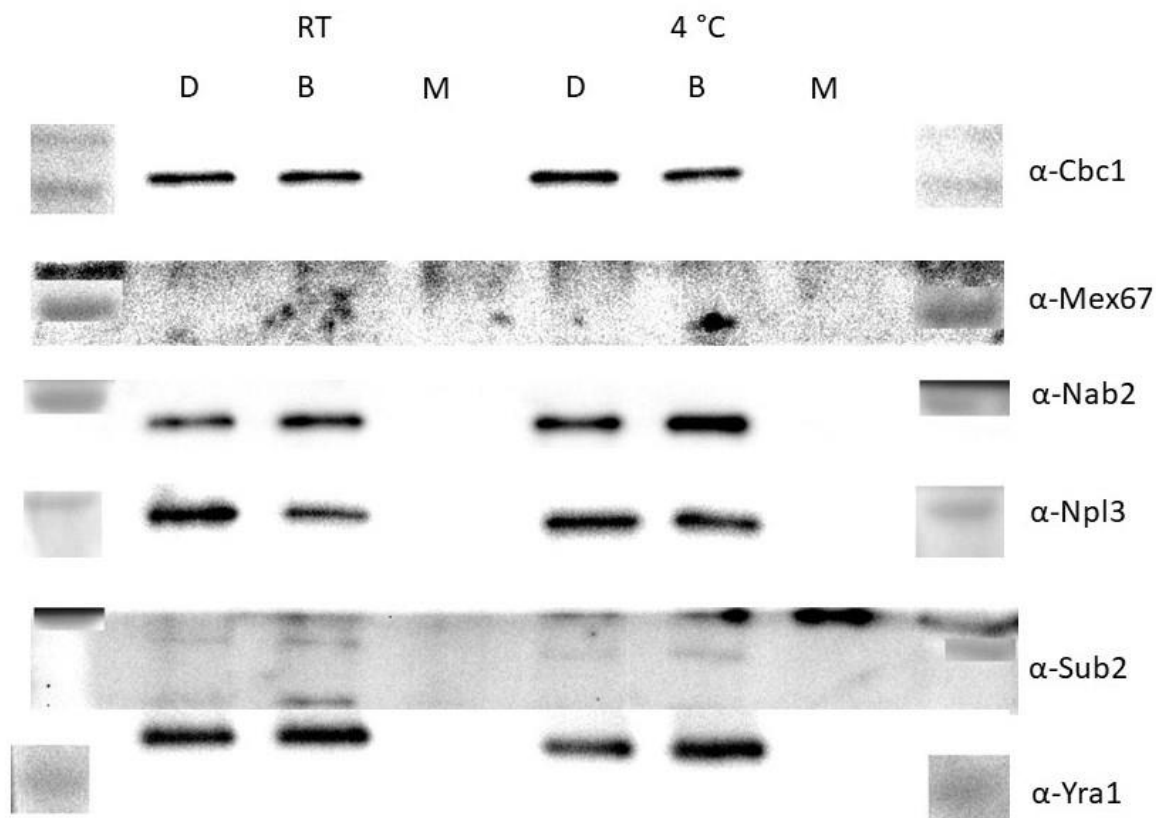


Figure 45. *CCW12* mRNA purification with two ASO 3 at 4 °C vs RT annealing temperature

WB compares the purification of the *CCW12* biotinylated ASO 3 (B) with the desthiobiotinylated ASO 3 (D) at 4°C and RT (while ASO 3 annealing). Nearly all proteins except Mex67 were detected in all samples and are enriched compared to the mock control. Only Sub2 showed a stronger signal in the Mock from 4 °C compared to all other samples.

Table 36. qPCR from mRNP purification using ASO 3 at 4°C and RT during the annealing step

Temperature	Sample	<i>CCW12</i>	<i>PGK1</i>	<i>CCW12-PGK1</i>
	TEV	18,1	21,5	-3,4
4 °C	M	32,4	35	
4 °C	B	21,8	28,7	-6,9
4 °C	D	24,3	31,5	-7,2
RT	M	32	34	-2
RT	B	22,7	30	-7,3
RT	D	24,8	34,4	-9,6

TEC: TEV eluate M: Mock B: biotin ASO 3 *CCW12* D: desthiobiotin ASO 3 *CCW12*

Table 37. qPCR from denatured mRNP purification using ASO 3 at 4 °C and RT

Sample	<i>CCW12</i>	<i>PGK1</i>	<i>CCW12-PGK1</i>
TEV 4 °C	21,4	24,4	-3
Mock 4 °C	34,6	33,6	
Biotin 4 °C	31,5	33,4	-1,9
Desthiobiotin 4 °C	29,9	32,5	-2,6
TEV RT	19,4	20,9	-1,5
Mock RT	30	31,7	
Biotin RT	24,7	26,5	-1,8
Desthiobiotin RT	26,9	30	-3,1
TEV 4 °C RT	20,4	22,6	-2,4
Mock 4 °C RT	30,2	30,8	
Biotin 4 °C RT	25,1	28,2	-3,1
Desthiobiotin 4 °C	25,5	27,9	-2,4
TEV 4 °C 2h	21,3	23,2	-1,9
Mock 4 °C 2h	29,9	31,2	
Biotin 4 °C 2h	23,4	26,2	-2,8
Desthiobiotin 4 °C 2h	22,9	25,9	-3

4 °C: whole mRNP purification done at 4 °C RT: whole mRNP purification done at RT

4 °C RT: whole mRNP purification done at 4 °C only M280 bead incubation at RT for 30 min

4 °C 2h: whole mRNP purification done at 4 °C with 2 h M280 bead incubation

3.2.14 Analysing the binding efficiency of *CCW12* ASO 1-3 to their mRNA via dilution and via RNase H assay

Since in 3.2.8 the data suggested that using the displacement oligo for purification at certain concentration already led to self-interacting of this primers, a dilution of *CCW12* ASOs for purification was tested. 1 and 12 µl of ASO1,2 and 3 have been compared in mRNP purifications. The WB levels of the dilutions were comparable in all three ASOs.

The qPCR data for ASO 1 and 3 showed a significant increase in the mRNA level comparing 12 and 1 µl while a dilution for ASO 2 did not influence the ct-values (Table 38).

To elucidate binding specificity for *CCW12* ASO 1 to 3 the RNase H assay was performed (2.2.2.15). If the specific ASO is binding the complementary target mRNA the emerged complex is targeted by the RNase H and cleaved. Comparing samples with or without RNase H and using specific primers in qPCR experiments revealed if the enzyme was active.

In the ASO 2 sample, no changes in the ct-values were detected (Table 39). For ASO 1 and 3, changes in the samples treated with RNase H were also observed (Table 39). Here, the ct-values with the enzyme are higher compared to the untreated starting material. Therefore, it can be concluded that ASO 1 and 3 are effective in binding their complementary parts in the *CCW12* mRNA. This observation goes along with findings in Table 38 where the purification of *CCW12* mRNA was more effective with 1 µl ASO

1 or 3 instead of 12 μ l. Less ASO reduces the chances of unwanted self-interactions of the anti-sense oligos and results in a more effective binding at the target mRNA. Therefore, 1 μ l of ASO 3 was used for all mRNP experiments. This adjustment saved money and materials and as well increase the efficiency of the purification of the specific nuclear mRNP.

Table 38. qPCR results from *CCW12* mRNP purification using 1, 6 and 12 μ l ASO 1-3

Sample	<i>CCW12</i>	<i>PGK1</i>	<i>CCW12-PGK1</i>
ASO 1 (12 μ l)	25	28,5	-3,5
ASO 1 (1 μ l)	22,8	28	-5,2
ASO 2 (12 μ l)	21,4	26,5	-4,9
ASO 2 (1 μ l)	21,3	27	-5,7
ASO 3 (12 μ l)	23,2	27,2	-4
ASO 3 (1 μ l)	20,2	28	-8,2

Table 39. qPCR results from RNase H assay using ASO 1 to 3

Sample	<i>CCW12</i>
ASO 1	20,8
ASO 1 + RNase H	28,3
ASO 2	21,6
ASO 2 + RNase H	21,4
ASO 3	21,4
ASO 3 + RNase H	28,9
Mock (no ASO)	32,7
Mock + RNase H	31,8

3.2.15 Purifying nuclear *CCW12* mRNPs at the different pH values

The purification of proteins in general is a very tough procedure where many factors play important roles. Many parameters have been already optimized for the mRNP purification and this includes temperature, buffer composition, input sample (origin and concentration) or the amount of ASO. Another crucial factor is the pH in which the purification takes place. Important here is the isoelectric point (pI) of the target. Since the goal is to purify a specific nuclear mRNA which has many proteins surrounding it, the calculation of an exact pI for the target is impossible (because the RBP coverage of the mRNPs is unknown). Therefore, three standard pH from the international literature were tested. The pH used were 6.8, 7.8 and 8.0. For the purification of the *CCW12* mRNP HEPES buffer and 1 μ l of ASO 3 were used. The first influence of different pH values was observed on the SDS PAGE. The Cbc1 and Cbc2 bands which are characteristic for the Cbc2-TAP purification were found in two of three purifications on the gel (not in pH 6.8 (6) (Figure 46)). Overall samples 6 had the least detected proteins on the gel. The pattern for p 7.8 (7) and 8.0 (8) looked identical but the most protein input was in sample 7. All the four control genes were detected on the three TEV eluates which served as input for the experiment (Figure 47). Like the observation from the SDS PAGE, the two higher pH values seem to have more protein input as the sample at pH 6.8. In both independent purifications A and B, the sample at 6.8 had the highest amount of the Sub2 degradation product as input (Figure 47).

Analysing the denatured elution (as in 3.2.13 explained) of the samples on WB showed reduced amounts of all target genes (Figure 48). Sub2 and Mex 67 were empty and the signal pattern for Tho1, Npl3 and Yra1 did not match in the two independent experiments. In general, most of the proteins were found at pH 7.8 which was the standard pH value for mRNP purification.

In the qPCR results, the mRNA of *CCW12* was found in higher amounts at pH 7.8 and 8.0. Even though the TEV eluates had quite similar ct-values (apart from TEV B Table 40), the lower pH seems not to be suited well for the M280 beads because the binding was quite weak compared to the other pH values. Taking the results from the pH values into account, the pH value for mRNP purification should remain at 7.8.

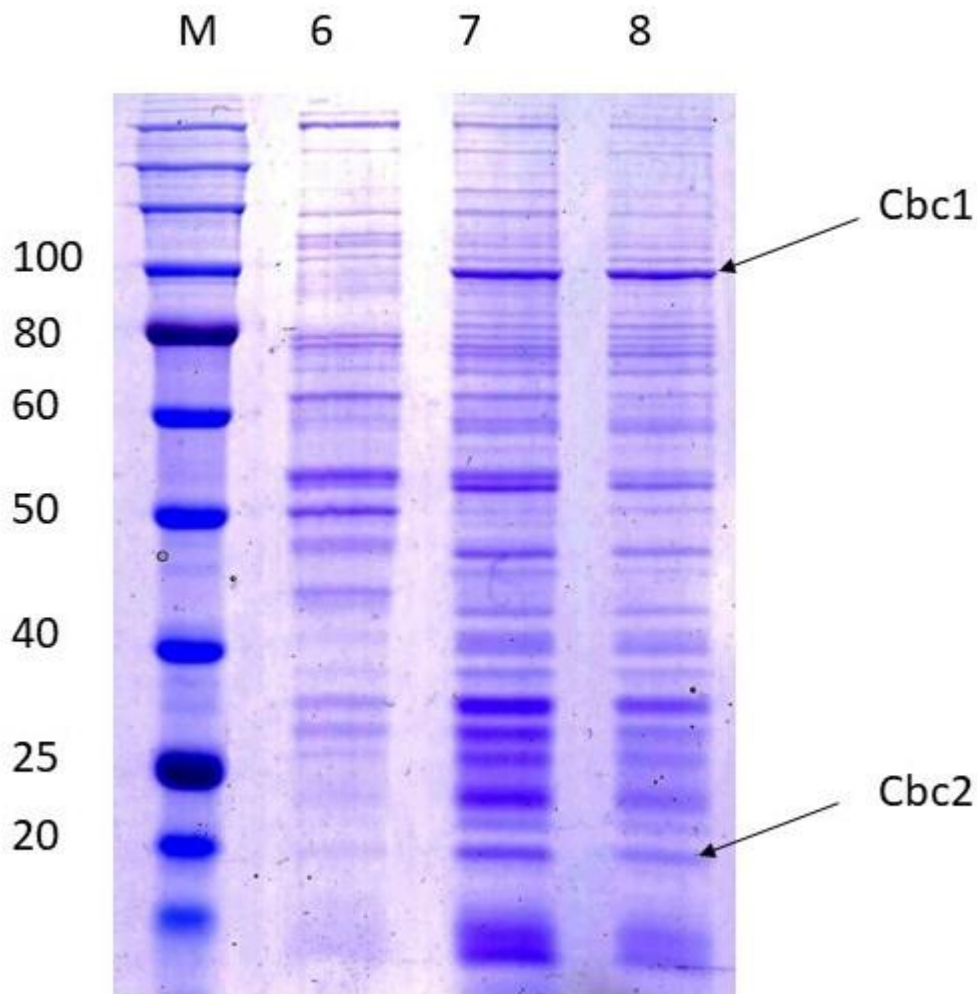


Figure 46. SDS PAGE of *CCW12* mRNA purification at different pH values

The sample at pH 6.8 (6) shows weaker protein bands and the pattern differs from the other samples at pH 7.8 (7) and pH 8.0 (8). Compared to 7 and 8, it seems that some bands were missing, for example, the characteristic Cbc1 and Cbc2 bands marked with an arrow at around 100 and 20 kDa. Samples 7 and 8 have more similar patterns compared to 6. Some protein bands are missing or are less prominent in the purification at pH 6.8. Altogether, the highest amounts of protein were obtained at pH 7.8.

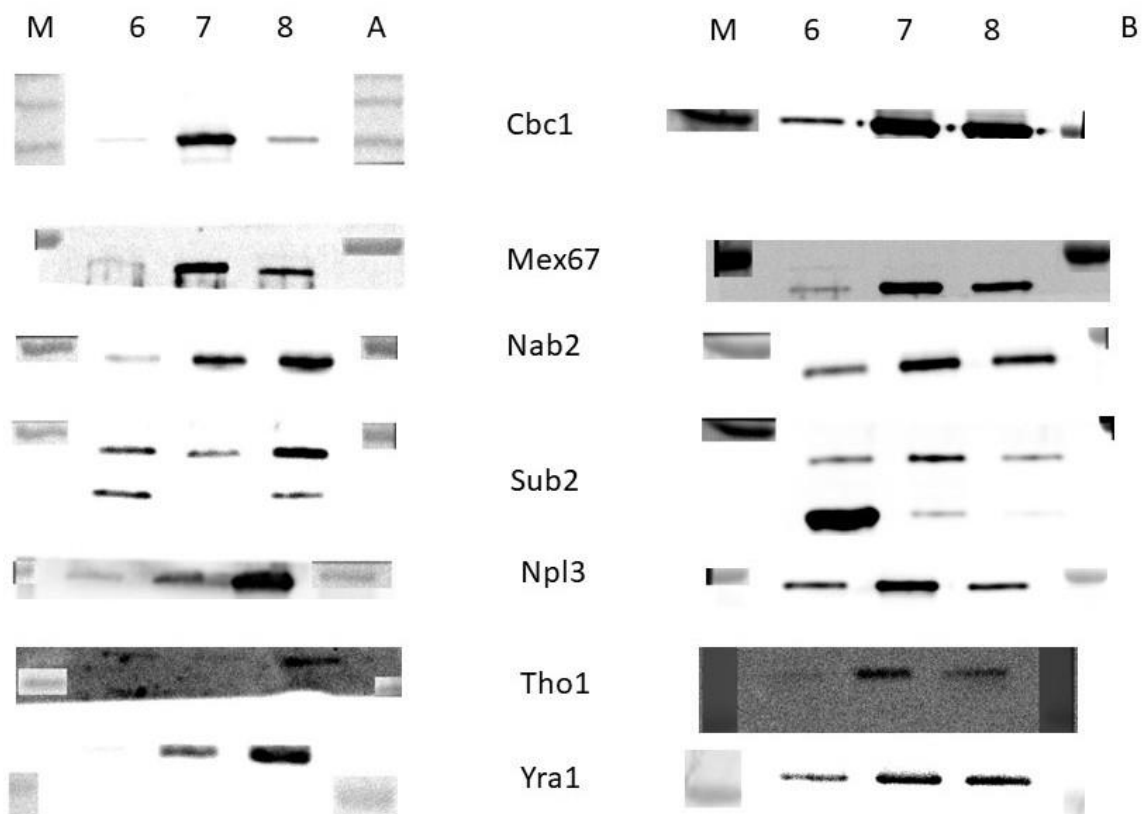


Figure 47. WB of TEV eluates at different pH values

From the input TEV elutes of two different purifications, A and B, at pH 6.8, 7.8 and 8.0 were analysed (same label as Figure 46). Sample 6 had less signals for most of the proteins but the highest amount of Sub2 degradation product (lower band). The results resemble the SDS PAGE findings in Figure 46. Less signals were observed in TEV of sample 6 compared to 7 and 8. Molecular weight of the marker bands is listed in Figure 27.

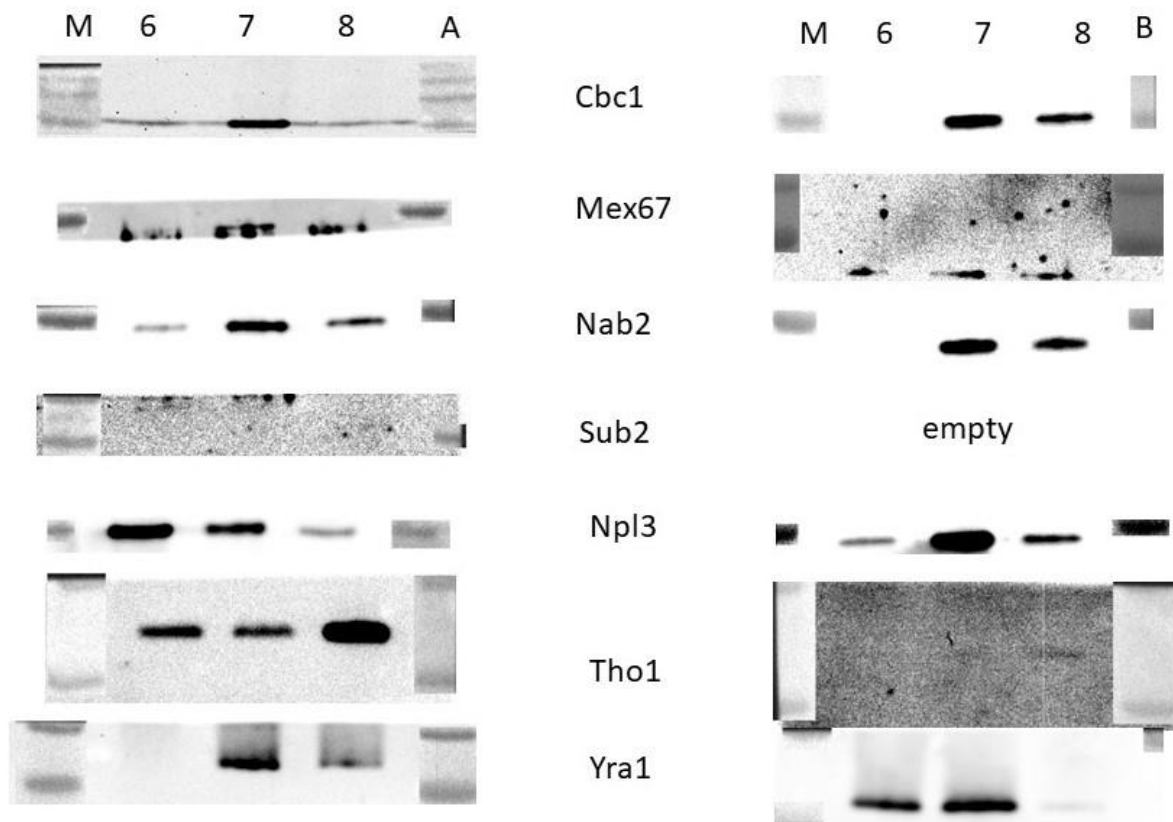


Figure 48. WB of denatured mRNP elutions at different pH values

In the WB of the denatured eluates (same label as Figure 47), no consistent pattern of signals was observed in the two purification A and B. Only the Nab2 signal distribution did not change. Signals for Mex67 and Sub2 have not been detected in both experiments. Npl3, Tho1 and Yra1 have consistently been detected in sample 7. At pH 7.8 the purification detected the most bound RBPs on WB.

Table 40. qPCR results from *CCW12* mRNP purification at pH 6.8, 7.8 and 8.0

Sample	<i>CCW12</i>	<i>PGK1</i>	<i>CCW12-PGK1</i>
TEV 6.8 A	21,7	25,7	
TEV 7.8 A	18,4	22,2	
TEV 8.0 A	21,7	24,2	
ASO 3 6.8 A	29,1	32,9	-3,8
ASO 3 7.8 A	25	30	-5
ASO 3 8.0 A	26,5	31,3	-4,8
Mock A	34,3	35,2	
TEV 6.8 B	26	27,2	
TEV 7.8 B	18,2	20,8	
TEV 8.0 B	17,4	20,6	
ASO 3 6.8 B	29	32,6	-3,6
ASO 3 7.8 B	25,6	28,2	-2,6
ASO 3 8.0 B	26,4	29	-2,5
Mock B	29,5	33,3	

A first experiment; B second experiment; 6.8 = pH 6.8; 7.8 = pH 7.8 8.0 = pH 8.0

3.2.16 Specific nuclear mRNP in $\Delta ccw12$ and $\Delta ilv5$ as control strains

For the mRNP purification a Cbc2-TAP was used as mock control with no addition of the ASO to purify a specific mRNP. To check for background impurities, the deletion strains of *CCW12* and *ILV5* were used for mRNP purification. Therefore, the deletion strains (Table 41) were purchased from Euroscarf and the deletion cassettes inserted into the Cbc2-TAP strain (2.2.2.6). Successful deletion was confirmed by qPCR (Table 41 and Table 42). The Cbc2-TAP *CCW12* mRNP purification was performed using ASO 1 to 3 in the $\Delta ccw12$, and ASO 10 in the $\Delta ilv5$ Cbc2-TAP strain. For the purification in the Cbc2-TAP strain the known western blot pattern for ASO 1 to 3 was observed detecting the highest amount of purified RBPs in the purification with ASO3 (Figure 49). In the mock control, apart from a quite strong Npl3 signal, only weak visible signals have been detected for the other proteins. Analyzing the purification with the new made *CCW12* deletion strain reveal the same patten for ASO 1 to 3 as in former purification with Cbc2-TAP strain on western blot (Figure 49). The ASO 3 sample showed the highest signal detected in this study. For Cbc1, Nab2, Sub2 and Yra1 the ASO 3 displays visible signals in both strains.

Since the purification of *CCW12* mRNP in the $\Delta ccw12$ should not work because the gene is deleted (Table 41), the WB in Figure 49 shows the background “noise” of the purification done. Similar observation was made regarding the $\Delta ilv5$ strain. $\Delta ilv5$ Cbc2-TAP showed high background in the protein set. In the qPCR, high amounts of *CCW12* mRNA were exhibited in the *ILV5* specific nuclear mRNP purification (Table 42)

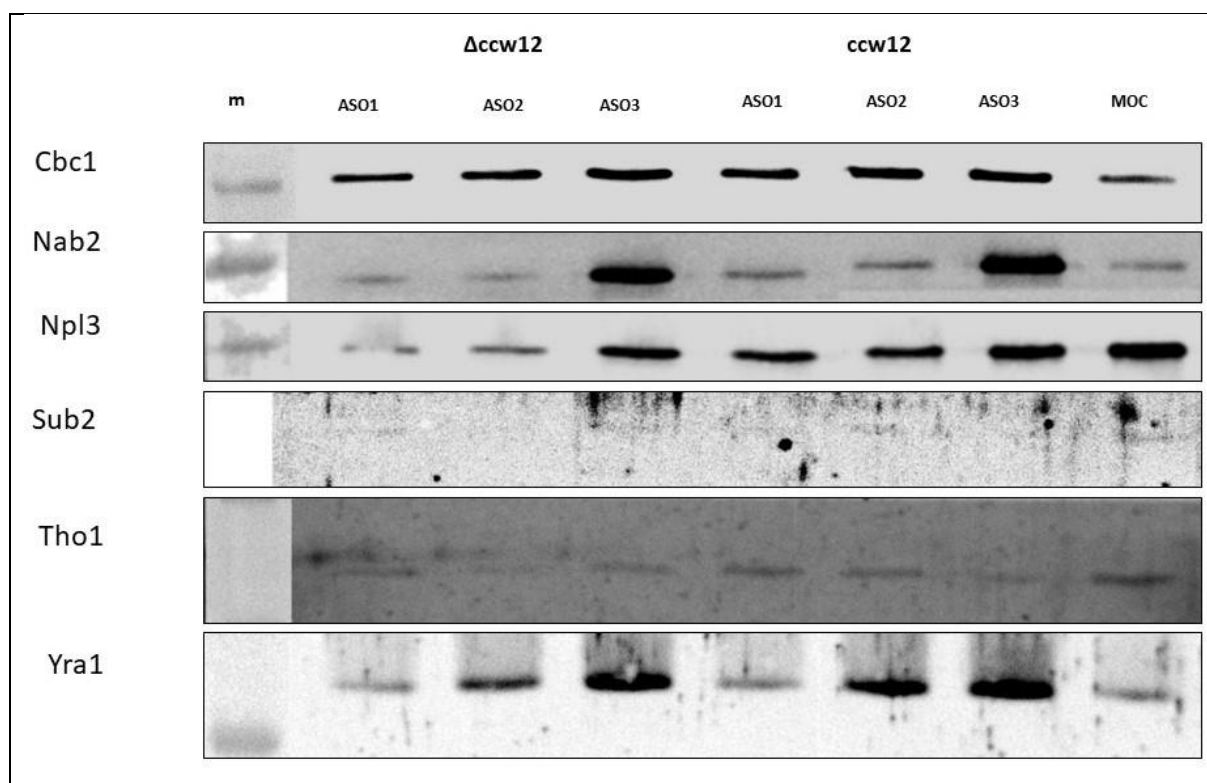


Figure 49. WB analysis of *CCW12* purification using ASO 1 to 3 in Cbc2-TAP ± *CCW12* strains
 The right side of the figure shows the known purification pattern of CCB2-TAP with ASO 1 to 3 where the most protein signals were found in the ASO 3 sample. The mock (moc) had an extremely high signal for Npl3. Apart from that, other signals, if visible, were less abundant compared to the proteins in ASO 1 to 3 (Cbc1, Nab2 and Yra1). On the left side, the signal pattern for the purification in the new $\Delta ccw12$ strain is shown. The pattern is the same as on the right side but less intense. This shows that all the signals on the right side contain the background on the left so the enrichment of RBPs in ASO 1 to 3 purification on protein level are not as high as previous expected (Figure done by Nataliia).

Table 41. qPCR results of CCW12 mRNP purification in Cbc2-TAP with and without CCW12

Sample	<i>CCW12</i>	<i>PGK1</i>	<i>CCW12-PGK1</i>
Lysate	16,8	17,9	
TEV	16	17,7	
ASO 1	20,7	30,3	-9,5
ASO 2	20,6	26,2	-5,6
ASO 3	20,4	27,5	-7,1
Lysate $\Delta ccw12$	28,8	18,4	
TEV $\Delta ccw12$	27,1	18,3	
ASO 1 $\Delta ccw12$	32	30,7	
ASO 2 $\Delta ccw12$	29,9	26,7	
ASO 3 $\Delta ccw12$	29,9	28,1	
Mock	30,2	32,5	

Table 42. qPCR results of ILV5 mRNP purification in Cbc2-TAP with and without ILV5

Sample	<i>CCW12</i>	<i>PGK1</i>	<i>ILV5</i>	<i>CCW12-PGK1</i>
TEV	18,3	21	23,6	
ASO 10 <i>ILV5</i>	27	33,6	26,2	-6,6
TEV $\Delta ilv5$	19,2	22,4	29,3	
ASO 10 $\Delta ilv5$	26,5	29,9	30	-3,4

To improve the mRNP purification in addition to the mock control, the corresponding deletion strain must be purified side by side to evaluate the purification results.

4 Discussion

4.1 A role for Tho1 in transcription

Tho1 protein is a known suppressor of the Hpr1 deletion (Jimeno *et al.* 2006). It has been shown in a metagenome analysis that Tho1 resembles the pattern of Hpr1 and Yra1 (Meinel 2013). Using a ChIP experiment with a mutated Spt5-CTR, the occupancy levels of Paf1 and Tho1 were reported to be decreased while TREX components (Sub2, Yra1 and Hrp1) increased (Meinel 2013).

In the first part of the results in this thesis, the interactions of Tho1 (Tho1-TAP) with TREX (Hpr1-TAP), the PAF1 complex (Paf1-TAP) and the adapter Spt5 (Spt5-TAP) were analysed with ChIP.

A Tho1 overexpression in a Paf1-Tap strain did not reveal any change in the PAF1 occupancy (Figure 11. ChIP of Paf1-TAP with and without THO1 overexpression Figure 11). On the other hand, it has already been demonstrated that overexpression of Tho1 reduced the occupancy of Sub2 and Hpr1 on the genes while there was no effect on Yra1 (Meinel, 2013). In this regard, neither the presence nor excess of Tho1 affect the occupancy of Paf1 on the control genes.

Performing the experiment in a Δ tho1 strain led to a decrease in the occupancy of PAF1 at the control genes by at least 15 % in several experiments (Figure 19). Therefore, it can be stated that the absence of Tho1 negatively affect the function of PAF1 complex. This finding could be further verified and analysed with different experiments like a TAP purification in the Δ tho1 strain followed by a MS analysis.

Analysing the Spt5-TAP occupancy in the Δ tho1 compared to the wt strain did not reveal any changes in the Spt5 occupancy at the tested genes (Figure 15). Previous data have shown that changes in Spt5-CTR are able to modify Tho1 levels at the genes in both directions (Meinel 2013).

For each tested TAP tagged protein (Paf1 and Spt5), the analysed RNAPII did not change (Figure 13 and Figure 17) which indicated that the transcription of this strains is not impaired. The impairment of transcription was observed in Δ paf1 and Δ hpr1 strains, an observation already described in literature. All the ChIP experiments performed in this study and by Birte Bucker (unpublished data) will help to elucidate a possible role for Tho1 in transcription. Taken together, this study revealed a complex interaction pattern between the three complexes and Tho1 which cannot be resolved exclusively by ChIP.

Therefore, further investigations are recommended, for example, the co-purification of TAP-tagged proteins from all strains mentioned in 3.1.4. This is important since previous pull-down coupled MS experiment of Spt5-Flag showed Tho1 as an interacting partner (Lindstrom *et al.* 2003). Interestingly, recent data using XL-MS approach have shown an interaction of Tho1 with Sub2 (Manuel Koschiza 2017). To verify physical interaction of proteins found in MS analysis, classical ITC and NMR titration experiments could be performed to validate this interaction and further describe their affinity (KD values).

Recently, it was shown that Mex67, the main mRNA exporter in yeast works different under head stress conditions (Carmody *et al.* 2010 and Zander *et al.* 2016). It would be interesting to know if Tho1 or the other complexes are affected by previous experiments performed under similar stress conditions as described in literature. It is speculative that under heat stress, Tho1 could serve as an adapter for Mex67 or be an alternative transporter for heat-shock mRNA.

For the human homologue of Tho1, the formation of a trimeric complex with UAP56 (yeast Sub2) and Aly (yeast Yra1) in an ATP-dependent manner is already described (Dufu *et al.* 2009), and CIP29 has been shown to be part of the human TREX (Schumann *et al.* 2016a).

Tho1 in yeast seems to have multiple functions as it is not yet known whether the protein is part of TREX. Therefore, it is important that further studies can characterize the functions of Tho1. The experiments performed in this study will complement the work about Tho1 which is soon to be published by Birte Bucker.

4.2 A purification for specific nuclear mRNPs

During this study, a working protocol for nuclear mRNP was established and modified (3.2) to prepare samples for various biophysical applications like NMR, (XL-) MS and various EM techniques to study the structure and interactome of the target. With this protocol, investigation of each specific nuclear mRNP is possible. With some modifications, the protocol could be adapted for the purification of cytoplasmic mRNPs.

Table 43. Summary of adapted changes applied to the mRNP purification protocol

Stage	Pellet preparation		
Standard procedure	wt RS453 strain	2 l culture OD ₆₀₀ of 0.8	No cross-linking (cl)
Modification	TAP strain (Cbc2-TAP)	2 l culture OD ₆₀₀ of 3.3	UV cl and formaldehyde or glutaraldehyde cl
Section	3.2.4	3.2.4	3.2.4 and 3.2.6
Results	Increase fraction of nuclear mRNPs in the sample and enable easier purification through tag.	Nearly no difference in WB or qPCR levels but higher OD yield more input.	Cl with chemicals substances like formaldehyde only in low concentration up to 0.1 % possible. UV cl changes cannot be detected by WB or qPCR. Detection via MS based methods.
Stage	TAP purification		
Standard procedure	10 min at 3600 rpm at 4°C pelleting	45 min at 35 k rpm UZ	Following Tap protocol to TEV eluate with Tris based buffer
Modification	Time increased to 20 min	30 min at 10 k rpm or no UZ	Change Tris for HEPES in three different pH values from 6.8 to 8.0
Section	3.2.5	3.2.5	3.2.15
Results	Without UZ on WB proteins could be detected but the total number of mRNA was low compared to the other samples.	Decreasing the UZ speed has been proven to enhance protein detection on WB and leads to higher amount of mRNA in qPCR experiments.	Nuclear mRNP seem not so stable under rather acid (6.8) or basic (8.0) pH so experiments have been done at pH 7.8.

Stage	TAP purification		
Standard procedure	TAP buffer HEPES pH 7.8	TAP buffer HEPES pH 7.8 (1.5 mM MgCl ₂)	150 µl TEV eluate are taken for mRNP purification
Modification	+ 4 mM ATP-γ-S	Without or 3 mM MgCl ₂	Dilution 1:1 of TEV eluate with TAP buffer
Section	3.2.7	3.2.7	3.2.10
Results	The WB results did not show a consistent pattern for both experiments so no conclusion about the influence of ATP-γ-S on Sub2 presence during the mRNP purification can be drawn.	Purifications containing MgCl ₂ in the buffer yielded more mRNA detected by the qPCR.	Diluting the TEV eluate for ASO purification did not affect the outcome of the purification detected by WB or qPCR.
Stage	mRNP purification		
Standard procedure	Add 12 µl of one specific ASO	2 h at 4 °C incubation with ASO 3	Add 100 µl of M280 magnetic beads
Modification	12 µl ASO mixture or 1 µl ASO	30 min at RT or 10 min at 50 °C incubation with ASO	100 µl of three other magnetic beads (from same company)
Section	3.2.5 and 3.2.14	3.2.11 and 3.2.12	3.2.3
Results	In purifications with a <i>CCW12</i> ASO mixture more proteins have been detected on WB compared to ASO 2. Lower amount of <i>CCW12</i> ASO 1 and ASO 3 increased the amount of purified mRNA significant compared to no effect on the purification with ASO 2.	The hybridization at different temperatures showed that at higher temperatures (50 °C) the amount of protein captured on WB is increased while the mRNA is decreased compared to RT or 4 °C. Lower temperatures have been chosen for further optimizations.	100 µl of each magnetic bead were compared in a purification experiment and the M280 performed better as the other three candidates.
Stage	mRNP purification		
Standard procedure	Incubation with M280 beads at RT	4x wash with low salt buffer and 2x wash with high salt buffer at RT	6x wash with low salt buffer at RT
Modification	Incubation with M280 beads at 4 °C	6x wash with low salt buffer at RT	6x wash with low salt buffer at 4 °C RT and 37 °C
Section	3.2.13	3.2.4	3.2.11
Results	The qPCR could not detect high levels of the target mRNA for an incubation of 30 min. Performing this step at 4 °C only yielded	In samples only washed with low salt buffer, more proteins were detected on WB compared to samples washed with the high salt buffer.	Changing the temperature of the washing buffer was applied for the purification at three different temperatures

	comparable mRNA amounts after 2 h incubation.		from 4°C to 50°C. Lower mRNA amounts of the target and more signals in WB were detected for the 50 °C samples.
Stage	mRNP purification		
Standard procedure	6x wash with low salt buffer at RT	Denatured elution with biotin ASO at RT	Native elution with biotin ASO using biotin or displacement DNA at 30 min RT
Modification	Use “Gerber” buffer 6x at RT	Compared to denatured elution with desthiobiotin ASO at RT	Compared to native biotin elution with desthiobiotin ASO 30 min RT
Section	3	3.2.13	3.2.8
Results	Introducing the buffer from the Gerber protocol significantly reduced the detected amount of <i>PGK1</i> in the qPCR.	The interaction with biotin was stronger as with desthiobiotin thus, the western blot signals were stronger for biotin, and on the qPCR, more target mRNA was detected in the biotin samples.	The best elution was observed for the desthiobiotin ASO using biotin. Here the highest amount was detected on the qPCR and on WB level, some proteins were detected.

Using the combined protocol, the purification of a target nuclear mRNP was performed in one day without the qPCR quality control. Purifying proteins at lower temperatures is mostly good for their stability. If the routine is too long, damage might be done by losing their function or changing structure of the protein over time. Therefore, removing protein or protein complexes like mRNPs from their cellular environment require quick purification methods. The temperature is therefore, increased in several parts of the purification to RT for to increase binding of the ASO to the TEV eluate or to elute the mRNP from the M280 beads with biotin. The addition of an extremely low concentration of detergents like 0.0001 % NP40 is also recommended during the elution step.

The use of WB, qPCR, and negative staining under the transmission electron microscope (TEM) have been proven as good quality control for the purification presented in this study for further downstream applications.

4.3 Comparing the combined mRNP purification with other methods from the literature.

The Group of Andre Gerber established a protocol to purify mRNA called tandem RNA isolation procedure (TRIP Iadevaia *et al.* 2018). Cross-linked cells were lysed, and the mRNA captured by oligo(dT) beads from cellular extracts. Like in this study the target mRNA is captured by 3'-biotinylated 2'-O-methylated antisense RNA oligonucleotides. The identification of protein/RNA complexes afterwards was done by mass spectrometry (MS). For *CCW12* mRNP purification, the TRIP protocol was employed using the ASO 3 from this study. The results were not as satisfying as with the mRNA purification

described in this study. In purifying the PFK2 enzyme, the new TAP based mRNP purification proved to be more efficient as compared to publications which used TRIP in qPCR experiments.

Many other groups have aimed to identify the composition of mRNPs by proteolytic digestion coupled with MS. Even though this experiment was remarkably successful in terms of determining proteins which are purified with target mRNAs, there are still not much information on the structures of the mRNPs and how the composition of an mRNP determines the fate of its mRNA (Gehring *et al.* 2017).

The laboratory of Ed Hurt published on the overall structure of nuclear mRNP by analyzing the TAP purification of Nab2 (Batisse *et al.* 2009). The authors showed a correlation between the mRNP size and the bp length of the mRNA. The authors used another TAP tagged protein for the purification as this study. Here our study includes a second step which addressed a specific nuclear mRNP with the unique 3'-biotinylated 2'-O-methylated antisense RNA oligonucleotides. This additional level of purification increases the amount of a single nuclear mRNP species which can be further analyzed. In Figure 37, the observed particles from negative stained *CCW12* mRNPs matched the predicted particle size of an mRNP with around 1.1 k bp.

A follow up experiment using cryo – EM (Figure 50) is a handy technique to gain insight in the structure the target. This method measures the electron density map specific to the target nuclear mRNP. Additional cross-linking MS (XL-MS) experiments (Figure 51) further elucidate the interaction of the RBPs bound to the mRNA. Knowing exactly which and how proteins in the mRNP are interacting makes it easier to define stringent parameters for modelling the complex.

To build the 3D-structure of a yeast and nuclear specific mRNP, a combination of all known RBPs structures (or the described parts) stored in the PDB collected with methods such as nuclear magnetic resonance (NMR) x-ray crystallography and small angle scattering (SAS, SAXS) could serve as input data.

Understanding the yeast nuclear mRNP formation might support existing knowledge on mRNP formation in humans which may further help in preventing certain diseases.

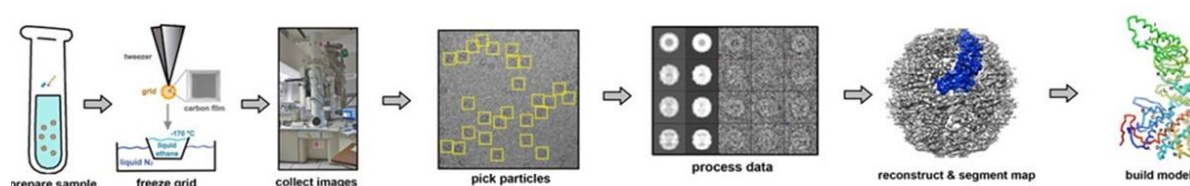


Figure 50. Workflow of cryo EM for mRNP sample analyses

The sample is purified as seen in figure 9. After the anti-sense purification, the sample is move on a grid and frozen. A lot of images are made and particles with the same seize are picked. A program is rendering and processing the data which can be used to reconstruct the nuclear specific mRNP and build a model of it combining data from other sources like NMR, EM and X-ray to it. (by Prof. Junjie Zhang (TAMU) (EM))

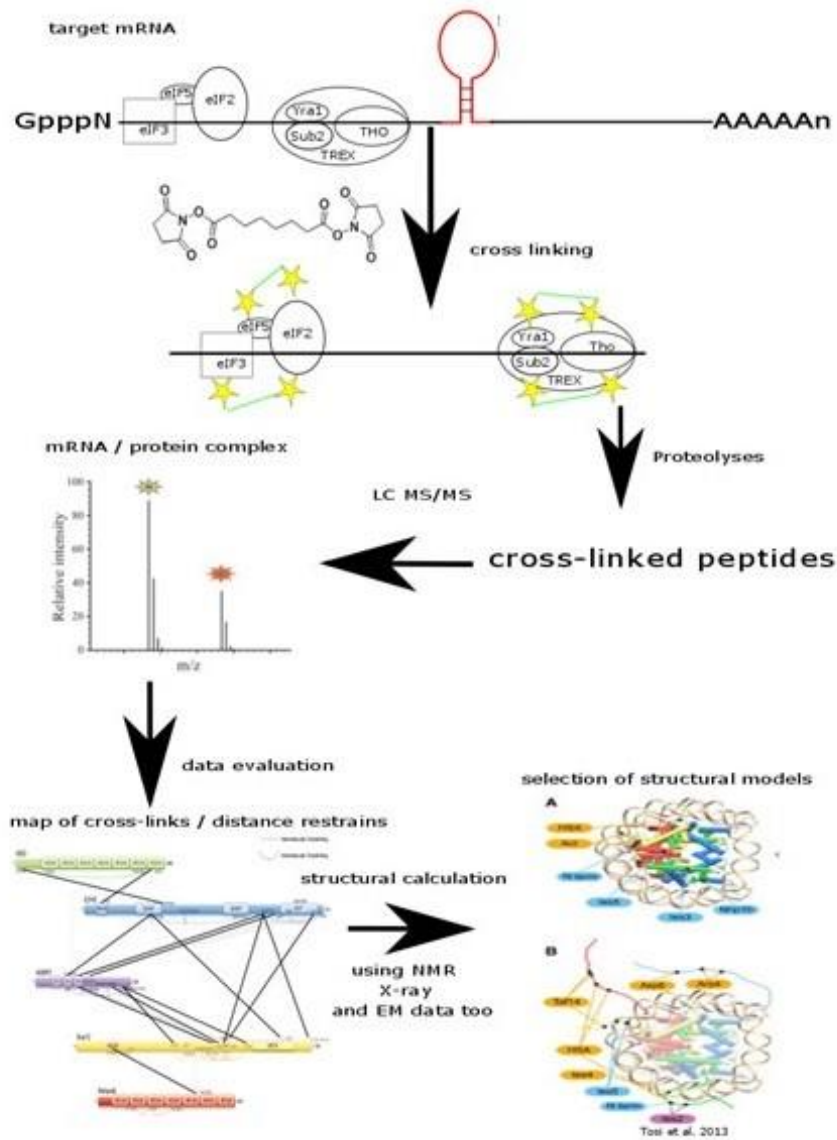


Figure 51. Purification scheme of nuclear mRNP for further structural XL-MS analyses

The target mRNA gets purified with an anti-sense oligo nucleotide (target sequence in red) after cross linking. Purification and proteolysis are followed by the XL-MS measurement, and the data is evaluated in cross-linked maps for distance restraints. In the last step structure from NMR, EM and X-ray are added to refine the 3D structures of the target mRNP.

5 Abbreviations

°C	Celsius
aa	Amino acid
app.	Approximately
APS	Ammonium persulfate
bp	Base pair
C-	carboxy-terminal
CBP	Calmodulin binding peptide
cDNA	Complementary DNA
ChIP	Chromatin Immunoprecipitation
conc.	concentration
CTD	C-terminal domain
CTR	C-terminal region
Dapi	4',6-diamidino-2-phenylindole
ddH ₂ O	double-distilled water
DMSO	dimethyl sulfoxide
DNA	deoxyribonucleic acid
dNTP	deoxyribonucleoside triphosphate
Ds	Double strand
DTT	dithiothreitol
<i>E. coli</i>	<i>Escherichia coli</i>
EDTA	ethylene diamine tetraacetic acid
fw	forward
H	Hour(s)
Ha	hemagglutinin
HEPES	4-(2-hydroxyethyl)-1-piperazineethanesulfonic acid
Ig g	immunoglobulin G
kDa	Kilo dalton
l	Liters
M	Molar
min	Minutes
mRNA	messenger ribonucleic acid
mRNP	messenger ribonucleo particles
N-	Amino- terminal
NPC	Nuclear pore complex
nt	nucleotides
NTC	Non template control
OD	optical density
ORF	Open reading frame
PAGE	polyacrylamide gel electrophoresis
PBS	phosphate buffered saline
PCI	phenol:chloroform:isoamyl
PCR	polymerase chain reaction
PDB	Protein data base
PEG	polyethylene glycol
pH	potential of hydrogen
PMSF	phenylmethylsulfonyl fluoride
Poly(A)	poly-adenosine
qPCR	quantitative PCR
RNAPII	RNA Polymerase II

RNAse	Ribonuclease
Rpm	revolutions per minute
RRM	RNA recognition motif
RT	room temperature
rv	reverse
<i>S. cerevisiae</i>	<i>Saccharomyces cerevisiae</i>
SDS	sodium dodecyle sulphate
sec	seconds
TAP	Tandem Affinity Purification
TCA	trichloro-acetic acid
TEMED	tetramethylethylenediamine
TEV	Tobacco etch virus
TREX	transcription and export complex
THO	suppressor of transcriptional defect of Hpr1 by overexpression
TRIS	tris(hydroxymethyl)aminomethane
UZ	Ultracentrifugation step
v/v	volume per volume
w/v	Weight per volume
wt	Wild type
α	alpha
β	beta
γ	gamma
μ	micro

6 Acknowledgements

First of all, I would like to thank my supervisor Prof. Katja Sträßer for giving me the opportunity to work on such an important, challenging and interesting project. I am grateful for our scientific discussions, their support and their ideas to solve problems along way. Whenever I needed something even if they could not help me directly, they always knew someone whom I shall send an email. Thank you for believing in me, let me do my work and always be a supporter.

I want to thank Prof. Dr. Elena Evguenieva-Hackenberg for being head of my thesis committee and my second supervisor. Moreover, I want to thank her for our scientific discussion at the GGL meetings and being our speaker of section 4. I will miss our annual conference in September and our section 4 meeting.

I would like to thank all other members of my thesis evaluation committee for their time, their opinion and scientific discourse on my thesis.

Many thanks to Dr. Martin Hardt and Anna Möbus from the imaging unit of the BFS in Giessen for helping me with sample preparation and picture interpretation at the EM. With their help we have been able to show that we can purify nuclear mRNPs with our method.

I am grateful to the European research council for funding two years of my research on the mRNP project with an ERC consolidation grand.

If I needed help with IT related matters Dr. Wolfgang Wende was always there to help me. I could ask him any time if he helping me fix an IT problem or for advice. Thanks, also to Apl. Prof. Dr. Peter Friedhoff, I very enjoyed his and Dr. Wolfgang Wende's scientific input into my progress report. Thanks both of them for sharing their expertise and ideas from "outside" the yeast field to broaden my biochemical horizon. It helped me a lot looking at my project from a different point of view to solve problems and move on.

Thanks also to Dr. Cornelia Kilchert for patiently answering my scientific question about methodology on working with *Saccharomyces cerevisiae* vs *Schizosaccharomyces pombe*.

Many thanks to Nataliia and Johanna, my lab mates and fellow PhD students who continue working on this fascinating project. It was a pleasure to introduce them to the fascinating world of nuclear mRNP and working together with them on this exciting topic. Thank them for being there and helping me to split the work among the three of us else I would be lost and would still test all temperatures and buffers. I believe in them and I am sure they will write a paper about a specific nuclear mRNP in the future. "Don't stop believing" (Journey 1981)

I want to thank Dr. Rashmi Minocha, a former student of the Sträßer lab, who worked with me for about three years in Giessen. It was a pleasure to work with you through the nights at the lab always waiting for latest results. I much enjoyed our talk about science and the philosophy of live. Thank you, many times, for your help and advice when I needed it. I really miss our night lab sessions. Thank you for taking the time and help correction the thesis.

Thanks also to the technicians in the lab, Bethy, Melanie, Merle, and Heike, for introducing me to the specific lab techniques. Thanks Melanie, for sharing her interesting insides about plant biology and horse stories to lighten up our days or try to motivate us with some quotes she found on the internet. I really appreciated it. Special thanks to Heike for purifying enzyme like TEV and Tac polymerase and being there over the whole five years. Her help was very appreciated, and it was always pleasant to talk with her and Carsten inside and outside the lab.

Thanks to the people in the Strässer lab (including AG Friedhoff, AG Kilchert and AG Wende) for being around and making work in the lab more enjoyable. Even during difficult times it was always nice to talk with them not only about work but also about life in general, Birte, Franzi, Kristin, Laura, Johanna, Nataliia, Philipp and Michael thank you all for being part of the AG Strässer and working around me in the lab on such exciting stuff. It was nice to share with them my experience and learn from them much about how to execute or improve my own methods. Their help in “killing the Haribo sweets” was appreciated. Thanks for the great memories from our lab retreats or our meeting outside the lab like a birthday, a “Polterabend”, a marriage or just a weekly social gathering. It was fun spending the time with them.

Thank you, Steven from AG Bindereif, for or lovely talks about science and God. May we never stop believing in doing the right for a better future. I wish you all the best mate follow the part and be happy. Do not let any negative influences bring you down.

Thanks to the students attending my “TAP purification” course. It was a pleasure to teach and I hope you learned something for life.

Thank you to Prof. Dr. Eveline Baumgart-Vogt for instituting the GGL, which was an important during my studies in Giessen. I am very thankful for the opportunity to meet and work with people from different scientific directions at the JLU during my time at GGL.

Special thanks to Eistine, Vannur and Wendell and the others (from India, Iran, Nepal, Czech Republic, China...) for spending so much time with me on the weekends to take a little break from science and playing soccer (with Silke and Greta), talking about life, playing music and Indians or just spending some time together. I will miss these weekends.

I am very thankful to Dr. Eistine “Einstein” Boateng for his spontaneous passion to proofread and correct my manuscript. Thank you for your help and input. Without you I could not have made it.

Also, thanks to Rashmi and Abhishri for additional proofreading and corrections too.

Working for five years in Giessen, one must sleep at night and call a place home. I got the possibility to live in a student dorm called Unterhof. Nearly 700 people live there in distance from my laboratory. I want to thank the people of my first WG like Sebastian and Kien for having a wonderful time before moving to the third floor. Room 531 Unterhof 59 was my hide out from the real life. Surrounded by lovely Roommates Lea, Samira, Lisa, Niclas, Luisa (Majid), Mathias and Marie. Words cannot express how much you all meant to me during my time living with you. Over the time we have become more like a family. There is not enough space to mention all the nice things we did together, but I will always love you and thank you from the bottom of my heart.

Fernab von meinem Arbeits- und Freundeskreis in Gießen gibt es noch Menschen in Rheinland-Pfalz und Bayern, die mir sehr wichtig sind und denen ich zu großem Dank verpflichtet bin.

Da wäre mein guter Freund Tobi, mein erster „Langzeit WG-Nachbar“. Ich denke die Zeit war nicht immer einfach für uns zwei, aber ich konnte dabei viel lernen. Danke, dass du mich immer unterstützt und an mich geglaubt hast.

Danke an der Stelle auch an die vielen Freunde, die ich in Regensburg kennen gelernt habe, wie z.B. Lais, Katja, Georg, Julko, Pavel, etc. Ich vermisse euch sehr und hoffe euch in Zukunft mal alle besuchen zu können.

Ich möchte mich auch bei Matthias bedanken. Danke für unsere Gespräche und die Freundschaft über Jahre hinweg verbunden durch den gemeinsamen Glauben an Gott. Danke mein Freund.

„Familie: Wo das Leben seinen Anfang nimmt und die Liebe niemals endet“ (Autor unbekannt)

Der größte Dank gilt meiner Familie. Danke an meine Eltern Paul und Ute, für ihre Liebe und Unterstützung in allen Lebenslagen. Danke auch an meinen Bruder Patrick, weil ich immer auf ihn zählen kann.

7 Figures

Figure 1. Regulation of gene expression	1
Figure 2. A schematic showing pre-mRNA splicing in yeast	3
Figure 3. Schema of early mRNP formation during mRNA processing.....	4
Figure 4. Steps of mRNP biogenesis.....	5
Figure 5. Schema of the Rbp1 CTD repeats.....	6
Figure 6. Scheme of TREX function in transcription and mRNA export	9
Figure 7. Schematic of domain organization comparison	12
Figure 8. Schematic view of interaction (Y-relationship) between Tho1 and TREX / PAF complex	14
Figure 9. Spt5-CTR S1A mutations lead to decreased Tho1 and Paf1 occupancies	34
Figure 10. Western blot of PAF1-TAP with and without overexpression of Tho1	35
Figure 11. ChIP of Paf1-TAP with and without THO1 overexpression.....	36
Figure 12. ChIP of Paf1-TAP with and without THO1.....	37
Figure 13. RNAPII ChIP THO1 overexpression.....	37
Figure 14. RNAPII ChIP THO1 overexpression.....	38
Figure 15. Spt5-TAP ChIP in RS453 strain $\pm \Delta tho1$	39
Figure 16. Spt5-TAP ChIP in a \pm Tho1 deletion RS453 strain	39
Figure 17. RNAPII ChIP in a RS453 strain $\pm \Delta tho1$	40
Figure 18. RNAPII ChIP in a \pm Tho1 deletion RS453 strain	40
Figure 19. Paf1-TAP ChIP in RS453 strain $\pm \Delta tho1$	41
Figure 20. Paf1-TAP ChIP in a \pm Tho1 deletion RS453 strain	42
Figure 21. RT-qPCR experiment in yeast WCE	44
Figure 22. Schematic view of a nuclear specific CCW12 mRNP	45
Figure 23. CCW12 Aso purification in RS453 WCE.....	46
Figure 24. Dynabeads Test with CCW12 ASO 2 and 8	47
Figure 25. nuclear mRNP purification with TEV and WCE in WB comparison.....	48
Figure 26. mRNP purification in a Hpr1-TAP strain with or without high salt buffer	49
Figure 27. WB set for mRNA purification experiments in a Cbc2-TAP strain.....	50
Figure 28. WB analysis of various CCW12 ASO mix compared to ASO 2 and lysate	51
Figure 29. WB of various CCW12 ASO mix compared to ASO 2 and lysate at 10 k rpm part I.....	52
Figure 30. WB of various CCW12 ASO mix compared to ASO 2 and lysate at 10 k rpm part II.....	52
Figure 31. WB analysis of CCW12 ASO 1-8 at 10 k rpm UZ.....	53
Figure 32. WB analysis of CCW12 ASO 1-8 without UZ.....	53
Figure 33. Cross-linking of Hpr1-TAP with formaldehyde and glutaraldehyde.....	55
Figure 34. Cbc2-TAP with or without ATP- γ -S and three different concentrations of MgCl ₂	56
Figure 35. WB analysis of biotin and desthiobiotin eluted samples for EM.....	57
Figure 36. Negative stains from CCW12 biotin elution and displacement oligonucleotide elution.....	58
Figure 37. Biotin elution samples of (desthio)biotinylated CCW12 ASO 3 under the EM.....	58
Figure 38. ILV5 11 and 10 mRNP elution with biotin from magnetic beads	59
Figure 39. First biotin elution of ILV5 ASO 11 under the EM.....	60
Figure 40. mRNA export defect in a Hpr1-TAP mex67-5 strain	61
Figure 41. mRNA export defect in a Cbc2-TAP mex67-5 strain.....	61
Figure 42. WB comparison of TRIS and HEPES buffer purified mRNP samples from Cbc2-TAP.....	62
Figure 43. Comparison of CCW12 ASO 3 annealing at 4°C, RT and 50°C	64
Figure 44. Old wash buffer and Gerber buffer at three different annealing temperatures.....	65
Figure 45. CCW12 mRNA purification with two ASO 3 at 4 °C vs RT annealing temperature.....	67
Figure 46. SDS PAGE of CCW12 mRNA purification at different pH values	70
Figure 47. WB of TEV eluates at different pH values	71
Figure 48. WB of denatured mRNP elutions at different pH values.....	72
Figure 49. WB analysis of CCW12 purification using ASO 1 to 3 in Cbc2-TAP \pm CCW12 strains	73
Figure 50. Workflow of cryo EM for mRNP sample analyses	79
Figure 51. Purification scheme of nuclear mRNP for further structural XL-MS analyses.....	80

8 Tables

Table 1. The level of CTD modifications through the transcription cycle.....	7
Table 2. Equipment	16
Table 3. yeast strains	17
Table 4. <i>e. coli</i> strains.....	18
Table 5. plasmids used	18
Table 6. Oligonucleotides for genomic tagging	19
Table 7. Oligonucleotides for qPCR	19
Table 8. anti-sense oligonucleotides for mRNP purification	20
Table 9. Composition of growth media.....	20
Table 10. Buffers and solutions.....	21
Table 11. Kits used.....	22
Table 12. List of primary antibodies used for Western-blotting	22
Table 13 List of secondary antibodies used for Western blotting	23
Table 14 KNOP PCR	23
Table 15 Fusion PCR	24
Table 16 colony PCR in yeast	24
Table 17 SDS polyacrylamide (PAA) gel preparation	25
Table 18 Working scheme for qPCR analysis.....	31
Table 19. Summary of Tho1 interaction results by ChIP	42
Table 20. Copy number of genes in yeast WCE	44
Table 21. Overview of CCW12 Aso purification in RS453 WCE for Figure 17.....	46
Table 22. Testing different OD600 and UV cross-linking for mRNP purification.....	48
Table 23. Testing different TAP strains and UV cross-linking for mRNP purification.....	48
Table 24. qPCR of Cbc2-TAP <i>CCW12</i> mRNP purification from Figure 27.....	50
Table 25. WB pattern comparison of <i>CCW12</i> ASO 2 with ASO mixes at 35k rpm.....	51
Table 26. WB pattern comparison of <i>CCW12</i> ASO 2 with ASO mixes at 10k rpm	52
Table 27. WB pattern comparison of <i>CCW12</i> ASO 1 to 8 at 10k rpm	53
Table 28. WB protein pattern comparison of <i>CCW12</i> ASO 1 to 8 without UZ.....	54
Table 29. copy number calculation for ASO 2 and 3 with different centrifugations	54
Table 30. qPCR of three <i>CCW12</i> ASO 3 purifications with different concentrations of MgCl ₂	56
Table 31. qPCR results of <i>ILV5</i> mRNP purification with ASOs 10 and 11	59
Table 32. qPCR results of <i>CCW12</i> mRNP purification with TRIS and HEPES buffer	63
Table 33. qPCR results of <i>CCW12</i> mRNP purification with diluted TEV eluate	63
Table 34. qPCR of <i>CCW12</i> mRNP purification with different annealing temperatures	64
Table 35. Buffer comparison at three different temperatures.....	65
Table 36. qPCR from mRNP purification using ASO 3 at 4°C and RT during the annealing step	67
Table 37. qPCR from denatured mRNP purification using ASO 3 at 4°C and RT.....	68
Table 38. qPCR results from <i>CCW12</i> mRNP purification using 1, 6 and 12 µl ASO 1-3	69
Table 39. qPCR results from RNase H assay using ASO 1 to 3	69
Table 40. qPCR results from <i>CCW12</i> mRNP purification at pH 6.8, 7.8 and 8.0.....	72
Table 41. qPCR results of <i>CCW12</i> mRNP purification in Cbc2-TAP with and without <i>CCW12</i>	74
Table 42. qPCR results of <i>ILV5</i> mRNP purification in Cbc2-TAP with and without <i>ILV5</i>	74
Table 43. Summary of adapted changes applied to the mRNP purification protocol	76

9 Equations

Equation 1 Quality criteria for nuclear mRNP purification by qPCR	32
Equation 2 copy number calculatio for qPCR.....	33

10 References

- Abruzzi KC, Lacadie S, Rosbash M (2004) Biochemical analysis of TREX complex recruitment to intronless and intron-containing yeast genes. *EMBO J* 23:2620–2631
- Aguilera A, Garcia-Muse T (2012) R loops: from transcription byproducts to threats to genome stability. *Mol Cell* 46:115–124
- Aibara S, Gordon JM, Riesterer AS, McLaughlin SH, Stewart M (2017) Structural basis for the dimerization of Nab2 generated by RNA binding provides insight into its contribution to both poly(A) tail length determination and transcript compaction in *Saccharomyces cerevisiae*. *Nucleic Acids Res* 45:1529–1538
- Alcázar-Román AR, Tran EJ, Guo S, Wentz SR. (2006) Inositol hexakisphosphate and Gle1 activate the DEAD box protein Dbp5 for nuclear mRNA export. *Nat Cell Biol* 8 (7): 711–716.
- Amos JS, Huang L, Thevenon J, Kariminedjad A, Beaulieu CL, Masurel-Paulet A, Najmabadi H, Fattahi Z, Beheshtian M, Tonekaboni SH et al (2017) Autosomal recessive mutations in THOC6 cause intellectual disability: syndrome delineation requiring forward and reverse phenotyping. *Clin Genet* 91:92–99
- Anderson JT, Wilson SM, Datar KV, Swanson MS (1993) NAB2: a yeast nuclear polyadenylated RNA-binding protein essential for cell viability. *Mol Cell Biol* 13:2730–2741
- Ares M, JR, Grate L, Pauling MH. (1999) A handful of intron-containing genes produces the lion's share of yeast mRNA. *RNA* 5 (9): 1138–1139.
- Bataille AR, Jeronimo C, Jacques P, Laramée L, Fortin M, Forest A, Bergeron M et al. (2012) A Universal RNA Polymerase II CTD Cycle Is Orchestrated by Complex Interplays between Kinase, Phosphatase, and Isomerase Enzymes along Genes. *Molecular Cell* 45 (2): 158–170.
- Batisse, J., Batisse, C., Budd, A., Böttcher, B., & Hurt, E. (2009). Purification of nuclear poly(A)-binding protein Nab2 reveals association with the yeast transcriptome and a messenger ribonucleoprotein core structure. *The Journal of biological chemistry*, 284(50), 34911–34917.
- Beaulieu CL, Huang L, Innes AM, Akimenko MA, Puffenberger EG, Schwartz C, Jerry P, Ober C, Hegele RA, McLeod DR et al (2013) Intellectual disability associated with a homozygous missense mutation in THOC6. *Orphanet J Rare Dis* 8:62
- Bienkowski RS, Banerjee A, Rounds JC, Rha J, Omotade OF, Gross C, Morris KJ, Leung SW, Pak C, Jones SK et al (2017) The conserved, disease-associated RNA binding protein dNab2 interacts with the fragile X protein ortholog in *drosophila* neurons. *Cell Rep* 20:1372–1384
- Bjork P, Wieslander L (2017) Integration of mRNP formation and export. *Cell Mol Life Sci* 74:2875–2897
- Blencowe BJ, Sproat BS, Ryder U, Barabino S, Lamond AI (1989). Antisense probing of the human U4/U6 snRNP with biotinylated 2'-OMe RNA oligonucleotides. *Cell*. 3;59(3):531-9.
- Boehringer A, Bowser R (2018) RNA nucleocytoplasmic transport defects in neurodegenerative diseases. *Adv Neurobiol* 20:85–101
- Boehringer A, Garcia-Mansfield K, Singh G, Bakkar N, Pirrotte P, Bowser R (2017) ALS associated mutations in Matrin 3 alter protein-protein interactions and impede mRNA nuclear export. *Sci Rep* 7:14529
- Bradford MM. (1976). A rapid and sensitive method for the quantitation of microgram quantities of protein utilizing the principle of protein-dye binding. *Anal Biochem*.7; 72:248-54.
- Bucheli ME, Buratowski S (2005) Npl3 is an antagonist of mRNA 3' end formation by RNA polymerase II. *EMBO J* 24:2150–2160
- Carey KT, Wickramasinghe VO (2018) Regulatory potential of the RNA processing machinery: implications for human disease. *Trends Genet* 34:279–290
- Carmody SR, Tran EJ, Apponi LH, Corbett AH, Wentz SR (2010) The mitogen-activated protein kinase Slt2 regulates nuclear retention of non-heat shock mRNAs during heat shock-induced stress. *Mol Cell Biol* 30:5168–5179

- Castellano-Pozo M, García-Muse T, Aguilera A. (2013). R-loops cause replication impairment and genome instability during meiosis. *EMBO Rep* 13: 923–929.
- Chanarat S, Burkert-Kautzsch C, Meinel DM, Strasser K (2012) Prp19C and TREX: interacting to promote transcription elongation and mRNA export. *Transcription* 3:8–12
- Chanarat S, Seizl M, Strasser K (2011) The Prp19 complex is a novel transcription elongation factor required for TREX occupancy at transcribed genes. *Genes Dev* 25:1147–1158
- Chang CT, Hautbergue GM, Walsh MJ, Viphakone N, van Dijk TB, Philipsen S, Wilson SA (2013) Chtop is a component of the dynamic TREX mRNA export complex. *EMBO J* 32:473–486
- Chang M, French-Cornay D, Fan HY, Klein H, Denis CL, Jaehning JA (1999) A complex containing RNA polymerase II, Paf1p, Cdc73p, Hpr1p, and Ccr4p plays a role in protein kinase C signaling. *Mol Cell Biol* 19: 1056–1067
- Chávez S, Beilharz T, Rondón AG, Erdjument-Bromage H, Tempst P, Svejstrup JQ, Lithgow T et al. (2000) A protein complex containing Tho2, Hpr1, Mft1 and a novel protein, Thp2, connects transcription elongation with mitotic recombination in *Saccharomyces cerevisiae*. *EMBO J.* 19 (21): 5824– 5834.
- Chavez S, Garcia-Rubio M, Prado F, Aguilera A. (2001) Hpr1 Is Preferentially Required for Transcription of Either Long or G+C-Rich DNA Sequences in *Saccharomyces cerevisiae*. *Molecular and Cellular Biology* 21 (20): 7054–7064.
- Cheng H, Dufu K, Lee CS, Hsu JL, Dias A, Reed R (2006) Human mRNA export machinery recruited to the 50 end of mRNA. *Cell* 127:1389–1400
- Chi B, Wang Q, Wu G, Tan M, Wang L, Shi M, Chang X, Cheng H (2013) Aly and THO are required for assembly of the human TREX complex and association of TREX components with the spliced mRNA. *Nucleic Acids Res* 41:1294–1306
- Chinnam M, Wang Y, Zhang X, Gold DL, Khoury T, Nikitin AY, Foster BA, Li Y, Bshara W, Morrison CD et al (2014) The Thoc1 ribonucleoprotein and prostate cancer progression. *J Natl Cancer Inst* 106
- Cho E, Kobor MS, Kim M, Greenblatt J, Buratowski S. (2001) Opposing effects of Ctk1 kinase and Fcp1 phosphatase at Ser 2 of the RNA polymerase II C-terminal domain. *Genes & Development* 15 (24): 3319–3329.
- Cho E, Takagi T, Moore CR, Buratowski S. (1997) mRNA capping enzyme is recruited to the transcription complex by phosphorylation of the RNA polymerase II carboxy-terminal domain. *Genes & Development* 11 (24): 3319–3326.
- Cooper-Knock J, Walsh MJ, Higginbottom A, Robin Highley J, Dickman MJ, Edbauer D, Ince PG, Wharton SB, Wilson SA, Kirby J et al (2014) Sequestration of multiple RNA recognition motif-containing proteins by C9orf72 repeat expansions. *Brain* 137:2040–2051
- Corbett AH (2018) Post-transcriptional regulation of gene expression and human disease. *Curr Opin Cell Biol* 52:96–104
- Cramer P. (2004) RNA polymerase II structure: from core to functional complexes. *Current Opinion in Genetics & Development* 14 (2): 218–226.
- David CJ, Boyne AR, Millhouse SR, Manley JL. (2011) The RNA polymerase II C-terminal domain promotes splicing activation through recruitment of a U2AF65-Prp19 complex. *Genes & Development* 25 (9): 972–983.
- Denning D, Patel S, Uversky V, Fink A, Rexach M (2003). Disorder in the nuclear pore complex: The FG repeat regions of nucleoporins are natively unfolded. *Proc Natl Acad Sci USA.* 100(5): 2450–5.
- Dermody JL, Dreyfuss JM, Villen J, Ogundipe B, Gygi SP, Park PJ, Ponticelli AS, Moore CL, Buratowski S, Bucheli ME (2008) Unphosphorylated SR-like protein Npl3 stimulates RNA polymerase II elongation. *PLoS One* 3:e3273
- Dominguez-Sanchez MS, Barroso S, Gomez-Gonzalez B, Luna R, Aguilera A (2011a) Genome instability and transcription elongation impairment in human cells depleted of THO/TREX. *PLoS Genet* 7:e1002386
- Dominguez-Sanchez MS, Saez C, Japon MA, Aguilera A, Luna R (2011b) Differential expression of THOC1 and ALY mRNP biogenesis/export factors in human cancers. *BMC Cancer* 11:77

- Dufu K, Livingstone MJ, Seebacher J, Gygi SP, Wilson SA, Reed R (2010) ATP is required for interactions between UAP56 and two conserved mRNA export proteins, Aly and CIP29, to assemble the TREX complex. *Genes Dev* 24:2043–2053
- Egloff S, Zaborowska J, Laitem C, Kiss T, Murphy S. (2012) Ser7 phosphorylation of the CTD recruits the RPAP2 Ser5 phosphatase to snRNA genes. *Mol. Cell* 45 (1): 111–122.
- Fabrega C, Shen V, Shuman S, Lima CD (2003). Structure of an mRNA Capping Enzyme Bound to the Phosphorylated Carboxy-Terminal Domain of RNA Polymerase II. *Molecular Cell* 11 (6): 1549– 1561.
- Fasken MB, Corbett AH (2016) Links between mRNA splicing, mRNA quality control, and intellectual disability. *RNA Dis* 3:e1448
- Ferguson Wilfred J., Braunschweiger K.I., W.R. Braunschweiger, James R. Smith, J. Justin McCormick, Cathy C. Wasmann, Nancy P. Jarvis, Duncan H. Bell, Norman E. Good (1980) Hydrogen ion buffers for biological research. *Analytical Biochemistry*, Volume 104, Issue 2, 1980, Pages 300-310
- Fleckner J, Zhang M, Valcarcel J, Green MR (1997) U2AF(65) recruits a novel human DEAD box protein required for the U2 snRNP-branchpoint interaction. *Genes Dev* 11:1864–1872
- Folco EG, Lee CS, Dufu K, Yamazaki T, Reed R (2012) The proteins PDIP3 and ZC11A associate with the human TREX complex in an ATP-dependent manner and function in mRNA export. *PLoS One* 7:e43804
- Fukuda S, Wu DW, Stark K, Pelus LM (2002) Cloning and characterization of a proliferation-associated cytokine-inducible protein, CIP29. *Biochem Biophys Res Commun* 292:593–600
- Gaillard H, Wellinger RE, Aguilera A (2007) A new connection of mRNP biogenesis and export with transcription-coupled repair. *Nucleic Acids Res* 35:3893–3906
- Gatfield D, Le Hir H, Schmitt C, Braun IC, Kocher T, Wilm M, Izaurralde E (2001) The DEXH/D box protein HEL/UAP56 is essential for mRNA nuclear export in *Drosophila*. *Curr Biol* 11:1716–1721
- Gehring NH, Wahle E, Fischer U (2017) Deciphering the mRNP code: RNA-bound determinants of post-transcriptional gene regulation. *Trends Biochem Sci* 42:369–382
- Germain H, Qu N, Cheng YT, Lee E, Huang Y, Dong OX, Gannon P, Huang S, Ding P, Li Y et al (2010) MOS11: a new component in the mRNA export pathway. *PLoS Genet* 6:e1001250
- Ghosh A, Shuman S, Lima CD. (2011) Structural Insights to How Mammalian Capping Enzyme Reads the CTD Code. *Molecular Cell* 43 (2): 299–310.
- Gilbert W, Guthrie C (2004) The Glc7p nuclear phosphatase promotes mRNA export by facilitating association of Mex67p with mRNA. *Mol Cell* 13:201–212
- Gilbert W, Siebel CW, Guthrie C (2001) Phosphorylation by Sky1p promotes Npl3p shuttling and mRNA dissociation. *RNA* 7:302–313 63
- Gomez-Gonzalez B, Garcia-Rubio M, Bermejo R, Gaillard H, Shirahige K, Marin A, Foiani M, Aguilera A (2011) Genome-wide function of THO/TREX in active genes prevents R-loop-dependent replication obstacles. *EMBO J* 30:3106–3119
- Gonatopoulos-Pournatzis T, Cowling VH (2014) Cap-binding complex (CBC). *Biochem J* 457:231–242
- Good N.E., S. Izawa (1972) Hydrogen ion buffers. *Methods in Enzymology*, Academic Press, Volume 24, Pages 53-68,
- Green DM, Marfatia KA, Crafton EB, Zhang X, Cheng X, Corbett AH (2002) Nab2p is required for poly(A) RNA export in *Saccharomyces cerevisiae* and is regulated by arginine methylation via Hmt1p. *J Biol Chem* 277:7752–7760
- Gromadzka AM, Steckelberg AL, Singh KK, Hofmann K, Gehring NH (2016) A short conserved motif in ALYREF directs cap- and EJC-dependent assembly of export complexes on spliced mRNAs. *Nucleic Acids Res* 44:2348–2361
- Guo S, Hakimi MA, Baillet D, Chen X, Farber MJ, Klein-Szanto AJ, Cooch NS, Godwin AK, Shiekhattar R (2005) Linking transcriptional elongation and messenger RNA export to metastatic breast cancers. *Cancer Res* 65:3011–3016

- Guo S, Liu M, Godwin AK (2012) Transcriptional regulation of hTREX84 in human cancer cells. *PLoS One* 7:e43610
- Gwizdek C, Iglesias N, Rodriguez MS, Ossareh-Nazari B, Hobeika M, Divita G, Stutz F, Dargemont C (2006) Ubiquitin-associated domain of Mex67 synchronizes recruitment of the mRNA export machinery with transcription. *Proc Natl Acad Sci U S A* 103:16376–16381
- Hahn S. (2004) Structure and mechanism of the RNA polymerase II transcription machinery. *Nat. Struct. Mol. Biol.* 11 (5): 394–403.
- Harlen KM, Churchman LS (2017) The code and beyond: transcription regulation by the RNA polymerase II carboxy-terminal domain. *Nat Rev Mol Cell Biol* 18:263–273
- Harlen, K. M., K. L. Trotta, E. E. Smith, M. M. Mosaheb, S. M. Fuchs and L. S. Churchman (2016). "Comprehensive RNA Polymerase II Interactomes Reveal Distinct and Varied Roles for Each Phospho-CTD Residue." *Cell reports* 15(10): 2147-2158.
- Hartmann R, Bindereif A, Schön A and Westhof E (2005) *Handbook of RNA Biochemistry*
- Hartzog GA, Fu J. (2013) The Spt4–Spt5 complex: A multi-faceted regulator of transcription elongation. *RNA polymerase II Transcript Elongation* 1829 (1): 105–115.
- Hashii Y, Kim JY, Sawada A, Tokimasa S, Hiroyuki F, Ohta H, Makiko K, Takihara Y, Ozono K, Hara J (2004) A novel partner gene CIP29 containing a SAP domain with MLL identified in infantile myelomonocytic leukemia. *Leukemia* 18:1546–1548
- Hautbergue GM, Castelli LM, Ferraiuolo L, Sanchez-Martinez A, Cooper-Knock J, Higginbottom A, Lin Y-H, Bauer CS, Dodd JE, Myszczyńska MA et al (2017) SRSF1- dependent nuclear export inhibition of C9ORF72 repeat transcripts prevents neurodegeneration and associated motor deficits. *Nat Commun* 8:16063
- Hautbergue GM, Hung ML, Golovanov AP, Lian LY, Wilson SA (2008) Mutually exclusive interactions drive handover of mRNA from export adaptors to TAP. *Proc Natl Acad Sci U S A* 105:5154–5159
- Hautbergue GM, Hung ML, Walsh MJ, Snijders AP, Chang CT, Jones R, Ponting CP, Dickman MJ, Wilson SA (2009) UIF, a new mRNA export adaptor that works together with REF/ALY, requires FACT for recruitment to mRNA. *Curr Biol* 19:1918–1924
- Heath CG, Viphakone N, Wilson SA (2016) The role of TREX in gene expression and disease. *Biochem J* 473:2911–2935
- Hector RE, Nykamp KR, Dheur S, Anderson JT, Non PJ, Urbinati CR, Wilson SM et al. (2002) Dual requirement for yeast hnRNP Nab2p in mRNA poly(A) tail length control and nuclear export. *EMBO J.* 21 (7): 1800–1810.
- Hobeika M, Brockmann C, Guessing F, Neuhaus D, Divita G, Stewart M, Dargemont C et al. (2009) Structural Requirements for the Ubiquitin-associated Domain of the mRNA Export Factor Mex67 to Bind Its Specific Targets, the Transcription Elongation THO Complex Component Hpr1 and Nucleoporin FXFG Repeats. *Journal of Biological Chemistry* 284 (26): 17575–17583.
- Huang Y, Gattoni R, Stevenin J, Steitz JA (2003) SR splicing factors serve as adapter proteins for TAP-dependent mRNA export. *Mol Cell* 11:837–843
- Huertas P, Aguilera A. (2003) Cotranscriptionally formed DNA:RNA hybrids mediate transcription elongation impairment and transcription-associated recombination. *Mol. Cell* 12 (3): 711–721.
- Hurt, E., Luo, M. -j., Rother, S., Reed, R., and Strasser, K. (2004). Cotranscriptional recruitment of the serine-arginine-rich (SR)-like proteins Gbp2 and Hrb1 to nascent mRNA via the TREX complex. *Proc. Natl. Acad. Sci.* 101, 1858–1862.
- Hurt JA, Obar RA, Zhai B, Farny NG, Gygi SP, Silver PA (2009) A conserved CCCH-type zinc finger protein regulates mRNA nuclear adenylation and export. *J Cell Biol* 185:265–277
- Iadevaia V, Matia-González AM, Gerber AP (2018). An Oligonucleotide-based Tandem RNA Isolation Procedure to Recover Eukaryotic mRNA-Protein Complexes. *J Vis Exp.* 18;(138):58223.

- Iglesias N, Tutucci E, Gwizdek C, Vinciguerra P, Von Dach E, Corbett AH, Dargemont C, Stutz F (2010) Ubiquitin-mediated mRNP dynamics and surveillance prior to budding yeast mRNA export. *Genes Dev* 24:1927–1938
- Jackson BR, Noerenberg M, Whitehouse A (2014) A novel mechanism inducing genome instability in Kaposi's sarcoma-associated herpesvirus infected cells. *PLoS Pathog* 10:e1004098
- Jacobsen, J. O., Allen, M. D., Freund, S. M., & Bycroft, M. (2016). High-resolution NMR structures of the domains of *Saccharomyces cerevisiae* Tho1. *Acta crystallographica. Section F, Structural biology communications*, 72(Pt 6), 500–506.
- Jaehning JA. (2010) The Paf1 complex: Platform or player in RNA polymerase II transcription? *Biochimica et Biophysica Acta (BBA) - Gene Regulatory Mechanisms* 1799 (5-6): 379–388.
- Jensen TH, Boulay J, Rosbash M, Libri D (2001) The DECD box putative ATPase Sub2p is an early mRNA export factor. *Curr Biol* 11:1711–1715
- Jimeno S, Luna R, García-Rubio M, Aguilera A. (2006) Tho1, a novel hnRNP, and Sub2 provide alternative pathways for mRNP biogenesis in yeast THO mutants. *Mol Cell Biol* 26(12):4387-98.
- Jimeno S, Rondón AG, Luna R, Aguilera A. (2002) The yeast THO complex and mRNA export factors link RNA metabolism with transcription and genome instability. *EMBO J.* 21 (13): 3526–3535.
- Johnson SA, Cubberley G, Bentley DL (2009) Cotranscriptional recruitment of the mRNA export factor Yra1 by direct interaction with the 30 end processing factor Pcf11. *Mol Cell* 33:215–226
- Katahira J, Katahira J, Strässer K, Podtelejnikov A, Mann M, Jung JU, Hurt E. (1999) The Mex67p-mediated nuclear mRNA export pathway is conserved from yeast to human. *EMBO J.* 18 (9): 2593–2609.
- Kelly SM, Leung SW, Pak C, Banerjee A, Moberg KH, Corbett AH (2014) A conserved role for the zinc finger polyadenosine RNA binding protein, ZC3H14, in control of poly(A) tail length. *RNA* 20:681–688
- Kelly SM, Bienkowski R, Banerjee A, Melicharek DJ, Brewer ZA, Marena DR, Corbett AH, Moberg KH (2015) The *Drosophila* ortholog of the Zc3h14 RNA binding protein acts within neurons to pattern axon projection in the developing brain. *Dev Neurobiol.* 76:93–106
- Keminer O, Peters R. (1999) Permeability of single nuclear pores. *Biophys J.* 77(1):217-28.
- Kim M, Suh H, Cho E, Buratowski S. (2009) Phosphorylation of the Yeast Rpb1 C-terminal Domain at Serines 2, 5, and 7. *Journal of Biological Chemistry* 284 (39): 26421–26426.
- Kistler AL, Guthrie C (2001) Deletion of MUD2, the yeast homolog of U2AF65, can bypass the requirement for sub2, an essential spliceosomal ATPase. *Genes Dev* 15:42–49
- Klein BJ, Bose D, Baker KJ, Yusoff ZM, Zhang X, Murakami KS. (2011) RNA polymerase and transcription elongation factor Spt4/5 complex structure. *Proceedings of the National Academy of Sciences* 108 (2): 546–550.
- Koschiza Manuel (Master Thesis 2017)
- Kota KP, Wagner SR, Huerta E, Underwood JM, Nickerson JA (2008) Binding of ATP to UAP56 is necessary for mRNA export. *J Cell Sci* 121:1526–1537
- Kress TL, Krogan NJ, Guthrie C (2008) A single SR-like protein, Npl3, promotes pre-mRNA splicing in budding yeast. *Mol Cell* 32:727–734
- Krishnamurthy S, He X, Reyes-Reyes M, Moore C, Hampsey M. (2004) Ssu72 Is an RNA Polymerase II CTD Phosphatase. *Molecular Cell* 14 (3): 387–394.
- Krogan NJ et al. (2003a) The Paf1 complex is required for histone H3 methylation by COMPASS and Dot1p: linking transcriptional elongation to histone methylation. *Mol Cell* 11: 721–729
- Krogan NJ, Kim M, Ahn SH, Zhong G, Kobor MS, Cagney G, Emili A, Shilatifard A, Buratowski S, Greenblatt JF (2002a) RNA polymerase II elongation factors of *Saccharomyces cerevisiae*: a targeted proteomics approach. *Mol Cell Biol* 22: 6979–6992
- Krogan NJ, Minkyu Kim, Amy Tong, Ashkan Golshani, Gerard Cagney, Veronica Canadien, Dawn P. Richards, Bryan K. Beattie, Andrew Emili, Charles Boone, Ali Shilatifard, Stephen Buratowski, Jack Greenblatt (2003b)

- Methylation of Histone H3 by Set2 in *Saccharomyces cerevisiae* Is Linked to Transcriptional Elongation by RNA Polymerase II. *Molecular and Cellular Biology*, 23 (12) 4207-4218
- Kumar R, Corbett MA, van Bon BW, Woenig JA, Weir L, Douglas E, Friend KL, Gardner A, Shaw M, Jolly LA et al (2015) THOC2 mutations implicate mRNA-export pathway in X-linked intellectual disability. *Am J Hum Genet* 97:302–310
- Kumar R, Gardner A, Homan CC, Douglas E, Mefford H, Wieczorek D, Ludecke HJ, Stark Z, Sadedin S, Broad CMG et al (2018) Severe neurocognitive and growth disorders due to variation in THOC2, an essential component of nuclear mRNA export machinery. *Hum Mutat* 39:1126–1138
- Laemmli UK. (1970). Cleavage of structural proteins during the assembly of the head of bacteriophage T4. *Nature*.15;227(5259):680-5.
- Lai MC, Tarn WY (2004) Hypophosphorylated ASF/SF2 binds TAP and is present in messenger ribonucleoproteins. *J Biol Chem* 279:31745–31749
- Lapek JD Jr, Greninger P, Morris R, Amzallag A, Pruteanu-Malinici I, Benes CH, Haas W (2017) Detection of dysregulated protein-association networks by high-throughput proteomics predicts cancer vulnerabilities. *Nat Biotechnol* 35:983
- Leaw CL, Ren EC, Choong ML. (2004). Hcc-1 is a novel component of the nuclear matrix with growth inhibitory function. *Cell Mol Life Sci* 61: 2264–2273.
- Lee MS, Henry M, Silver PA (1996) A protein that shuttles between the nucleus and the cytoplasm is an important mediator of RNA export. *Genes Dev* 10:1233–1246
- Li Y, Lin AW, Zhang X, Wang Y, Wang X, Goodrich DW (2007) Cancer cells and normal cells differ in their requirements for Thoc1. *Cancer Res* 67:6657–6664
- Li Y, Wang X, Zhang X, Goodrich DW (2005) Human hHpr1/p84/Thoc1 regulates transcriptional elongation and physically links RNA polymerase II and RNA processing factors. *Mol Cell Biol* 25:4023–4033
- Lidschreiber M, Leike K, Cramer P. (2013) Cap completion and C-terminal repeat domain kinase recruitment underlie the initiation-elongation transition of RNA polymerase II. *Molecular and Cellular Biology* 33 (19): 3805-3816.
- Linder P, Jankowsky E (2011) From unwinding to clamping – the DEAD box RNA helicase family. *Nat Rev Mol Cell Biol* 12:505–516
- Lindstrom DL, Squazzo SL, Muster N, Burckin TA, Wachter KC, Emigh CA, McCleery JA et al. (2003) Dual Roles for Spt5 in Pre-mRNA Processing and Transcription Elongation Revealed by Identification of Spt5-Associated Proteins. *Molecular and Cellular Biology* 23 (4): 1368–1378.
- Liu C, Yue B, Yuan C, Zhao S, Fang C, Yu Y, Yan D (2015) Elevated expression of Thoc1 is associated with aggressive phenotype and poor prognosis in colorectal cancer. *Biochem Biophys Res Commun* 468:53–58
- Liu Y, Warfield L, Zhang C, Luo J, Allen J, Lang WH, Ranish J et al. (2009) Phosphorylation of the Transcription Elongation Factor Spt5 by Yeast Bur1 Kinase Stimulates Recruitment of the PAF Complex. *Molecular and Cellular Biology* 29 (17): 4852–4863
- Loya, T. J. and D. Reines (2016). Recent advances in understanding transcription termination by RNA polymerase II. *F1000Research* 5: F1000 Faculty Rev-1478.
- Lund MK, Guthrie C. (2005) The DEAD-box protein Dbp5p is required to dissociate Mex67p from exported mRNPs at the nuclear rim. *Mol. Cell* 20 (4): 645–651.
- Luo MJ, Zhou ZL, Magni K, Christoforides C, Rappsilber J, Mann M, Reed R (2001) Pre-mRNA splicing and mRNA export linked by direct interactions between UAP56 and Aly. *Nature* 413:644–647
- Ma WK, Cloutier SC, Tran EJ (2013) The DEAD-box protein Dbp2 functions with the RNA-binding protein Yra1 to promote mRNP assembly. *J Mol Biol* 425:3824–3838
- MacMorris M, Brocker C, Blumenthal T (2003) UAP56 levels affect viability and mRNA export in *Caenorhabditis elegans*. *RNA* 9:847–857

- Mandel, C. R., Y. Bai and L. Tong (2008). Protein factors in pre-mRNA 3'-end processing. *Cellular and molecular life sciences* 65(7-8): 1099-1122.
- Margaritis T, Holstege FC. (2008) Poised RNA Polymerase II Gives Pause for Thought. *Cell* 133 (4): 581– 584.
- Martinez-Rucobo FW, Sainsbury S, Cheung ACM, Cramer P. (2011) Architecture of the RNA polymerase–Spt4/5 complex and basis of universal transcription processivity. *EMBO J* 30 (7): 1302–1310.
- Maeder CI, Kim JI, Liang X, Kaganovsky K, Shen A, Li Q, Li Z, Wang S, Xu XZS, Li JB et al (2018) The THO complex coordinates transcripts for synapse development and dopamine neuron survival. *Cell* 174:1436–1449.e1420
- Masuda S, Das R, Cheng H, Hurt E, Dorman N, Reed R (2005) Recruitment of the human TREX complex to mRNA during splicing. *Genes Dev* 19:1512–1517
- Matia-González AM, Iadevaia V, Gerber AP (2017). A versatile tandem RNA isolation procedure to capture in vivo formed mRNA-protein complexes. *Methods*. 15;118-119:93-100.
- Mayer A, Schrieck A, Lidschreiber M, Leike K, Martin DE, Cramer P. (2012b) The spt5 C-terminal region recruits yeast 3' RNA cleavage factor I. *Mol. Cell. Biol.* 32 (7): 1321–1331.
- Mayer, A., M. Heidemann, M. Lidschreiber, A. Schrieck, M. Sun, C. Hintermair, E. Kremmer, D. Eick and P. Cramer (2012). CTD tyrosine phosphorylation impairs termination factor recruitment to RNA polymerase II. *Science* 336(6089): 1723-1725.
- Mayr C, Bartel DP. (2009) Widespread Shortening of 3'UTRs by Alternative Cleavage and Polyadenylation Activates Oncogenes in Cancer Cellst. *Cell* 138 (4): 673–684.
- McHugh, C. A., Chen, C. K., Chow, A., Surka, C. F., Tran, C., McDonel, P., Pandya-Jones, A., Blanco, M., Burghard, C., Moradian, A., Sweredoski, M. J., Shishkin, A. A., Su, J., Lander, E. S., Hess, S., Plath, K., & Guttman, M. (2015). The Xist lncRNA interacts directly with SHARP to silence transcription through HDAC3. *Nature*, 521(7551), 232–236.
- Meignin C, Davis I (2008) UAP56 RNA helicase is required for axis specification and cytoplasmic mRNA localization in *Drosophila*. *Dev Biol* 315:89–98
- Meinel Dissertation 2013
- Meinel, D. M. and K. Strasser (2015). Co-transcriptional mRNP formation is coordinated within a molecular mRNP packaging station in *S. cerevisiae*. *Bioessays* 37(6): 666-677.
- Meinel, D. M., C. Burkert-Kautzsch, A. Kieser, E. O'Duibhir, M. Siebert, A. Mayer, P. Cramer, J. Soding, F. C. Holstege and K. Strasser (2013). Recruitment of TREX to the transcription machinery by its direct binding to the phospho-CTD of RNA polymerase II. *PLoS Genet* 9(11): e1003914.
- Minajigi A, Froberg J, Wei C, Sunwoo H, Kesner B, Colognori D, Lessing D, Payer B, Boukhali M, Haas W, Lee JT (2015). Chromosomes. A comprehensive Xist interactome reveals cohesin repulsion and an RNA-directed chromosome conformation. *Science*. 17;349(6245):10.1126/science.aab2276 aab2276
- Mohr, Dagmar; Frey, Steffen; Fischer, Torsten; Güttler, Thomas; Görlich, Dirk (2009). Characterisation of the passive permeability barrier of nuclear pore complexes. *The EMBO Journal*. 28 (17): 2541–2553.
- Morris DPGA. (2000) The Splicing Factor, Prp40, Binds the Phosphorylated Carboxyl-terminal Domain of RNA Polymerase II. *Journal of Biological Chemistry* 275 (51): 39935–39943.
- Mosley AL, Pattenden SG, Carey M, Venkatesh S, Gilmore JM, Florens L, Workman JL et al. (2009) Rtr1 Is a CTD Phosphatase that Regulates RNA Polymerase II during the Transition from Serine 5 to Serine 2 Phosphorylation. *Molecular Cell* 34 (2): 168–178.
- Mueller CL, Jaehning JA (2002) Ctr9, Rtf1, and Leo1 are components of the Paf1/RNA polymerase II complex. *Mol Cell Biol* 22: 1971–1980
- Muller-McNicoll M, Botti V, de Jesus Domingues AM, Brandl H, Schwich OD, Steiner MC, Curk T, Poser I, Zarnack K, Neugebauer KM (2016) SR proteins are NXF1 adaptors that link alternative RNA processing to mRNA export. *Genes Dev* 30:553–566

- Ng H.H., Dole S. and Struhl K. (2003) The Rtf1 component of the Paf1 transcriptional elongation complex is required for ubiquitination of histone H2B. *J. Biol. Chem.* 278: 33625-33628
- Nino CA, Herissant L, Babour A, Dargemont C (2013) mRNA nuclear export in yeast. *Chem Rev* 113:8523–8545
- Noble KN, Tran EJ, Alcazar-Roman AR, Hodge CA, Cole CN, Wentz SR. (2011) The Dbp5 cycle at the nuclear pore complex during mRNA export II: nucleotide cycling and mRNP remodeling by Dbp5 are controlled by Nup159 and Gle1. *Genes & Development* 25 (10): 1065–1077.
- Noble SM, Guthrie C (1996) Transcriptional pulse-chase analysis reveals a role for a novel snRNP-associated protein in the manufacture of spliceosomal snRNPs. *EMBO J* 15:4368–4379
- Nojima T, Hirose T, Kimura H, Hagiwara M (2007) The interaction between cap-binding complex and RNA export factor is required for intronless mRNA export. *J Biol Chem* 282:15645–15651
- Oeffinger M, Zenklusen D. (2012) To the pore and through the pore: A story of mRNA export kinetics. *Biochimica et Biophysica Acta (BBA) - Gene Regulatory Mechanisms* 1819 (6): 494–506.
- Ohl MD, Vander Kooi CW, Rosenberg JA, et al. (2005) Structural and functional analysis of essential pre-mRNA splicing factor Prp19p. *Mol Cell Biol.* 25(1):451-460.
- Ozsolak F, Kapranov P, Foissac S, Kim SW, Fishilevich E, Monaghan AP, John B et al. (2010) Comprehensive Polyadenylation Site Maps in Yeast and Human Reveal Pervasive Alternative Polyadenylation. *Cell* 143 (6): 1018–1029.
- Peters R (2006). Introduction to nucleocytoplasmic transport: molecules and mechanisms. *Methods Mol Biol. Methods in Molecular Biology™.* 322. pp. 235–58
- Piruat JI, Aguilera A. (1998) A novel yeast gene, THO2, is involved in RNA pol II transcription and provides new evidence for transcriptional elongation-associated recombination. *EMBO J.* 17;17(16):4859-72.
- Pokholok DK, Hannett NM, Young RA (2002) Exchange of RNA polymerase II initiation and elongation factors during gene expression in vivo. *Mol Cell* 9: 799–809
- Proudfoot NJ. (2011) Ending the message: poly(A) signals then and now. *Genes & Development* 25 (17): 1770–1782.
- Puig, O., F. Caspary, G. Rigaut, B. Rutz, E. Bouveret, E. Bragado-Nilsson, M. Wilm and B. Seraphin (2001). The tandem affinity purification (TAP) method: a general procedure of protein complex purification. *Methods* 24(3): 218-229.
- Qiu H, Hu C, Gaur NA, Hinnebusch AG. (2012a) Pol II CTD kinases Bur1 and Kin28 promote Spt5 CTR-independent recruitment of Paf1 complex. *EMBO J* 31 (16): 3494–3505.
- Qiu H, Hu C, Hinnebusch AG (2009). Phosphorylation of the Pol II CTD by KIN28 Enhances BUR1/BUR2 Recruitment and Ser2 CTD Phosphorylation Near Promoters. *Molecular Cell* 33 (6): 752–762.
- Reichelt, R; Holzenburg, A; Buhle Jr., E L; Jarnik, M; Engel, A; Aebi, U. (1990) Correlation between Structure and Mass Distribution of the Nuclear Pore Complex and of Distinct Pore Complex Components. *Journal of Cell Biology.* 110(4): 883–894.
- Ren Y, Schmiege P, Blobel G (2017) Structural and biochemical analyses of the DEAD-box ATPase Sub2 in association with THO or Yra1. *Elife* 6
- Reuter LM, Meinel DM, Strasser K (2015) The poly(A)-binding protein Nab2 functions in RNA polymerase III transcription. *Genes Dev* 29:1565–1575
- Richard, P., and J. L. Manley (2009). Transcription termination by nuclear RNA polymerases. *Genes Dev* 23(11): 1247-1269
- Röther, S., Burkert, C., Brünger, K. M., Mayer, A., Kieser, A., & Strässer, K. (2010). Nucleocytoplasmic shuttling of the La motif-containing protein Sro9 might link its nuclear and cytoplasmic functions. *RNA (New York, N.Y.)*, 16(7), 1393–1401.
- Rout MP, Blobel G. (1993) Isolation of the yeast nuclear pore complex. *J. Cell Biol.* 123(4): 771–83.

- Saguez C, Gonzales FA, Schmid M, Boggild A, Latrick CM, Malagon F, Putnam A, Sanderson L, Jankowsky E, Brodersen DE et al (2013) Mutational analysis of the yeast RNA helicase Sub2p reveals conserved domains required for growth, mRNA export, and genomic stability. *RNA* 19:1363–1371
- Saito Y, Kasamatsu A, Yamamoto A, Shimizu T, Yokoe H, Sakamoto Y, Ogawara K, Shiiba M, Tanzawa H, Uzawa K (2013) ALY as a potential contributor to metastasis in human oral squamous cell carcinoma. *J Cancer Res Clin Oncol* 139:585–594
- Salas-Armenteros I, Pérez-Calero C, Bayona-Feliu A, Tumini E, Luna R, Aguilera A (2017) Human THO–Sin3A interaction reveals new mechanisms to prevent R-loops that cause genome instability. *EMBO J* 36:3532–3547
- Sambrook and Russell (2001): *Molecular cloning A Laboratory manual*
- Sandberg R, Neilson JR, Sarma A, Sharp PA, Burge CB. (2008) Proliferating Cells Express mRNAs with Shortened 3' Untranslated Regions and Fewer MicroRNA Target Sites. *Science* 320 (5883): 1643–1647.
- Santos-Pereira JM, Aguilera A (2015) R loops: new modulators of genome dynamics and function. *Nat Rev Genet* 16:583–597
- Santos-Rosa H, Moreno H, Simos G, Segref A, Fahrenkrog B, Panté N, Hurt E et al. (1998) Nuclear mRNA export requires complex formation between Mex67p and Mtr2p at the nuclear pores. *Mol. Cell. Biol.* 18 (11): 6826–6838.
- Schumann S, Baquero-Perez B, Whitehouse A (2016a) Interactions between KSHV ORF57 and the novel human TREX proteins, CHTOP and CIP29. *J Gen Virol* 97:1904–1910
- Segref A, Sharma K, Doye V, Hellwig A, Huber J, Luhrmann R, Hurt E (1997) Mex67p, a novel factor for nuclear mRNA export, binds to both poly(A)⁺ RNA and nuclear pores. *EMBO J* 16:3256–3271
- Shen JP, Zhang LD, Zhao R (2007) Biochemical characterization of the ATPase and helicase activity of UAP56, an essential pre-mRNA splicing and mRNA export factor. *J Biol Chem* 282:22544–22550
- Shi M, Zhang H, Wu X, He Z, Wang L, Yin S, Tian B, Li G, Cheng H (2017) ALYREF mainly binds to the 50 and the 30 regions of the mRNA in vivo. *Nucleic Acids Res* 45:9640–9653
- Shi, H., Cordin, O., Minder, C. M., Linder, P., & Xu, R. M. (2004). Crystal structure of the human ATP-dependent splicing and export factor UAP56. *Proceedings of the National Academy of Sciences of the United States of America*, 101(51), 17628–17633.
- Sikorski, R. S. and P. Hieter (1989). A system of shuttle vectors and yeast host strains designed for efficient manipulation of DNA in *Saccharomyces cerevisiae*. *Genetics* 122(1): 19-27.
- Simone R, Balendra R, Moens TG, Preza E, Wilson KM, Heslegrave A, Woodling NS, Niccoli T, Gilbert-Jaramillo J, Abdelkarim S et al (2018) G-quadruplex-binding small molecules ameliorate C9orf72 FTD/ALS pathology in vitro and in vivo. *EMBO Mol Med* 10:22–31
- Sims, R. J., 3rd, R. Belotserkovskaya and D. Reinberg (2004). Elongation by RNA polymerase II: the short and long of it. *Genes Dev* 18(20): 2437-2468.
- Squazzo SL, Costa PJ, Lindstrom DL, Kumer KE, Simic R, Jennings JL, Link AJ, Arndt KM, Hartzog GA (2002) The Paf1 complex physically and functionally associates with transcription elongation factors in vivo. *EMBO J* 21: 1764–1774 Volume 162, Issue 5, Pages 1016-1028
- Strahm Y, Fahrenkrog B, Zenklusen D, Rychner E, Kantor J, Rosbash M, Stutz F (1999) The RNA export factor Gle1p is located on the cytoplasmic fibrils of the NPC and physically interacts with the FG-nucleoporin Rip1p, the DEAD-box protein Rat8p/Dbp5p and a new protein Ymr255p. *EMBO J* 18:5761–5777
- Strasser K, Bassler J, Hurt E (2000) Binding of the Mex67p/Mtr2p heterodimer to FXFG, GLFG, and FG repeat nucleoporins is essential for nuclear mRNA export. *J Cell Biol* 150:695–706
- Strasser K, Hurt E (2000) Yra1p, a conserved nuclear RNA-binding protein, interacts directly with Mex67p and is required for mRNA export. *EMBO J* 19:410–420
- Strasser K, Hurt E (2001) Splicing factor Sub2p is required for nuclear mRNA export through its interaction with Yra1p. *Nature* 413:648–652

- Strasser, K., S. Masuda, P. Mason, J. Pfannstiel, M. Oppizzi, S. Rodriguez-Navarro, A. G. Rondon, A. Aguilera, K. Struhl, R. Reed and E. Hurt (2002). "TREX is a conserved complex coupling transcription with messenger RNA export." *Nature* 417(6886): 304-308.
- Student (1908). The Probable Error of a Mean. In: *Biometrika*. Band 6, Nr. 1, S. 1–25,
- Taniguchi I, Ohno M (2008) ATP-dependent recruitment of export factor Aly/REF onto intronless mRNAs by RNA helicase UAP56. *Mol Cell Biol* 28:601–608
- Thomas, B. J. and R. Rothstein (1989). Elevated recombination rates in transcriptionally active DNA. *Cell* 56(4): 619-630.
- Tian B, Manley JL. (2013) Alternative cleavage and polyadenylation: the long and short of it. *Trends in Biochemical Sciences* 38 (6): 312-320.
- Tietjen JR, Zhang DW, Rodríguez-Molina JB, White BE, Akhtar MS, Heidemann M, Li X et al. (2010) Chemicalgenomic dissection of the CTD code. *Nat Struct Mol Biol* 17 (99): 1154–1161.
- Topisirovic, I., Y. V. Svitkin, N. Sonenberg and A. J. Shatkin (2011). Cap and cap-binding proteins in the control of gene expression. *Wiley Interdiscip Rev RNA* 2(2): 277-298.
- Tran EJ, Zhou Y, Corbett AH, Wentz SR. (2007) The DEAD-box protein Dbp5 controls mRNA export by triggering specific RNA:protein remodeling events. *Mol. Cell* 28 (5): 850–859.
- Viphakone N, Cumberbatch MG, Livingstone MJ, Heath PR, Dickman MJ, Catto JW, Wilson SA (2015) Luszp4 defines a new mRNA export pathway in cancer cells. *Nucleic Acids Res* 43:2353–2366
- Viphakone N, Hautbergue GM, Walsh M, Chang CT, Holland A, Folco EG, Reed R, Wilson SA (2012) TREX exposes the RNA-binding domain of Nxf1 to enable mRNA export. *Nat Commun* 3:1006
- Vitaliano-Prunier A, Babour A, Herissant L, Apponi L, Margaritis T, Holstege FC, Corbett AH, Gwizdek C, Dargemont C (2012) H2B ubiquitylation controls the formation of exportcompetent mRNP. *Mol Cell* 45:132–139
- Walsh MJ, Cooper-Knock J, Dodd JE, Stopford MJ, Mihaylov SR, Kirby J, Shaw PJ, Hautbergue GM (2015) Invited review: decoding the pathophysiological mechanisms that underlie RNA dysregulation in neurodegenerative disorders: a review of the current state of the art. *Neuropathol Appl Neurobiol* 41:109–134
- Werner F, Grohmann D. (2011) Evolution of multisubunit RNA polymerases in the three domains of life. *Nat Rev Micro* 9 (2): 85–98.
- West, M. L. and J. L. Corden (1995). "Construction and analysis of yeast RNA polymerase II CTD deletion and substitution mutations." *Genetics* 140(4): 1223-1233.
- Wilkening S, Pelechano V, Jarvelin AI, Tekkedil MM, Anders S, Benes V, Steinmetz LM et al. (2013) An efficient method for genome-wide polyadenylation site mapping and RNA quantification. *Nucleic Acids Research* 41 (5): e65.
- Will CL, Luhrmann R. (2011) Spliceosome Structure and Function. *Cold Spring Harbor Perspectives in Biology* 3 (7): a003707.
- Woodcock, D. M., Crowther, P. J., Doherty, J., Jefferson, S., DeCruz, E., Noyer-Weidner, M., Smith, S. S., Michael, M. Z., & Graham, M. W. (1989). Quantitative evaluation of *Escherichia coli* host strains for tolerance to cytosine methylation in plasmid and phage recombinants. *Nucleic acids research*, 17(9), 3469–3478.
- Yamada T, Yamaguchi Y, Inukai N, Okamoto S, Mura T, Handa H. (2006) P-TEFb-Mediated Phosphorylation of hSpt5 C-Terminal Repeats Is Critical for Processive Transcription Elongation. *Molecular Cell* 21 (2): 227–237.
- Yamazaki T, Fujiwara N, Yukinaga H, Ebisuya M, Shiki T, Kurihara T, Kioka N, Kambe T, Nagao M, Nishida E et al (2010) The closely related RNA helicases, UAP56 and URH49, preferentially form distinct mRNA export machineries and coordinately regulate mitotic progression. *Mol Biol Cell* 21:2953–2965
- Yoh SM, Cho H, Pickle L, Evans RM, Jones KA (2007) The Spt6 SH2 domain binds Ser2-P RNAPII to direct Iws1-dependent mRNA splicing and export. *Genes Dev* 21:160–174

- Zander G, Hackmann A, Bender L, Becker D, Lingner T, Salinas G, Krebber H. mRNA quality control is bypassed for immediate export of stress-responsive transcripts. *Nature*. 2016 Dec 22;540(7634):593-596.
- Zenklusen, D., P. Vinciguerra, J.-C. Wyss and F. Stutz (2002). Stable mRNP Formation and Export Require Cotranscriptional Recruitment of the mRNA Export Factors Yra1p and Sub2p by Hpr1p. *Molecular and Cellular Biology* 22(23): 8241-8253.
- Zhang, D. W., J. B. Rodriguez-Molina, J. R. Tietjen, C. M. Nemecek and A. Z. Ansari (2012). "Emerging Views on the CTD Code." *Genet Res Int* 2012: 347214.
- Zhao J, Hyman L, Moore C. (1999) Formation of mRNA 3' ends in eukaryotes: mechanism, regulation, and interrelationships with other steps in mRNA synthesis. *Microbiol. Mol. Biol. Rev* 63 (2): 405– 445.
- Zhou K, Kuo WHW, Fillingham J, Greenblatt JF. (2009) Control of transcriptional elongation and cotranscriptional histone modification by the yeast BUR kinase substrate Spt5. *Proceedings of the National Academy of Sciences* 106 (17): 6956–6961
- Zhou ZL, Luo M, Straesser K, Katahira J, Hurt E, Reed R (2000) The protein Aly links premessenger-RNA splicing to nuclear export in metazoans. *Nature* 407:401–405